Fall 1-31-1996

Design and analysis of environmentally safe cooling systems for machine tools

Haiping Xu
New Jersey Institute of Technology

Copyright Warning & Restrictions

The copyright law of the United States (Title 17, United States Code) governs the making of photocopies or other reproductions of copyrighted material.

Under certain conditions specified in the law, libraries and archives are authorized to furnish a photocopy or other reproduction. One of these specified conditions is that the photocopy or reproduction is not to be "used for any purpose other than private study, scholarship, or research." If a, user makes a request for, or later uses, a photocopy or reproduction for purposes in excess of "fair use" that user may be liable for copyright infringement,

This institution reserves the right to refuse to accept a copying order if, in its judgment, fulfillment of the order would involve violation of copyright law.

Please Note: The author retains the copyright while the New Jersey Institute of Technology reserves the right to distribute this thesis or dissertation

Printing note: If you do not wish to print this page, then select "Pages from: first page # to: last page #" on the print dialog screen

ABSTRACT

DESIGN AND ANALYSIS OF ENVIRONMENTALLY SAFE COOLING SYSTEMS FOR MACHINE TOOLS

by
Haiping Xu

Many cooling systems of metal cutting and both their advantages and disadvantages have been reviewed. The cutting forces' relationships, stress distribution, energy consumption and heat generation of orthogonal processes are discussed. A two-dimensional finite element model has been developed to design and analyze a new proposed cooling device, which comes from the idea of "A Novel Cooling Device" proposed by Billatos et al. First, a thermal calculation is completed to compare the temperature difference between two different shapes of coiled pipe. Then, three different cutting conditions, which were considered in the experiments by Childs et al, are conducted under three varying cooling environment: Dry Cutting, New Cooling Device, and Wet Cutting for case studies. The corresponding temperature distributions around the cutting edge have been obtained by using the ANSYS package. Results showed that the proposed new cooling device does reduce the temperature of cutting tool comparing with the Dry Cutting, but it increases the temperature and temperature boundary of cutting tool comparing with Wet Cutting. This makes the proposed cooling device to be suitable under some cutting conditions when: 1. it is necessary to eliminate the cutting fluids and; 2. the maximum temperature of tool by using the device is below the temperature of tool thermal failure.

DESIGN AND ANALYSIS OF ENVIRONMENTALLY SAFE COOLING SYSTEMS FOR MACHINE TOOLS

by
Haiping Xu

A Thesis
Submitted to the Faculty of
New Jersey Institute of Technology
in Partial Fulfillment of the Requirements for the Degree of
Master of Science in Manufacturing Systems Engineering

Department of Industrial and Manufacturing Engineering

January 1996

APPROVAL PAGE

DESIGN AND ANALYSIS OF ENVIRONMENTALLY SAFE COOLING SYSTEMS FOR MACHINE TOOLS

Haiping Xu

Dr. George Abdou, Thesis Advisor — Date
Associate Professor and Acting Chairperson
Industrial and Manufacturing Engineering Department, NJIT

Dr. Layek Abdel-Malek, Committee Member — Date
Professor of Industrial and Manufacturing Engineering, NJIT

Dr. Sanchoy K. Das, Committee Member — Date
Associate Professor of Industrial and Manufacturing Engineering, NJIT

BIOGRAPHICAL SKETCH

Author: Haiping Xu

Degree: Master of Science in Manufacturing Systems Engineering

Date: January 1996

Undergraduate and Graduate Education

- Master of Science in Manufacturing Systems Engineering
  New Jersey Institute of Technology,
  Newark, New Jersey, 1996

Major: Manufacturing Engineering

- Master of Science in Mechanical Engineering,
  Shanghai Jiao Tong University,
  Shanghai, P. R. China, 1989

- Bachelor of Science in Mechanical Engineering,
  Shanghai Jiao Tong University,
  Shanghai, P. R. China, 1984

Major: Mechanical Engineering

To my beloved family

ACKNOWLEDGMENT

I would like to express my deepest appreciation to Professor George Abdou, who not only served as my thesis advisor, providing valuable and countless resources, insight, and intuition, but also constantly gave me support, encouragement, and reassurance. Special thanks are given to Professor Layek Abdel-Malek and Professor Sanchoy K. Das for actively participating in my committee.

I wish to express my sincere gratitude to Dr. Samir B. Billatos, Department of Mechanical Engineering at University of Connecticut, who offered much more help on this research.

TABLE OF CONTENTS

TABLE OF CONTENTS
(Continued)

TABLE OF CONTENTS
(Continued)

TABLE OF CONTENTS
(Continued)

LIST OF TABLES

LIST OF FIGURES

LIST OF FIGURES
(Continued)

LIST OF FIGURES
(Continued)

LIST OF FIGURES
(Continued)

Figure **Page**

CHAPTER 1

INTRODUCTION

The traditional processes of metal cutting are of the type in which a component is produced by the removal of material from a workpiece as the action of the wedge-shaped cutting edge (or edges) of the tool used. The removed material is normally called swarf or chips. Typical machining processes of this kind include turning, milling, drilling, shaping, broaching and grinding. Metal is the most widely machined of all materials and it is quite common for machining processes to be called metal cutting processes. Conditions such as speed under which a process is carried out and the forces involved are usually refereed to as cutting conditions and cutting forces [6].

In recent years, some non-conventional methods of material removal appeared, such as Electron beam machining (EBM), Ion beam machining (IBM), Electrochemical machining (ECM), Laser machining, Electric discharge machining, Plasma arc machining, Ultrasonic machining (USM), Water-jet machining (WJM) and some other specialized methods of machining. All these non-conventional methods are non-chip-forming processes [8].

However, the traditional metal-cutting is a very large segment indeed of our industry. The automotive industry, electrical engineering, railroads, shipbuilding, aircraft manufacturing, and even the machine tool industry itself, all these have large machine shops with thousands of workers engaged in machining. Though much effort has been devoted to the development of ways of shaping components to reduce the material wasted such as cold-forging, precision casting and powder metallurgy, the metal-cutting

is till the cheapest way to make very many shapes and is likely to continue to be so for many years.

In a metal-cutting operation, it is necessary for a metal-cutting tool to take the form of a large-angled wedge, which derives asymmetrically into the work material, to remove a thin layer from a thicker body. The layer must be thin enough to enable the cutter and work to withstand the imposed stress and a clearance angle must be formed on the cutter to ensure that the clearance face does not reach the newly formed work surface.

In practical machining, the included angle of the tool edge varies between 55° and 90°, so that the removed layer, the chip, is diverted through an angle of at least 60° as it moves away from the workpiece, across the rake face of the tool. In this process, the whole volume of metal removed is plastically deformed, and thus a large amount of energy is required to form the chip and to move it across the tool face. In the process, two new surfaces are formed, the new surface of the workpiece (OA in Figure 1.1 [4]) and the under surface of the chip (BC). The formation of new surfaces requires energy, but in metal cutting, the theoretical minimum energy required to form the new surface is much of that required to deform plastically the whole of the metal removed [4].

The mechanical energy consumed in machining processes include energy associated with chip formation, energy associated with plastic deformation remaining in the deformed material. Many studies show that almost more than 98% of mechanical

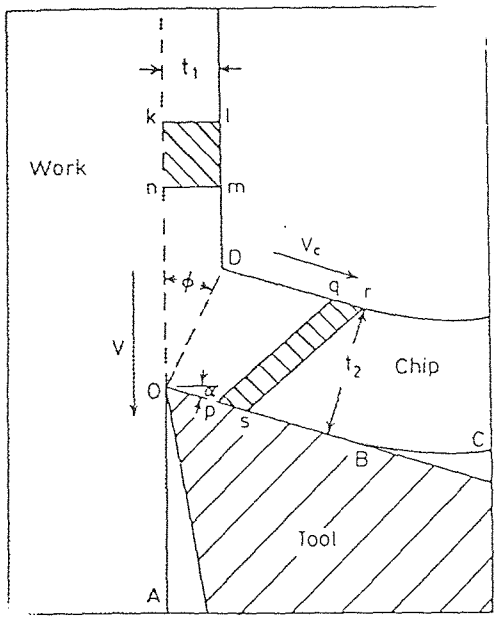

Figure 1.1 Metal Cutting Diagram [4]

energy associated with chip formation ends up as thermal energy [2], which causes the high temperature on tool face (θ_r) and on the relief surface (θ_R), then further effects the tool wear rate and the machined surface. The temperature during cutting is the single most important tool life variable. In general, tool life varies as some very high power of tool temperature. Taylor [23] demonstrated that the tool life in minutes (T) for a high speed steel (HSS) tool operating at a constant feed varies with cutting speed (V) as follows:

$$V\,T^n = \text{constant} \qquad (1.1)$$

The temperature at the tip of a cutting tool is found to vary approximately as follows [11]:

$$\theta \quad u\sqrt{vt / k\rho c} \qquad (1.2)$$

where: u = specific cutting energy (energy per unit volume of chips produced)

v = cutting speed

t = undeformed chip thickness(feed rate in a turning operation)

k = coefficient of thermal conductivity of the work material

ρc = volume specific heat of the work material

Combining equation(1.1) and (1.2) for a given material and feed rate:

$$T \quad V^{1/n} \quad \theta^{2/n} \qquad (1.3)$$

Table 1.1 Effects of Temperatures and Materials on Tool Life

HSS	n = 0.1	$T \quad \theta^{20}$
Tungsten Carbide (wc)	n = 0.2	$T \quad \theta^{10}$
Ceramic	n = 0.4	$T \quad \theta^{5}$

Thus, tool life varies with tool tip temperature to a high power, but the tool temperature exponent decreases as the tool material becomes more refractory [11].

In order to remove the heat generated during machining, cutting fluids are introduced. The major objectives of using cutting fluids are [4,9]:

1. Improve surface finish and workpiece quality and accuracy.

2. Increase tool life and minimize machine down-time.

3. Reduce feed forces, cutting forces and energy consumption and increase machining rates.
4. Wash away the chips.
5. Protect the newly machined surfaces from corrosion by leaving a residual film on the work surface.

1.1 Problem Definition

The main sources of heat in a cutting operation, as discussed later, are on the primary shear plane and at the tool-work interface (especially in the flow-zone in the tool rake face). The work done in shearing the work material in these two regions is converted into heat, while the work done by sliding friction makes a minor contribution to the heating under most cutting conditions. Heat generated in the primary shear zone is mostly carried away in the chip and a minor proportion is conducted into the workpiece. The removal of heat generated in the primary shear zone can have little effect on the life or performance of the cutting tools.

As discussed later, the heat generated near the tool/work interface is of much greater significance, particularly under high cutting speed conditions where the heat source is a thin flow-zone seized to the tool. The thin zone is the heat source and removal of this heat by conduction through the chip and through the body of the workpiece is likely to have relatively little effect on the temperature at the tool/work interface, since both chip and workpiece are constantly moving away from the contact area allowing very little time for heat to be conducted from the source.

For example, when cutting at 30 m/min (100 ft/min) the time required for the chip to pass over the region of contact with the tool is of the order of 0.005 second [4].

Since the tool is the only stationary part of the machining process, it is damaged by the high temperatures and, therefore, in most cases, cooling is most effective through the tool. The tool is cooled most effectively by directing the coolant towards those accessible surfaces of the tool that are at the highest temperatures, since these are surfaces from which heat is most rapidly moved, and the parts of the tool most likely to suffer damage. Knowledge of temperature distribution in the tool can, therefore, be in assistance in a rational approach to coolant application.

To reduce the effect of heat generation, fluids are used. The cutting fluids not only help in obtaining a component with desired dimensional accuracy and surfaces finish but also help do so more economically. The beneficial effect may be in one or more of the following [2]:

* Increased tool life due to lubrication and cooling effects.
* Improved surface finish.
* Easy removal of chips.
* Less distribution of workpiece due to cooling effect.
* Reduction in cutting forces, which reduce the distortion due to elastic deflection.

The use of cutting fluids should be justified economically. The value added to the product by way of better quality due to better dimensional accuracy and surface finish and the lower cost of the process due to the better tool life should outweigh the cost of cutting fluid consumed and the costs due to the cooling system [1].

CHAPTER 2

LITERATURE REVIEW

2.1 Types of Cutting Fluids

The major groups of the cutting fluids are [4]:

a) Straight or neat cutting oils

They are derived from petroleum, animal, marine, or vegetable substances which contain chlorine and/or sulphur for lubricating purpose. They are used without dilution with water usually for light-duty machining on metals of high machinability. Straight oils can be used alone or as oils compounded with various polar and/or chemically active lubricant additives. They have inadequate cooling effect.

b) Water-based cutting fluids or soluble oils

They consist of an emulsion or a solution, usually a mineral oil fortified with emulsifiers and diluted with water in proportion between 1:10 and 1:60. Because of their high specific heat, high thermal conductivity and high heat of vaporization, they are convenient for cooling purposes in high temperature machining. They contain inhibitors of rust and of the growth of bacteria and fungi. Lubricant additives are also commonly added for medium to heavy duty machining.

c) Synthetic cutting fluids

They are water-based fluids containing no mineral oil and formulated with multiple rust and fungi's inhibitors and lubricant additives. They provide better cooling and longer tank life, but less lubricant and harder waste treatability. Defoams, wetting agent and dyes are also auxiliary additives.

d) Semisynthetic cutting fluids

They are water-based fluids contain oil-based additives. Usually, they contain 5 - 20% mineral oil, emulsified into water to form a microemulsion. They have the advantages of both of soluble oils and synthetic fluids without many of their individual disadvantages. They can be used on some difficult machining applications.

2.2 Application Methods

Cutting fluids can be applied to the cutting zone by one of the following techniques:

a) Flood cooling

Flood cooling is the most commonly used method in industry. Cutting fluids are flooded with rates ranging from 10 liters/min for single-point tools to 225 liters/min per cutter for multiple-tooth cutters. In some operations, high pressures extending from 0.7 to 14 Mpa are used to wash away the chips [26]. The system usually consists of containers, circulating pumps, electrical and pneumatic controls, piping and jets for directing the fluids to the tool, and return troughs, chip conveyors, and filters for clearing the used fluid [4].

b) Mist cooling

This method supplies finely divided or atomized cutting fluid in pressurized air at 0.07 to 0.6 MPa. This enables the fluid to reach inaccessible areas, and provides better visibility to the machined part. Some mist systems as shown in Figure 2.1 use a vortex tube to cool the pressurized air and produce cold mist. This technique has a

limited cooling capacity and needs good ventilation to save the machine operator from inhaling the used fluid [26].

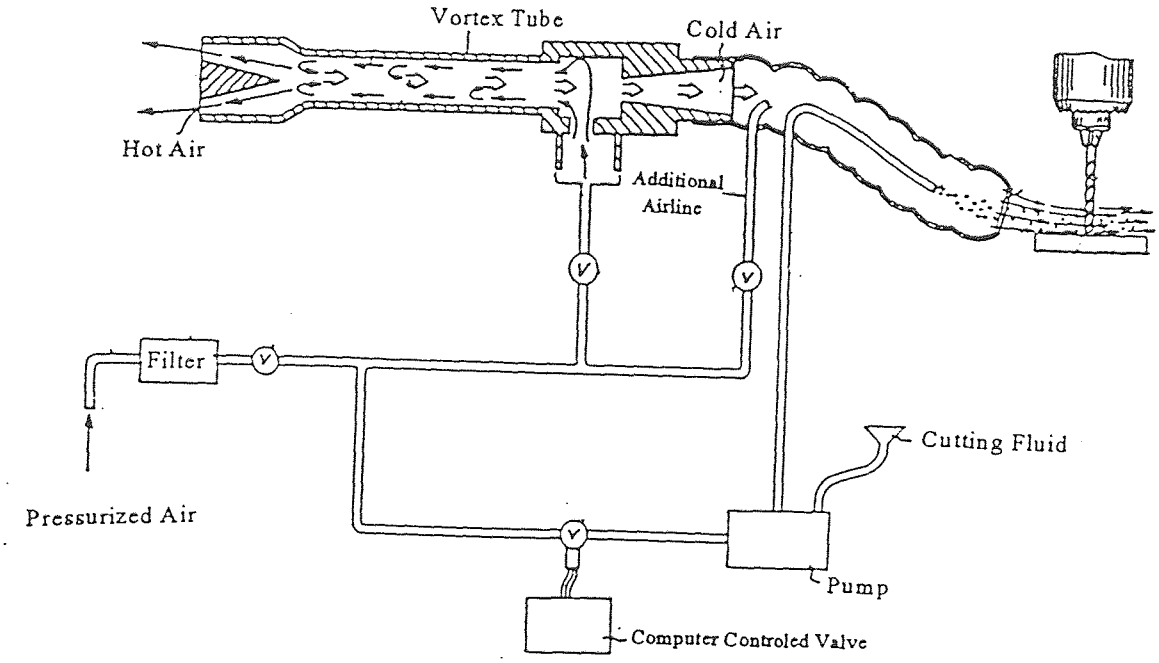

Figure 2.1 Mist Cooling System [26]

2.3 Cutting -Fluid Actions

The action of the cutting fluids can be as coolants or lubricants. This depends on type and conditions of the cutting operation.

a) Cooling action

The cutting fluid cools the cutting zone: the tool, the chip, and the workpiece and thus reduces the temperatures, the tools wear, and the thermal distortion of the tool and the workpiece.

b) Lubrication action

The cutting fluid reduces the weldability and the contact area between the chip and the tool surface which results in less friction, heat, wear, and built-up-edge. Also, it can modify the flow pattern around the cutting edge and increase the shear angle as shown in Figure 2.2 which consequently reduces the generated heat at the shear plane and provides less chip thickness [4].

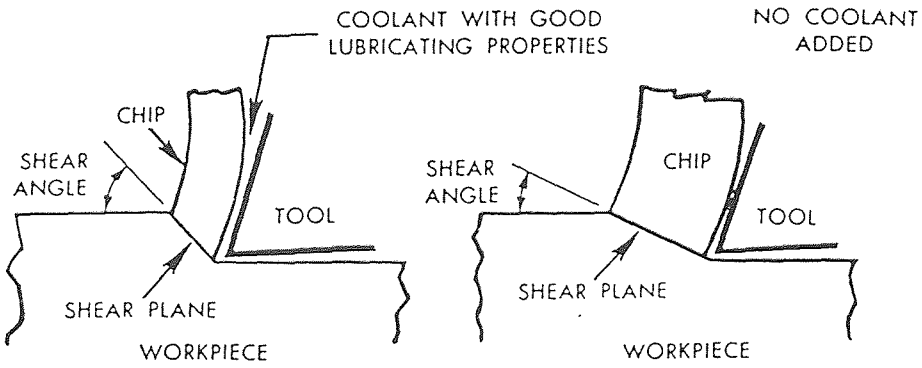

Figure 2.2 Lubrication Action [4]

2.4 Cutting Fluid Function at High Speed Machining

To study the effect of coolant on heat removal, Trent and Smart [4,2] examined temperature contours on the rake face of high speed steel tools used in cutting iron at 183 m/min. They conducted their experiments under three different cooling conditions: (a) dry (air), (b) wet (tool flooded with coolant over rake face), and (c) wet (jet of coolant directed at end clearance face) and results are shown graphically in Figure 2.3. They found that in case of high speed machining, the heat source at the chip-tool

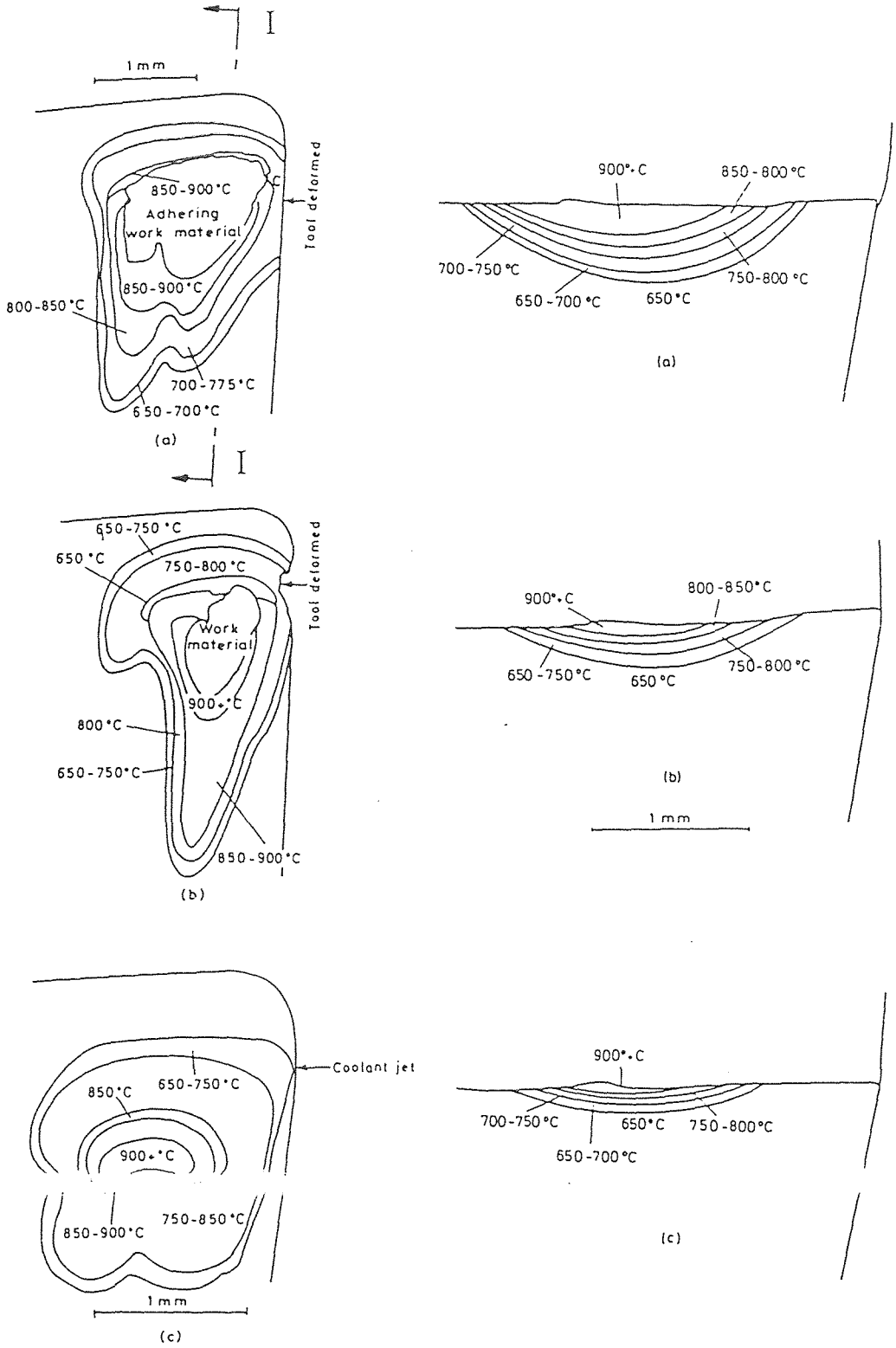

Figure 2.3 Temperature Contours on the Rake Face and on Section I-I [4]
(a) For Dry Cutting (b) For Tool Flooded with Coolant over Rake Face
(c) For Tool with Jet of Coolant Directed at End Clearance Face

interface is a thin flow-zone seized to the tool. Coolant cannot reach this zone but can only reduce the volume of the tool material which was seriously affected by overheating by removing heat from the surrounding accessible surfaces of the chip, the workpiece and the tool. They also found that directed coolant jet has better cooling effect than flooding the rake face by coolant from top.

Trent [4] found very little effect of the coolant on the tool-work interface temperature when cooling through the workpiece or the chip. This occurs due to the high moving speed of the chip and the workpiece at the contact area without allowing enough time for heat to be transferred, Trent also noted that at high metal removal rates, all possible mechanisms of wear are very sensitive to the high temperature at the work-tool interface. For example, the rate of diffusion wear in high speed steel tools will be doubled for an increment increase in temperature of about 20°.

Kalpakjian [26] pointed out that at high cutting temperatures the cutting fluid is converted to a gaseous state of small molecular size that penetrates the tool-chip interface causing more lubrication effects. But, for high speed machining there is less probability that an effective capillary action will take place and the main role of the cutting fluid becomes only of cooling the cutting zone.

Kurimoto and Barrow [27] studied the influence of different cutting fluids in turning of an alloy steel using carbide tool with cutting speed range from 30 to 240 m/min. They indicated that under particular cutting conditions, cutting fluids had no lubricating action and did not penetrate into the chip-tool interface, and hence, they can be considered solely as coolants. Various cutting fluids' performances were investigated

on each region of tool wear: crater, flank, groove and notch wear. It was concluded that:

* Cutting fluids can reduce the rate of crater wear.
* Dry cutting has slightly better effect than all cutting fluids on the flank wear.
* All the fluids increase the groove wear at the trailing edge (see Figure 2.4), particularly at low feeds. This can be considered due to the corrosive or oxidizing action of the fluids. Since the groove wear affects the surface finish and the dimensional accuracy of the workpiece, in finishing processes tool life can decrease with the use of fluids.
* There is no significant effect of using cutting fluids on notch wear.

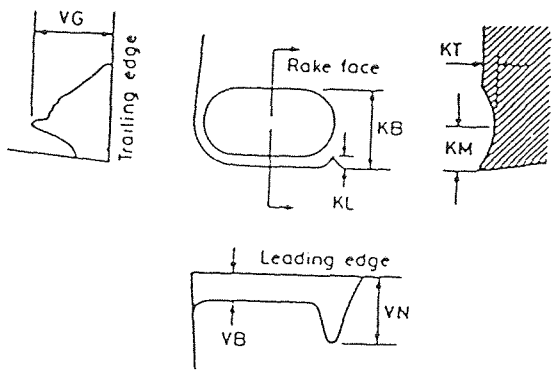

Figure 2.4 General Forms of Tool Wear [27]

From the above studies, it can be concluded that the main roles of the cutting fluids, under general conditions, at high speed machining are to:

1. Cool the cutting tool,
2. Decrease the crater wear,

3. Removes the chip, and 4. Cool the workpiece.

Despite these advantages and functions of the cutting fluids, they cause harmful effects to the operators and serious problems of pollution to the environment. Additional disadvantages are listed below.

2.5 Disadvantages Of Cutting Fluids [26]

1. Potential health problems resulting from direct contact or inhalation of fluids.
2. Environmental and pollution problem resulting from degrading, recycling, disposing of unwanted waste chemicals and treatment of waste waters.
3. Machines must be fitted with complicated systems for handling, circulating, pumping and filtering the cutting fluids.
4. Additives must be added such as: bioresistant chemicals and rust inhibitors.
5. Damage to tool itself in some situations. For examples, in milling process, cutting fluid may cause big variation of the cutter teeth temperature leading to thermal cracks.
6. In some case, cutting fluid can cause the chip to curl into a very small radius, and thus increase the temperatures and the stresses near the tip of the tool and reduce the tool life.

To overcome these disadvantages and limitations of cutting fluids, other cooling methods were invented, as discussed in the following section.

2.6 Inventive Cooling Systems

2.6.1 Cryogenic Systems

In these systems, a stream of a cryogenic coolant, such as Freon-12 or nitrogen, is routed internally through a conduit inside the tool and directed at close range to the interface between the cutting edge and the workpiece as shown in Figure 2.5 [28]. The coolant stream is directed in such a manner that the cutting chips do not obstruct. The coolant evaporates completely and effectively cools the cutting edge and the workpiece. To prevent the coolant from boiling until it is released at the cutting edge, proper insulation and minimum diameter of the internal conduit should be used. Also, there are other similar systems that use a liquefied gas, such as carbon dioxide, or a mist of a mixture of Freon and butyl Cellosolve and direct it externally in a stream toward the cutting zone. This method applies refrigerants which are not advantageous to use now due to their harmful environmental effect.

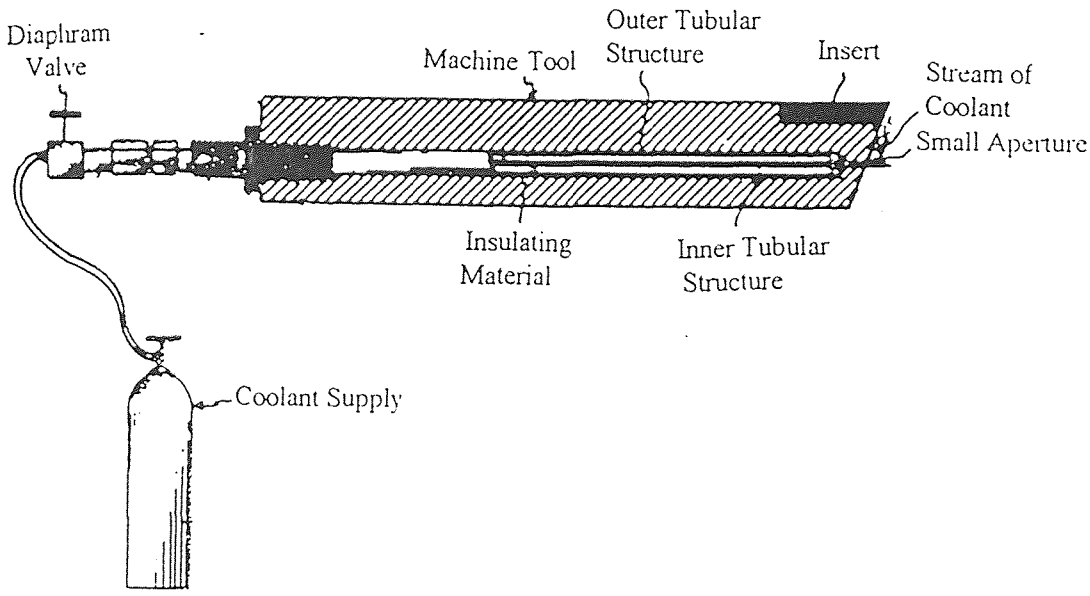

Figure 2.5 Cooling Using Cryogenic Fluid [28]

2.6.2 Internal Cooling by Vaporization Systems

In these systems, a vaporizable liquid, such as water, is introduced inside the shank of the tool and vaporized on the underside surface of the insert as shown in Figure 2.6 [29]. A capillary wick is used to pump the fluid automatically to this surface and there is a vent hole in the tool for the vapor generated in the cooling process. The generated heat at the cutting edge is transferred to the underside surface of the insert by conduction and then removed by nucleate boiling of the coolant. Although this method provides very good environmental solution, it has been shown that in heavy duty cutting operations, the cutting temperatures are about the same as dry cutting [29].

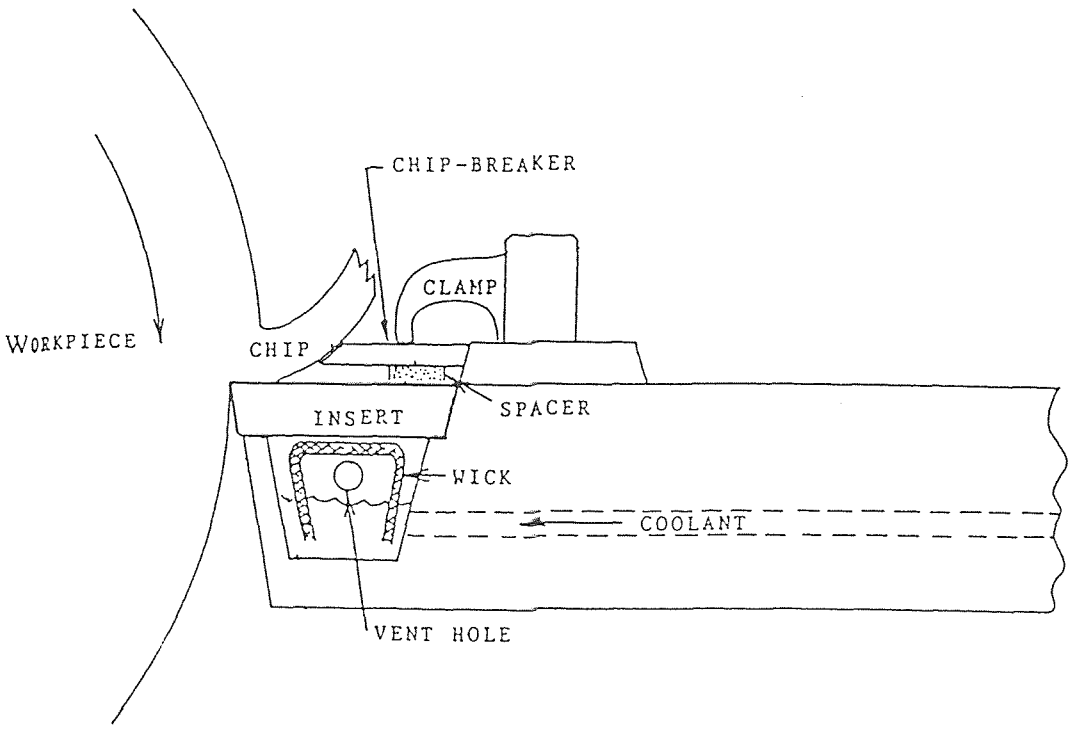

Figure 2.6 Internal Cooling by Vaporization [29]

2.6.3 Thermoelectric Cooling Systems

In these systems, a module of couples of thermoelectric material elements connected electrically to one another is used as shown in Figure 2.7 (a) [31] . When an electric current is passed through the thermoelectric elements a cold junction and a hot junction is created at the opposite ends of each of these elements. The thermocouples are so oriented that all the cold junctions are located in one side of the module which can be called the cold face.

The apparatus, as shown in Figure 2.7 (b), has no moving parts. The cutting tool is clamped to the tool holder. The tool holder is made of copper and includes two flat side surfaces. Each of these surfaces contacts the cold face of a thermoelectric module. The hot face of the module engages the inner wall of a heat exchanger unit which includes a cavity filled with a heat absorbing and transferring fluid, such as water, and fins to enhance the cooling process.

The heat generated in the cutting tool is transferred to the cold face of the module and removed by the thermoelectric cooling effect. The temperature difference between the cold and the hot face should be maintained as low as possible to maximize heat pumping. This can be achieved by using the heat exchanger unit which cools the hot face and transfers heat to the ambient air by natural or forced convection.

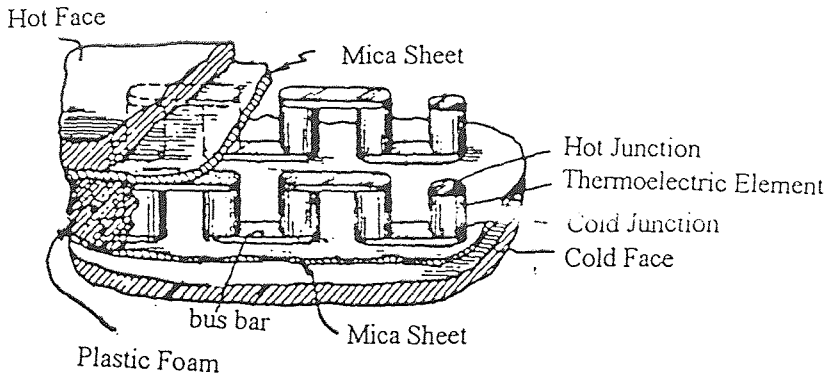

Figure 2.7 (a) The Thermoelectric Model [31]

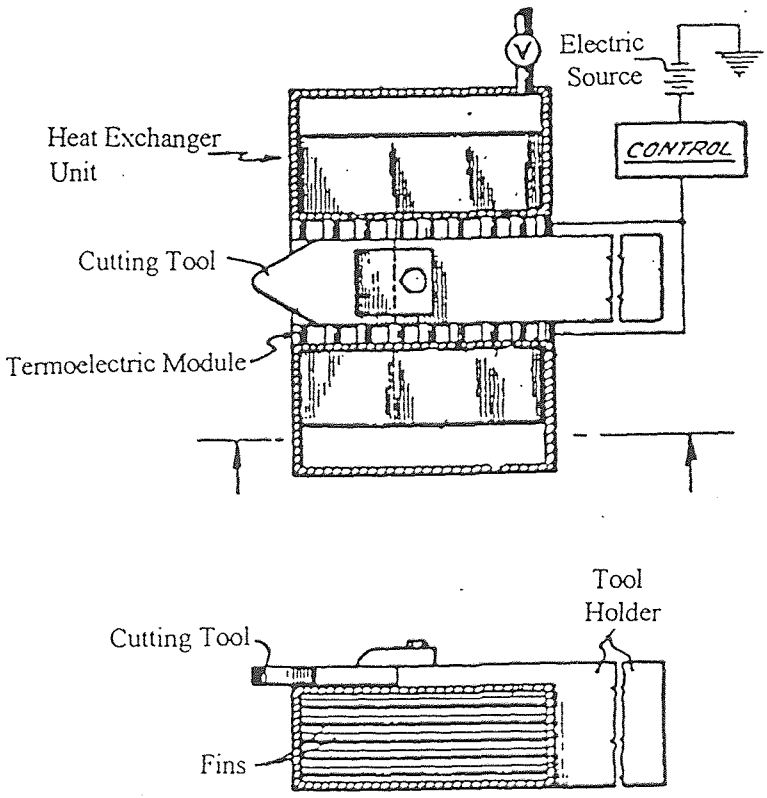

Figure 2.7 (b) The Thermoelectric Cooling Apparatus [31]

2.6.4 Cold Gun Air Cooling Systems

In these systems, a vortex tube is used to cool supplied compressed air to about 30°C below its temperature without using any moving parts as shown in Figure 2.8 [32]. The cold air is then discharged through a flexible hose and directed to the point of use. This system can be used in grinding, drilling, milling and sawing operations [32].

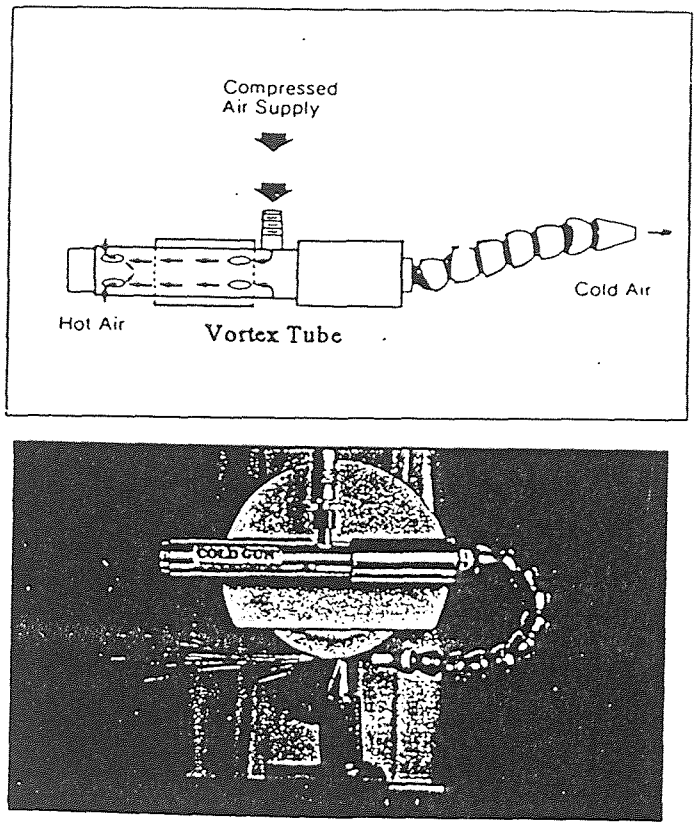

Figure 2.8 Cold Gun Air Cooling [32]

2.6.5 High Pressure Water-Jet Cooling Systems

In these systems, high pressure water-jet (35 to 280 MPa) is directed under the produced chip as shown in Figure 2.9 [33]. Mazurkiewicz compared this method with

the dry and flood cooling methods. He pointed out in his studies that for a given cutting speed and rake angle, this method reduces the contact length and the coefficient of friction on the tool rake face, and thus greatly reduces cutting and feed forces. Also, the chip quality can be used after filtration (5 microns) in an open cycle. Therefore, no additives or recirculation systems are required. Whether this method with such high pressure jets can be used with a large scale in industry is a matter of interest [4].

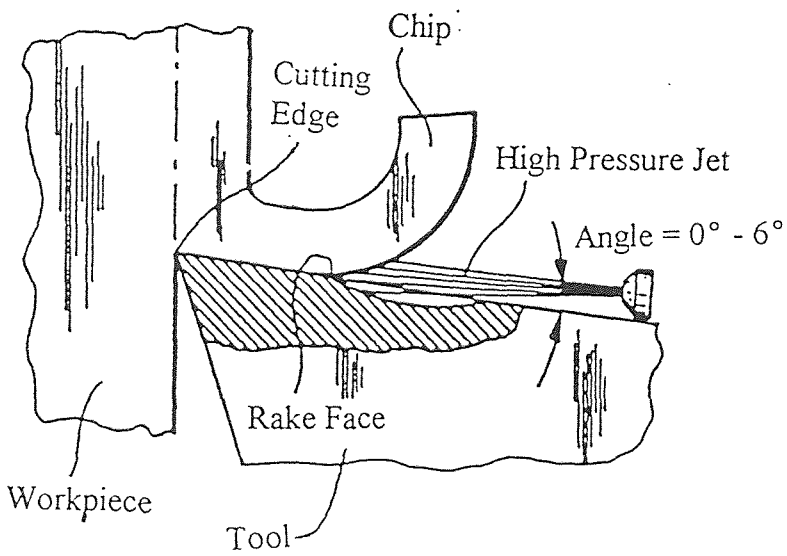

Figure 2.9 High Pressure Water-Jet Cooling [33]

2.6.6 Under-Cooling Systems

Ber and Goldlatt [22] studied the temperature distribution at the tool tip during cutting process at velocities higher than 100 m/min. They investigated the influence of the temperature gradient on the wear behavior of the cutting tool and its life. They showed that the thermal failure of the cutting tool depends on the temperature

gradient. Large temperature gradient results in smaller rate of crater wear and lower level of crater and flank wear. They explained, by using the two temperature gradients model for friction failure [34], shown in Figure 2.10, that as the temperature gradient decreases the shearing process becomes deeper and causes more damage (see Figure 2.11). Therefore, they recommend limiting the effect of the shearing process to a small possible layer of the surface [35]. To achieve large temperature gradient, an "under-cooling" system, shown in Figure 2.12, was used. In this system, the coolant flows through channels located under the insert then out to the environment. A thin copper foil is attached to the lower face of the tool to remove maximum heat. The system produced larger temperature gradient and lowered wear compared to the traditional upper-cooling method used in industry.

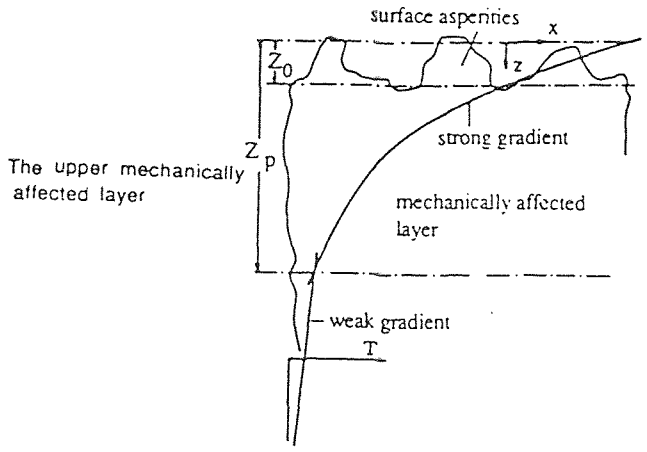

Figure 2.10 Two Temperature Gradients Model [34]

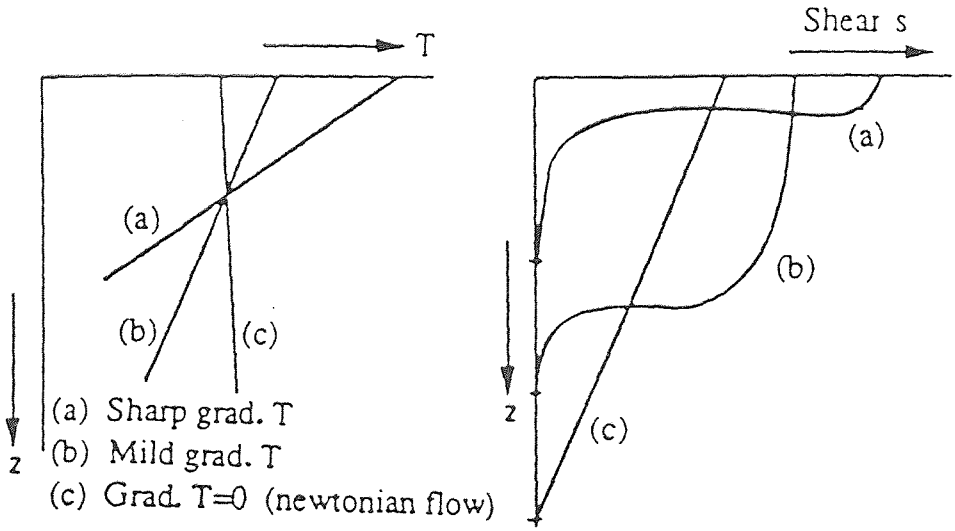

Figure 2.11 The Shear Rates in the Mechanically Affected Layer [35]

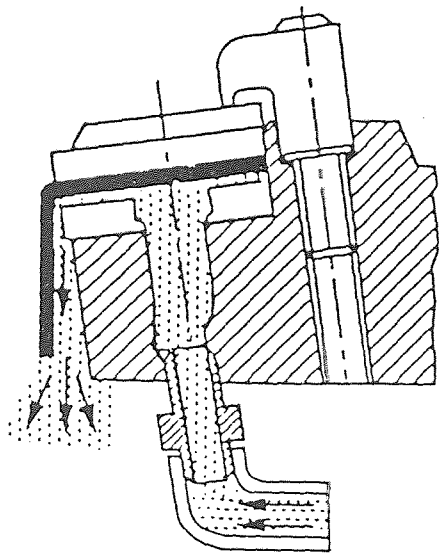

Figure 2.12 The Under-Cooling System [22]

2.6.7 Internal Cooling by Flushing Systems

Maekawa et al [36] developed a two-dimensional finite element model, shown in Figure 3.13, to study the effect of the internal cooling, using water flushing, on the tool. They found that the less distance between the coolant path and the rake face of the tool and the larger area from which heat is taken away, the lower the maximum temperature on the rake face (T_{max}) becomes. They showed that T_{max} can be decreased by 30° C to 200° C by the internal cooling method and there is no influence on the strength of the tool (see Figure 3.14). Also, displacement of the internally cooled tool edge, shown in Figure 3.15, is found to be less than the normal one, and thus internal cooling method achieves more precision in machining. This method needs special technology to construct a tiny coolant path (about 2 mm in diameter) inside the tool itself which is usually made of very hard material.

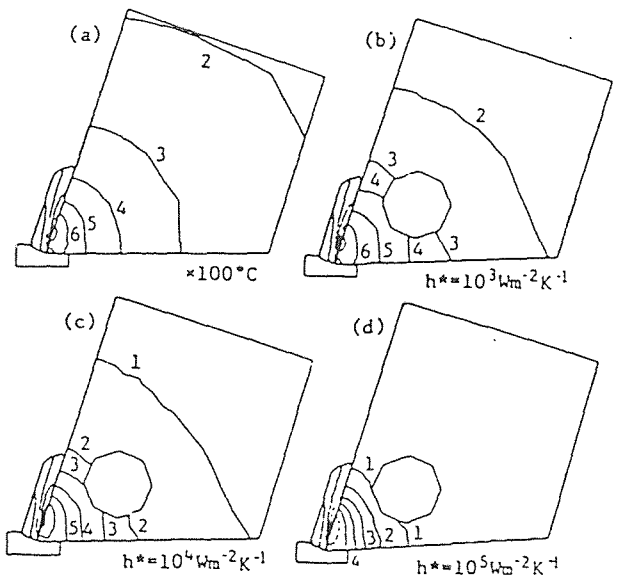

Figure 2.13 Temperature Contours at
Various Heat Transfer Coefficients of Coolant Path [36]

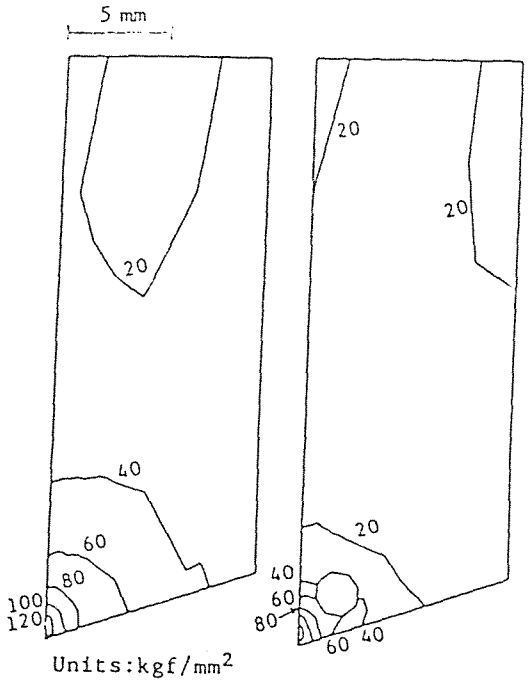

Figure 2.14 Contours of Equivalent Stress Within Cutting Tool [36]

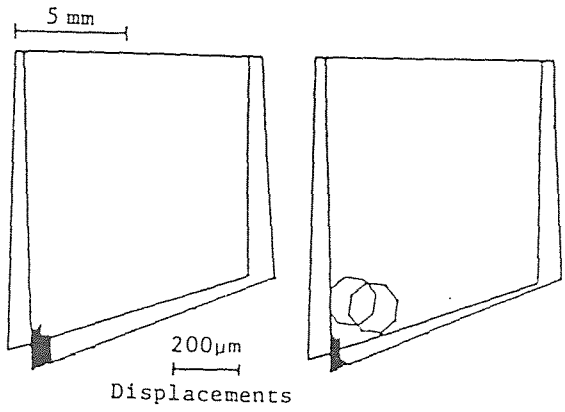

Figure 2.15 Deformation of Cutting Edge and Yielded Zone [36]

2.7 Objectives

Considering the previous review for the existing and the inventive cooling methods, it has been shown that:

1. Many methods use chemical compounds or cryogenic coolants that have harmful effects on the environment and humans.
2. Some methods, such as the internal cooling by vaporization and the cold gun air cooling, have limited cooling effect on the cutting tools and can not be used in heavy - duty machining.
3. Other methods, such as the high-pressure water-jet cooling and the internal flushing, need special techniques to be used with a large scale in industry.

Therefore, The objective of this research is to investigate analytically a new practical and environmental safety to cool the cutting tool effectively. The new method applies the principles of heat transfer to the area of high temperature of cutting tool, which need to design a heat exchanger by using closed loop water as coolant. There are many expected economic benefits from this method such as: longer tool life, increased productivity, improved accuracy, eliminated cutting fluids disposing applications and safe to environments.

The present work pertains to single-point cutting tools, such as those used on a lathe. It focuses on orthogonal cutting processes at high speed machining. Orthogonal cutting processes are selected for use in the present investigation because they are basically two-dimensional cutting processes. In high speed machining,

problems due to the generated heat are severe and, therefore, reducing tool temperature results in higher metal removal rate.

Procedure of this thesis is organized as follows: A simplified model for the orthogonal cutting process and its parameters are presented in Chapter 3. Chapter 4 provides the description of the new proposed cooling device and FEA heat transfer. Chapter 5 provides the case studies under varying cooling environment. Chapter 6 analyzes the results of these cases from the ANSYS package calculations. Chapter 7 gives some conclusions and recommendations.

CHAPTER 3

MACHINING PROCESSES

In orthogonal cutting the tool edge is straight, it is normal to the direction of cutting, and normal also to the feed direction. On a lathe, these conditions are secured by using a tool with the cutting edge horizontal, on the center line, and at right angles to the axis of rotation of the workplace. Strictly orthogonal cutting can be carried out on a planing or shaping machine, in which the work material is in the form of a plate, the edge of which is machined.

Simple case of orthogonal machining can clearly show the formation of chip. In this process as shown in Figure 3.1, a tool with a plane cutting face and a single, straight cutting edge, which is set normal to the cutting velocity U, removes a layer of work material of uniform thickness t, and width w, which is greater than the width of cut, and by the two angles α and β. The angle α between the tool cutting face and

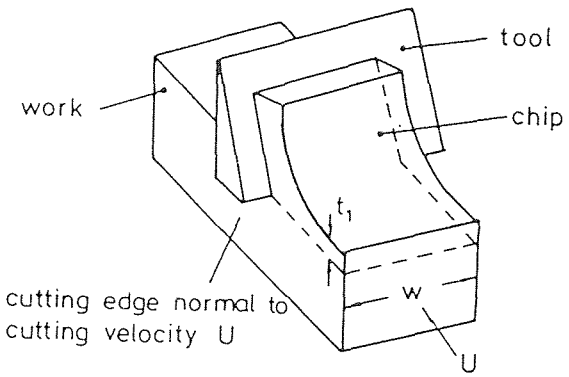

Figure 3.1 Orthogonal Machining Process [6]

the normal to the cutting velocity U is the rake angle. The angle β between the clearance face of the tool and the work surface is the clearance angle.

Lots of research work on the zone of deformation between work and chip had been done. Ernst [37] used high speed motion pictures to distinguish the different types of chips, namely discontinuous, continuous and continuous with built-up edge. Sketches of these are given in Figure 3.2.

Based on the experimented observation made by Ernst [37] and others. A shear plane model of chip formation was present to describe the continuous chip formation by plastic deformation in a narrow zone that runs from the tool cutting edge to the work-chip free surface. This is represented by the shear plane AB in Figure 3.3 across which the work speed U (the tool is assumed stationary) is instantaneously changed to the chip velocity V. This requires a discontinuity (jump) in the tangential component of velocity across AB equal to Vs as shown by the velocity diagram in Figure 3.3.

For an idealized rigid-perfectly plastic (non-hardening) work material, the elastic strain is disregarded and during deformation the volume of an element remains constant, then the model as described is valid. Conservation of mass requires that the normal component of velocity is continuous across AB, that is the components of U and V normal to AB are equal.

$$V\cos(\phi - \alpha) = U\sin\phi \qquad (3.1)$$

$$Vs\cos(\phi - \alpha) = U\cos\phi \qquad (3.2)$$

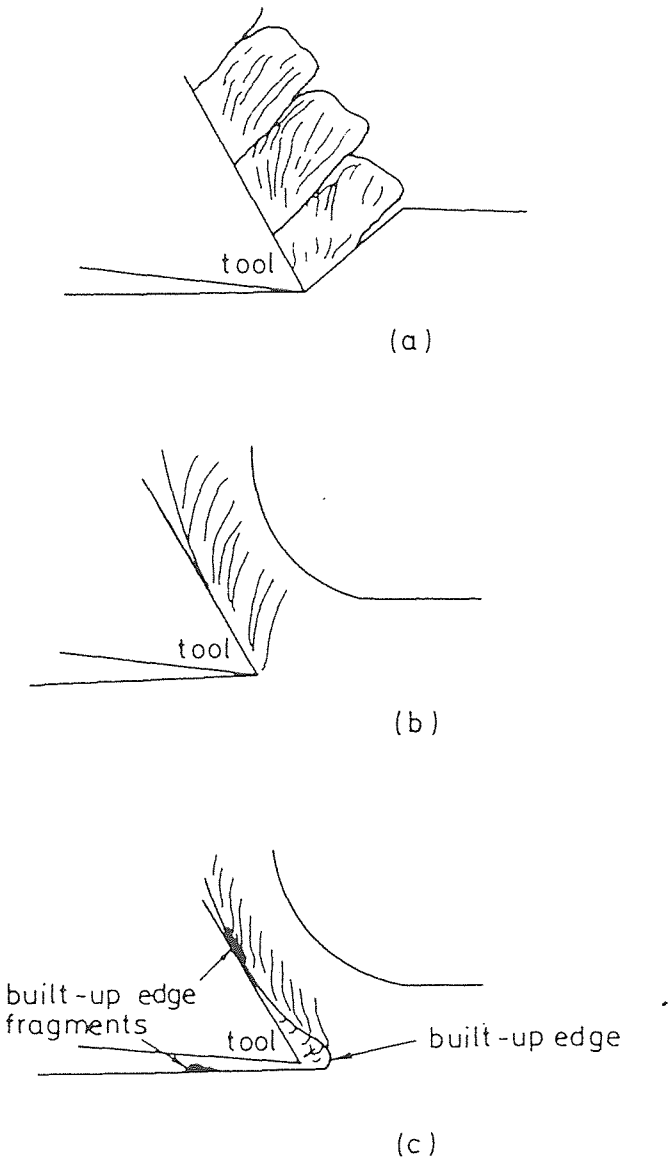

Figure 3.2 Sketches of Different Chip types [37]: (a) Discontinuous; (b) Continuous; (c) Continuous with Built-Up

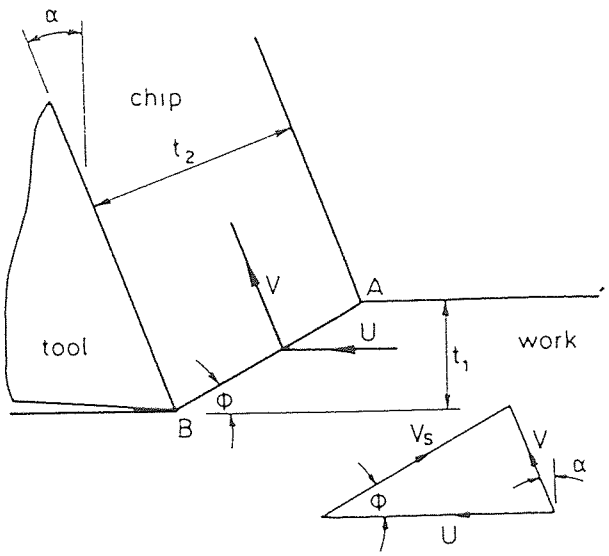

Figure 3.3 Shear Plane Model [6]

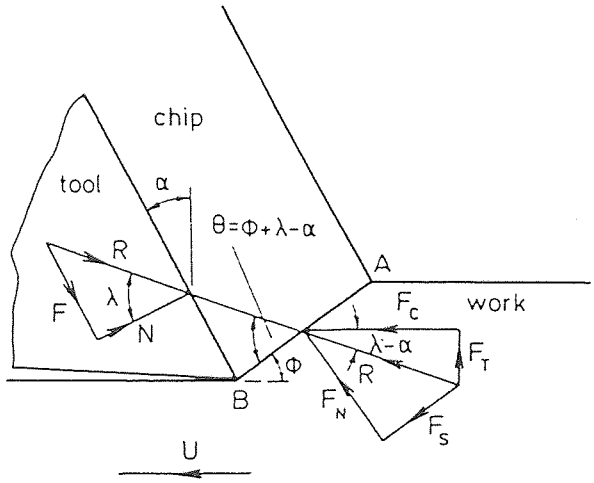

Figure 3.4 Forces Associated with Shear Plane Model [6]

3.1 Forces Relations

If the tool is assumed to be perfectly sharp, and the shear plane AB is taken to be straight. It is convenient to obtain three sets of forces:

1. In the cutting direction and normal to this direction, F_C and F_T
2. Along and perpendicular to the shear plan, F_S and F_N
3. Along and perpendicular to the tool face, F_n and F_n

$$F_S = F_C \cos\phi - F_T \sin\phi \qquad (3.3)$$

$$F_N = F_T \cos\phi + F_C \sin\phi = F_S \tan(\phi + \lambda - \alpha) \qquad (3.4)$$

Similarly

$$F = F_C \sin\alpha + F_T \cos\alpha \qquad (3.5)$$

$$N = F_C \cos\alpha - F_T \sin\alpha \qquad (3.6)$$

The tool face components are of importance since they enable the coefficient of friction for the tool face:

$$\mu = \tan\lambda \qquad (3.7)$$

will be determined by

$$\mu = \frac{F}{N} = (F_C \sin\alpha + F_T \cos\alpha) / (F_C \cos\alpha - F_T \sin\alpha) \qquad (3.8)$$

3.2 Stresses

The shear plane model gives the relation of forces, which are of importance since they enable the mean shear and normal stresses on the shear plane to be determined,

Thus,

$$\tau = \frac{F_s}{A_s} \qquad (3.9)$$

where : As is the area of the shear plane.

The force required to form the chip is determined by the shear yield strength of work material under cutting conditions and the area of the shear plane. The shear yield strength can be obtained by calculation and using data from dynamoments and chip thickness measurements. In general the shear strength of metals and alloys in cutting has been found to vary only slightly over a wide range of cutting speeds and feed rates, and the values obtained are not greatly different from the yield strengths of the same materials measured in laboratory tests at appropriate amounts of strain.

If the shear plane area remain constant, the force required to form the chip is only depended on shear yield strength of the material. However, the area of the shear plane is very variable, and it is the area which exerts the dominant influence on the cutting force, often more than outweighting the effect of the shear strength of the metal being cut.

In orthogonal cutting the area of the shear plane is related to the undeformed chip thickness t_1 (the feed), to the chip width w (depth of cut) and to the shear angle ϕ .

$$A_s = \frac{Wt_1}{\sin\phi} \qquad (3.10)$$

The feed and depth of cut are two of the major variables under the control of the machine tool operator. However, the shear plane angle is not directly under the control of the operator, and in practice it is found to vary greatly under different conditions of cutting, from a maximum of approximately 45^0 to a minimum which may be 5^0 or less. The forces increase in direct proportion to increments in the feed and

depth of cut and to decrease in the shear plane angle. If cutting forces are to be controlled or even predicted, it is possible to investigate the factors which regulate the shear plane angle. Much of the work done on analysis of machining has been devoted to methods of predicting the shear plane angle.

From equation (3.3), (3.4), (3.9), and (3.10):

$$\tau = \frac{(F_C \cos\phi - F_T \sin\phi)\sin\phi}{Wt_1} \tag{3.11}$$

Similarly,

$$\sigma = \frac{F_N}{A_N} = \frac{(F_C \sin\phi + F_T \cos\phi)\sin\phi}{Wt_1} \tag{3.12}$$

3.3 The Shear Angle

For a given rake angle α and undeformed chip thickness t_1 it can be seen that the geometry of Figure 3.18 is not completely defined unless the shear angle ϕ (or the chip thickness t_2) is known and hence no estimate can be made of cutting forces, etc. Many equations have been proposed for predicting ϕ. Ernst and Merchnt (1941) expressed the shear stress along the shear plane in terms of R, w, t_1, α, λ and ϕ and then, making a number of simplifying assumptions, selected ϕ to make AB a direction of maximum shear stress which gave

$$\phi = \frac{\pi}{4} + \frac{\alpha}{2} - \frac{\lambda}{2} \tag{3.13}$$

If we relax some restrictions of Ernst and Merchant (1941) model, some different equations are given, for instance, Merchant (1945) obtained shear angle ϕ be

expressing the cutting force F_H in terms of the shear flow stress along AB, w, t_1, α, λ and ϕ.

$$2\phi = \cot^{-1} s + \alpha - \lambda \qquad (3.14)$$

where s is the slope of the shear stress against normal stress relation.

Oxley [38] shown that Merchant's result was the upper bound solutions to the problem. There are many other models in shear plane solutions. This thesis does not represent them, it does not mean they are not important, but they beyond the focus of this discussion.

3.4 The Shear Plane Angle And Minimum Energy Theory

As we mentioned before, the thickness of the chip is not constrained by the tool, then we must answer the question - what does determine whether there is a thick chip with a small shear plane angle and high cutting force, or a thin chip with large shear plane angle and minimum cutting force? Analysis the energy consumed in cutting provides at least a qualitative answer to this question by Rove and Spick [24]. Their hypothesis is that, since it is not externally constrained, the shear plane will adopt such a position that the total energy expanded in the system (energy on the shear plane plus energy on the rake face) is a minimum.

Consider the rate of work done on the shear plane with the simple conditions for the rake angle $\alpha = 0^0$, it can be shown that

$$\frac{dW_s}{dt} = \frac{t_1 W \tau U}{\sin\phi\cos\phi} \qquad (3.15)$$

Thus if all the cutting conditions are held constant, it is found that the rate of works on the shear plane is proportional to $\frac{1}{\sin\phi}$, Curve 1 in Figure 3.5 shows how the work done on the shear plane varies with the shear plane angle with a minimum at $\phi = 45^o$. Thus, if the feed force FT and the work done on the rake face are so small that they can be neglected, the minimum energy theory proposes that the shear plane angle would be 45^o, with the chip thickness t_2 equal to the feed t_1. If the rake angle is higher than zero, the minimum work is at a shear plane angle higher than 45^o, but always at a value where $t_2 = t_1$. In practice, the chip is sometimes approximately equal in thickness to the feed, never thinner, but often much thicker.

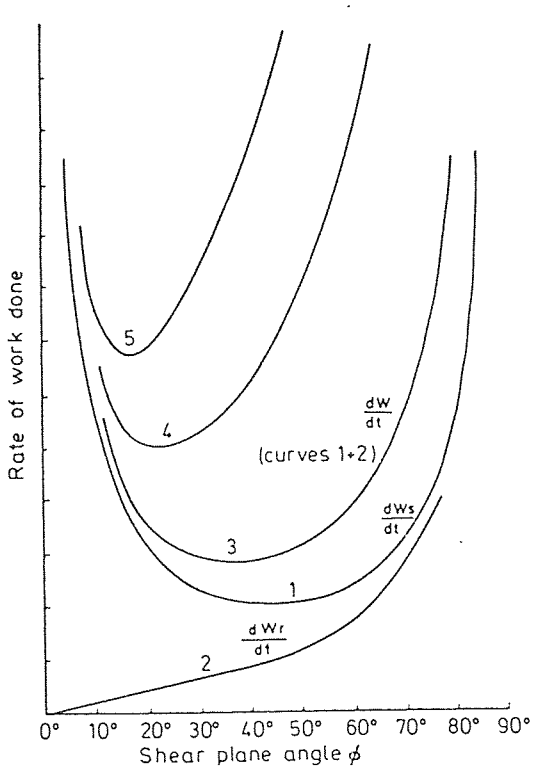

Figure 3.5 Rate of Work Done vs. Shear Plane Angle ϕ [4]

We also must consider the work done on the rake face in order to assess the total energy consumed. For the simple conditions where $\alpha = 0^{o}$.

$$\frac{dW_r}{dt} = F_T V \qquad (3.16)$$

W_r = work done at the rake face.

where V = velocity of chip

$V = U \tan\phi$

and, where there is no chip spread.

we have $$\frac{dW_r}{dt} = w\, L\, Kr\, U \tan\phi \qquad (3.17)$$

Thus, if all cutting conditions are held constant, including L, the length of contact on the rake face, the rate of doing work on the rake face is proportion to $\tan\phi$. The curve 2 in Figure 3.5 shows that $\frac{dW_r}{dt}$ increases with the shear plane angle and becomes very large as ϕ, approaches 90^{o}. The contact length L is one of the major variables in cutting, and its influence can be demonstrated by plotting a series of curves for different values of L. Curve 4 and 5 show the total rate of work done for values of L four and eight times that of curve 3.

So the consequence of increasing either the shear yield strength at the rake face, or the contact area (length) is to raise not only the feed force F_T but also the cutting force Fc. The contact area on the tool rake face in particular is seen to be a most important region, controlling the mechanics of cutting, and becomes a point of focus for research on machining [4].

3.5 Energy Considerations

When metal is cut in a two-dimensional cutting operation, the total energy consumed per unit time is

$$P = Fc\ U = \frac{F_s U \cos(\lambda - \alpha)}{\cos(\phi + \lambda - \alpha)} \tag{3.18}$$

Specific energy which is the energy consumed per unit volume of metal removed will therefore be

$$p = \frac{P}{Vwt_1} = \frac{F_c}{wt_1} \tag{3.19}$$

The specific energy consists of following components:

(1) As shear energy per unit volume (p_s)on the shear plane

(2) As friction energy per unit volume (p_F) on the tool face

(3) As surface energy per unit volume (p_A) due to the formation of new surface area in cutting

(4) As momentum energy per unit volume (p_M) due to the momentum change associated with the metal as it crosses the shear plane.

The Shear specific energy may be obtained as follows:

$$p_s = \frac{F_s V_s}{Uwt_1} \tag{3.20}$$

The friction specific energy may be similarly found

$$p_F = \frac{FV}{Uwt_1} = \frac{F_r}{wt_1} \tag{3.21}$$

When a new surface is generated in a solid substance, sufficient energy must be supplied to separate the ions at interface. A certain energy is thus associated with the formation of new surface and this is usually referred to as the surface energy of the substance (T). The surface specific energy in cutting will be

$$p_A = \frac{T2Uw}{Uwt_1} = \frac{2T}{t_1} \tag{3.22}$$

The quantity 2 in equation (3.22) comes from the fact that two surfaces are generated simultaneously when a cut is made. The value of T for most metal s is about 0.006 in lb. in^{-2} (1000 dyne cm^{-1}).

The resultant momentum force associated with the change in momentum of the metal as it crosses the shear plane will obviously be in the direction of slip or along the shear plane. This resultant momentum force (F_M) may, therefore, be obtained by applying the linear momentum law of applied mechanics along the shear plane:

$$F_m = \rho\ (U\ w\ t_1)[\ V\sin(\phi - \alpha) + U\cos\phi\ ] \tag{3.23}$$

where ρ is the mass density of the metal. Thus the momentum specific energy will be

$$p_M = \rho[V\sin(\phi - \alpha) + U\cos\phi\ ] \tag{3.24}$$

The magnitudes of these energy components may be compared, respectively [2].

p = 400,000 psi

p_s = 292,000 psi

p_F = 108,000 psi

p_A = 3.2 psi

p_M = 1.1 psi

It is evident from this example that p_A and p_M are negligible compared with p and that the sum of p_s and p_F is therefore equal to the total specific energy p. So it can be represented by

$$p = p_s + p_F \tag{3.25}$$

Practically all the energy associated with a cutting operation is consumed in either plastic deformation or friction, and essentially all of this ends up as thermal energy.

3.6 Thermal Energy In Metal-Cutting

The mechanical energy consumed in metal cutting is largely converted into heat at the zone of shear plane and friction area, as shown in Figure 3.6, and many of the economic and technical problems of machining are caused directly or indirectly by this heating action. The cost of metal removal, and may be reduced by increasing the cutting speed and /or the feed rate, but there are limits to the speed and feed rate above which the life of the tool is shortened excessively. The bulk of cutting, however, is carried out on steel and cast iron, and it is in the cutting of these, together with the nickel - based alloys, that the most serious technical and economic problems occur. With these higher melting point metals and alloys, the tools are heated to high temperatures as metal removal rate increase, and above certain critical speeds, the tools tend to collapse after a very short cutting time under the influence of stress and temperature.

Therefore, it is important to understand the factors which influence the generation of heat, the flow of heat and the temperature distribution in the tool and work material near tool edge. As early as in 1905, Nicolson[39] point out "there is little doubt that when

the laws of variation of the temperature of shaving and tool with different cutting angles, sizes and shapes of cut, and of the rate of abrasion... are definitely determined, it will be possible to indicate how a tool should be ground in order to meet with the best efficiency... the various conditions to be found in practice." However, determination of temperatures and temperature distribution in vitally important region near the cutting edge is technically difficult, and progress has been slow in the 90 years since the problem was clearly stated.

It causes the high temperatures of shear plane, tool face and relief surface. These temperatures are of importance for their influence on flow stresses, crater wear rate and rate of wear-land development, respectively.

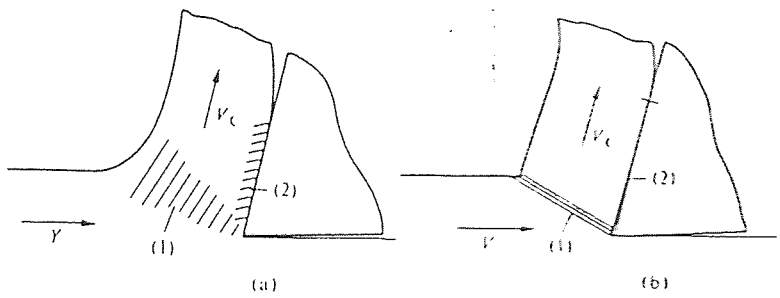

Figure 3.6 Heat heat source in Orthogonal Metal - Cutting
(a) Actual and (b) Idealized Heat Source

Of the total energy consumed in the cutting process, the maximum portion (about 80%) is consumed in the shear plane. The frictional loss at the rake face takes up to 18% and the frictional loss at flank face may account for 2% [39]. A small fraction of energy consumed in deformation is stored in the chip and the rest appears as heat.

Figure 3.7 shows that maximum heat is developed in the material which forms the chip and hence it is the hottest portion of metal in the machining process. Some heat from the chip may get conducted into the workpiece and into the tool through the chip-tool interface. The distribution of heat generated among tool, chip and workpiece may vary according to the condition of the process. [5].

Figure 3.7 also shows the temperature distribution in the workpiece and the chip of orthogonal metal cutting. Print X, which is moving towards the cutting tool,

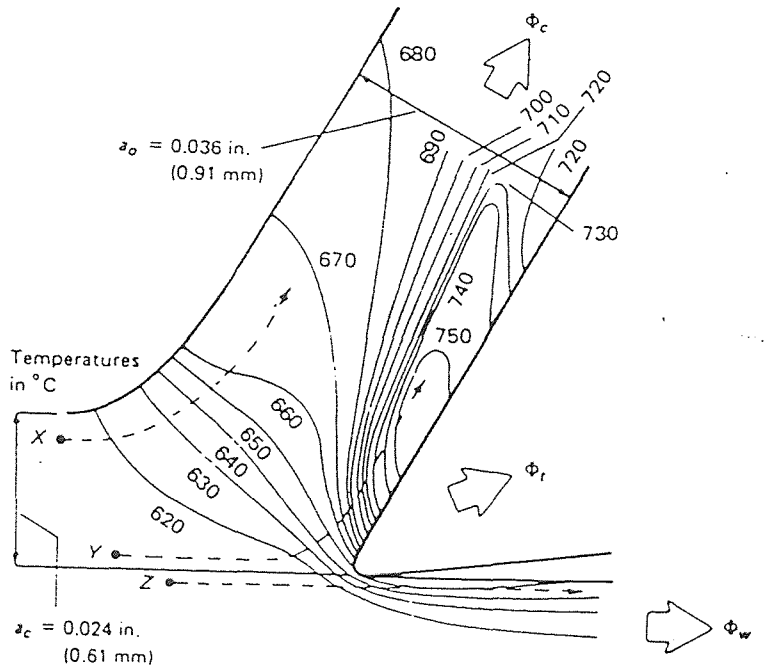

Figure 3.7 Temperature Distribution in Workpiece and Chips During Orthogonal Cutting (Obtained from an Infrared Photograph) [5]

approaches and passes through the primary deformation zone. It is heated until it leaves the zone and is carried away into the chip. Point Y, however, passes through both primary and secondary deformation zones, and it is heated until it has left the zone of secondary

deformation. It then cooled as the heat is conducted into the body of the chip, and eventually the chip achieves a uniform temperature throughout. Thus the maximum temperature occurs along the tool face some distance from the cutting edge. Point Z, which remains in the workpiece, is heated by the conduction of heat from the primary deformation zone. Some heat is conducted from the secondary deformation zone into the body of the tool. Thus the total rate of heat generation, P, can be expressed as [5]

$$P = \Phi_c + \Phi_w + \Phi_t \qquad (3.26)$$

where : Φ_c = rate of heat transportation by the chip

Φ_w = rate of heat conduction to the workpiece

Φ_t = rate of heat conduction to the tool

Because the chip material near the tool face is flowing rapidly, it has a much greater capacity for the removed of heat that the tool. For this reason, Φ_t usually forms a very small proportion of p and may be neglected except at very low cutting speed.

3.6.1 Heat in Chip Formation

The work done in (1) deforming the bar to form the chip, (2) moving the chip and freshly cut work surface over the tool, is nearly all converted into heat. Because of the very large amount of plastic strain, it is unlikely that 1% of the work done is stored as plastic energy, the remain 99% going to heat the chip, the tool and the work material.

Under most normal cutting conditions, the largest part of the work is done in forming the chip at the shear plane. In a simplified model of the action on the shear plane, the work material is heated instantaneously as it is sheared and all the heat is

carried away by the chip. Using this model, the temperature of chip increases according to the equation [25]

$$Tc = \frac{k\gamma}{J\rho C} \tag{3.27}$$

where Tc = temperature increase in chip body

k = shear flow stress

γ = shear strain

J = mechanical equivalent of heat

ρC = volume specific heat

A research estimate of the temperature increase in the body of the chip can be made using this simplified relationship for many conditions of cutting, particularly at relatively high speeds. The temperature of the chip can affect the performance of the tool only as long as the chip remains in contact; the heat remaining in the chip after it breaks contact is carried out of the system. Any small element of the body of the chip, after being heated in passing through the shear zone, is not further deformed and heated as it pass over the rake face, and the time required to pass over the area of contact is very short. For example, at a cutting speed of 50 m min^{-1} (150 ft/min), if the chip thickness ratio is 2, the chip velocity is 25 m min^{-1} (75 ft/ min). If the contact on the rake face (L) is 1 mm long, a small element of the chip will pass over this area in just over 2 milliseconds. Very little of the heat can be lost from the chip body in this short time interval by radiation or convection to the air, or by conduction into the tool.

Heat may also be lost from the body of the chip by conduction into the tool through the contact area. However, under many conditions of cutting, particularly at high rate of metal removal, the work done in overcoming the feed force, F_T, heats the flow zone at the under surface of the chip to a temperature higher than that of the body of the chip. Heat then tends to flow into the body of the chip from underneath, and no heat is lost from the body of the chip into the tool by conduction.

Some of the heat generated on the shear plane must be conducted into the work material, so it make the work material slightly higher temperature before being sheared to form the chip. If the shear zone was plane, extending from the cutting edge to the workpiece surface as is the idealized model, the heat conducted back into the workpiece would be insignificant unless the shear -plane angle were very small.

To sum up, most of the heat resulting from the work done on the shear plane to form the chip remains in the chip and is carried away with it, while a small but variable percentage is conducted into the workpiece and raises its temperature. This part of the work done in cutting makes a relatively unimportant contribution to the heating of the cutting tool.

3.6.2 Heat at the Tool/Work Interface

The heat generated at the tool/work interface is of major importance in relation to tool performance , and is particularly significant in limiting the rates of metal removal when cutting iron, steel and other metals and alloys of high melting point. The heat generated in this region is treated on the basis of classic friction theory or seizure theory.

It is necessary to study the pattern of strain in the flow-zone first, which constitutes the main heat source raising the tool temperature. With the help of photomicrographs of the quick-stop sections, we can obtain the information about the strain pattern in the flow-zone, and from this the thickness of the zone can be measured and a qualitative assessment made of its general character, Figure 3. shows a quick-stop section through the tool/chip interface of a low carbon steel cut by a 6° rake angle tool, the cutting speed is 153 m/min (500 ft/min) and the chip thickness ratio is 4:1. The body of the chip is therefore moving over the rake face at 38 m/min (125 ft ft/min), while, at the tool face, the two surfaces are not in relative movement. In general, values of shear strain (γ) on the shear plane are 2 to 4, and in the present example γ equals approximately 4. The flow-zone is, on the average, 0.025 mm (0.003 in.), thick over most of the seized contact which is 1.5 mm (0.06 in.) long. Shear in the flow-zone can be visualized by considering the change of shape of a unit cube 0.075 mm deep initially situation at the cutting edge on the rake face. When the top of this unit cube had moved to the position where the chip parted from the tool surface, a distance of 1.5 mm, it would have been subjected to a shear strain of 18 or four and one half times as great as the strain on the shear plane [2]. However, this is not the total extent of strain in the flow-zone. The bottom of the flow-zone still remains anchored to the tool surface, the material in that part very close to the tool surface continuous to be subjected to strain indefinitely, as the top of the original unit cube moves off on the underside of the chip when it leaves the tool. Thus the amounts of strain in the flow zone near the tool surface are very large indeed and cannot be estimated by the methods used for the shear plane.

The usual methods of measuring strain, such as making a grid on the surface and measuring its change of shape after deformation, are impossible to apply in such a small volume of metal subjected to such extremes of strain. It is clear, however, that the amounts of strain in the flow-zone are normally several orders of magnitude greater than on the shear strain plane. The ability of metals and alloys to withstand such enormous shear strains in the flow-zone without fracture, must be attributed to the very high compressive stresses in this region, which inhibit the initiation of cracks, and cause the re-welding of such small cracks as may be started or already existed in the working material before machining. One of examples is that the holes in highly porous powder metal components are often completely sealed on the under surface of the chip and on the machined surface where these areas have passed through the flow-zone. The compressive stress at the rake face decreases as the chip moves away from the cutting edge. When the compressive component of the stress contact inhibit the formation of cracks, the chip separates from the tool. Its under surface has being formed by fracture either at the tool surface or at points of weakness within the flow-zone.

A reasonably good estimate of total amount of heat generated at the tool-work interface can be made from the force and chip thickness measurements. For a zero rake angle tool the heat generated Q is

$$Q = \frac{F_T V_C}{J} \qquad (3.28)$$

The temperature of the body of the chip can be calculated with considerable accuracy, because there is little error involved in assuming even distribution of strain rate across the shear plane, and the neglecting heat losses during the short time interval involved.

However, this simplification is not possible in conduction of temperatures in the flow-zone for three reasons [2]:

1. Energy distribution in the flow-zone may be very non-uniform and the data from which to calculate it are unreliable because of the extremes of strain, strain rate, etc.
2. The thickness of the flow-zone, and the amount of metal passing through, are not accurately know.
3. The heat losses from the flow-zone may be large and difficult to calculate.

Many attempts have been made to calculate temperatures and temperature gradients on the rake face of the tool. Even for a two-dimensional section through a tool used for orthogonal cutting, there must be considerable doubt about the accuracy of the values of the temperature calculated. The temperature increase depends on the amount of work done on the quantity of metal passing through the flow-zone. The thickness of the flow-zone provides some measure of the latter, and the thinner the flow-zone the higher the temperature would be for the same amount of work done. The thickness varies considerably with the material being cut from more than 100 μm (0.004 in.) to less than 12 μm (0.0005 in.). It tends to be thicker at low speeds, but does not very greatly with the feed. In general the flow-zone is very thin compared with the body of the chip, it is commonly of the order of 5% of the chip thickness. Since the work done at the tool rake face is frequently about 20% of the work done on the shear plane, much high temperatures are found in the flow-zone than in the chip body, particularly at high cutting speed. The temperature in the heat flow-zone is influenced strongly by heat loss by conduction. The heat is generated in a very thin layer of the chip and with the tool. The temperature of

flow-zone is higher than that of the chip body. With the region moves away from cutting edge, the temperature of flow-zone is reduced by heat flows into the chip. After the chip leaves the tool surface, that part of the flow-zone, which passes off on the under surface of the chip, cools very rapidly to the temperature of the chip body, since cooling by metallic conduction is very efficient. The increase in temperatures of the chip body due to heat from the flow-zone is slight because of the relatively large volume of the chip body.

The conditions of heat transfer from the flow-zone into the tool are different from those at the flow-zone/chip body interface, because heat flows continuously into the same small volume of tool material. The tool acts as a heat sink into which heat flows from the flow-zone and a stable temperature gradients is build up within the tool. The amount of heat loss from the flow-zone into the tool depends on the thermal conductivity of the tool, the tool shape, and any cooling method used to lower its temperature. The heat flow into the tool from the flow-zone raises its temperature and this is the most important factor limiting the rate of metal removal when cutting the higher melting point metals [2]

3.6.3 Heat Flow at the Tool Clearance Face

Like the situation of heat transfer from flow-zone into rake face of tool, there may be heat generation between clearance face of tool and new cut surface. The clearance angle plays an important role to reduce the heat generation there, which must be large enough to ensure that the new surface is separated from the tool face and does not rub against it. Then the heat generated by deformation of the new surface is dissipated by conduction into the workpiece and has little heating effect on the tool.

The workpiece is a more rigid body than the chip, and the feed force cannot deflect it to maintain contact with the tool if a reasonable clearance angle of 5°-10° is used. But in some special cases, such as form tools or parting - off tools, such a large clearance angle would seriously weaken the tool or make it too expensive, and clearance angles as low as 1c are employed. With such small clearance angles there is a risk of creating a long contact path on the clearance face which becomes a third heat source, similar in character to the flow-zone on the rake face. Even with normal clearance angle, prolonged cutting results in "flank wear", in which a new surface is generate on the tool more or less parallel to the direction of cutting

3.6.4 Heat in the Absence of a Flow-Zone

There are two other conditions of heat sources affecting the tool temperatures, where the flow-zone is absent from the tool/work interface.

Where a build-up edge is formed there is usually a flow-zone but different in character and further from the tool surface, and is confined to a restricted region rather than spread out over the rake face. A different type of temperature distribution in the tool can be expected, with lower temperatures, and heat conducted into the tool only in a narrow region close to the tool edge. In most cases, the build-up edge which is formed when cutting speeds and other poly-phase materials, disappears as the cutting speed is raised, and is replaced by a flow-zone.

Where the conditions at tool/work interface are those of sliding conduct, the mode of heat generation is very different. The shearing of very small, isolated metallic junctions

provides numerous very short-lived temperature surges at the interface. This is likely to lead to a very different temperature pattern at the tool-work interface compared with that of the seized flow-zone. It seems probable that the mean temperatures will be lower, because a much smaller amount of work is required to shear the isolated junctions, but localized high temperatures could also occur at any part of the interface. There is likely to be more even temperature distribution over the contact area than under conditions of seizure. The direct effects of heat generated at sliding contact surfaces would have to be taken into consideration in a complete account of metal cutting.

CHAPTER 4

PRINCIPLES OF HEAT TRANSFER AND FINITE ELEMENT ANALYSIS OF THE MODEL

4.1 Principles of Heat Transfer for Modelling of New Cooling Device

The process of heat transfer is familiar to us all. On a cold day we put on more clothing to reduce heat transfer from our warm body to cold surroundings. When a hot object is placed in cold surroundings, it cools: the object loses internal energy, which the surroundings gain internal energy. The engineering discipline of heat transfer is concerned with methods of calculating rates of heat transfer. It is clear that heat transfer involves a great variety of physical phenomena and engineering systems. The phenomena must first be understood and quantified before a methodology for the thermal design of an engineering system can be developed. A common thermal design problem is the transfer of heat from one fluid to another. Devices for this purpose are called heat exchangers. In our cooling device, we will apply some basic formula of both heat conduction and heat convection. Though there exist thermal radiation, it is only a small portion compared with former two forms of heat transferred.

4.1.1 Heat Conduction

Analysis of heat transfer processes does require using some thermodynamics concepts. In particular, the first law of thermodynamics is used, generally in particularly of the principle of conservation of energy, which is a basic law of physics. In heat transfer, it is common practice to refer to the first law of as the energy conservation principle or simple as an

energy or heat balance when no work is done. A closed system containing a fixed mass of a solid is shown in Figure 4.1. The system has a volume (m^3), and the solid has a density ρ (kg/m^3). There is heat transfer into the system at a rate of $\dot{Q}$ (J/s or W),and heat may be generated within the solid at a rate of $\dot{Q}_v$ (W).The principle of conservation of energy requires that over a time interval Δt (s),

Change in internal energy within the system	=	Heat transferred into the system	+	Heat generated within the system

$$\Delta U = \dot{Q}\,\Delta t + \dot{Q}_v\,\Delta t \qquad (4.1)$$

Dividing by Δt and letting Δt go to zero gives

$$\frac{dU}{dt} = \dot{Q} + \dot{Q}_v$$

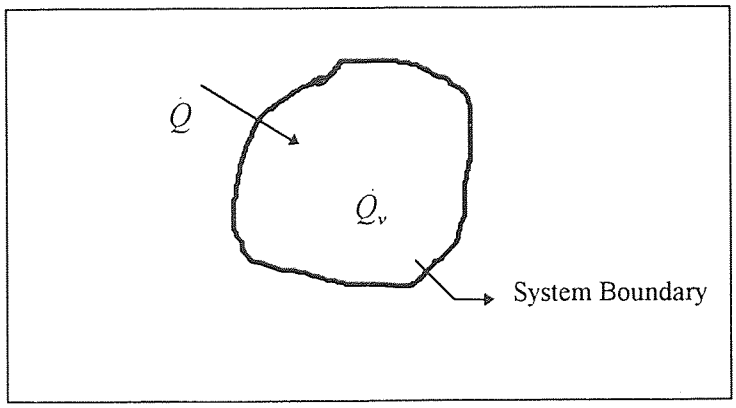

Figure 4.1 Application of the Energy Conservation Principle to a Closed System

The system contains a fixed mass (ρV); thus, we can write dU = ρVdu, where u is the specific internal energy (J/kg). For an incompressible solid, du = $C_v dT$, where C_v is the constant-volume specific heat (J/kgK), and T (K) is temperature. Since the solid has been

taken to be incompressible, the constant-volume and constant-pressure specific heat are equal, so we simply write du = cdT to obtain

$$\rho Vc\frac{dT}{dt} = \dot{Q} + \dot{Q}_v \qquad (4.2)$$

As early as in 1822, Fourier presented law of heat conduction: The conduction heat flux in a specified direction equals the negative of the product of the medium thermal conductivity and the temperature derivative in that direction. This law will be introduced here by considering the simple problem of one-dimensional heat flow across a plane wall — for example, a layer of insulation.

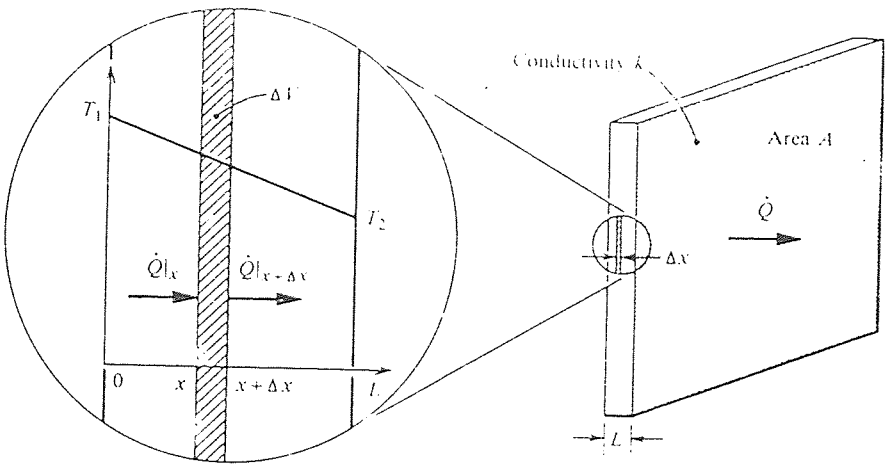

Figure 4.2 Steady One-Dimensional Conduction Across a Plane Wall [43]

Figure 4.2 shows a plane wall of surface area A and thickness L, with its face at x = 0 maintained at temperature T_1 and the face at x = L maintained at T_2. The heat flow $\dot{Q}$ through the wall is in the direction of decreasing temperature. In Cartesian coordinates,

with temperature varying in the x direction only,

$$\frac{\dot{Q}}{A} = q \qquad \text{and} \qquad q = -k\frac{dT}{dx} \tag{4.3}$$

where q is the heat flux, or heat flow per unit area perpendicular to the flow direction (W/m^2), k is the thermal conductivity of the substance and, by inspection of the equation, must have units (W/mK), T is the local temperature (K or $^{\circ}C$), and x is the coordinate in the flow direction (m).

In cylindrical or spherical coordinates, with temperature varying in the r direction only,

$$q = -k\frac{dT}{dr} \tag{4.4}$$

Figure 4.2 shows an elemental volume ΔV located between x and x+Δx; ΔV is a closed system, and the energy conversation principle in the form of equation 4.2 applies. If we consider a steady state, then temperatures are unchanging in time and $\frac{dT}{dt} = 0$; also, if there is no heat generated within the volume, $\dot{Q}_v = 0$. Then equation states that net heat flow into the system is zero. Since heat is flowing into ΔV across the face at x, and out of ΔV across the face at x+Δx,

$$\dot{Q}\big|_x = \dot{Q}\big|_{x=\Delta x} \qquad \text{or} \qquad \dot{Q} = \text{constant} \tag{4.5}$$

But from Fourier's law,

$$\dot{Q} = qA = -kA\frac{dT}{dx} \tag{4.6}$$

rearrange the variables

$$\frac{\dot{Q}}{A}\int_0^L dx = -\int_{T_1}^{T_2} k\,dT \tag{4.7}$$

$$\dot{Q} = \frac{kA}{L}(T_1 - T_2) = \frac{T_1 - T_2}{L/kA} \tag{4.8}$$

If we have a composite wall of two slabs of materials, as shown in Figure 4.3, the heat flow through each layer is the same:

$$\dot{Q} = \frac{T_1 - T_2}{L_A/k_A A} = \frac{T_2 - T_3}{L_B/k_B A} \tag{4.9}$$

or

$$\dot{Q} = \frac{T_1 - T_3}{L_A/k_A A + L_B/k_B A} = \frac{T_1 - T_2}{R_A + R_B} \tag{4.10}$$

where $R \equiv L/kA$ can be viewed as a thermal resistance analogous to electrical resistance.

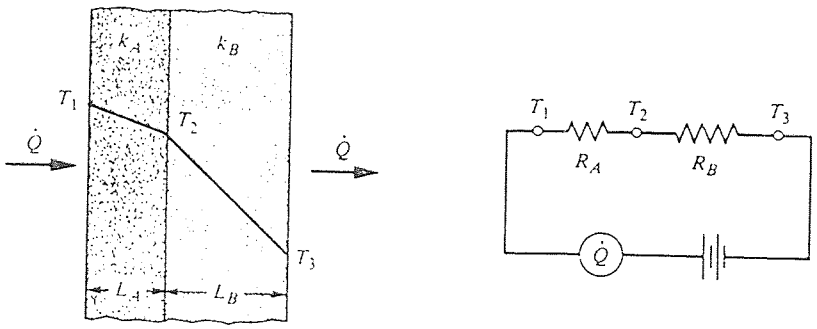

Figure 4.3 The Temperature Distribution for Steady Conduction Acorss a Composite Plane Wall and the Corresponding Thermal Circuit [43]

Steady one-dimensional conduction in cylinders or spheres requires that temperature be a function of only the radial coordinate r. In the case of a cylindrical or spherical shell, the area for heat flow changes in the direction of heat flow. For a cylindrical shell of length L, the area for heat flow is A = 2 πrL. A increases with increasing r. If the inner radius is

r_1 and outer radius is r_2, their corresponding temperature are T_1 and T_2, respectively, and if there is no heat generated within the body and $\dot{Q}_v = 0$. The energy conservation principle requires that the heat flow across the face at r equal to that at face $r + \Delta r$

$$\dot{Q}|_r = \dot{Q}|_{r+\Delta r} \tag{4.11}$$

this is,

$\dot{Q}$ = Constant, independent of r

Using Fourier's law in the form of equation (4.4),

$$\dot{Q} = Aq = 2\pi rL(-k\frac{dT}{dr}) \tag{4.12}$$

Dividing by 2πkL and assuming that the conductivity k is independent of temperature gives

$$\frac{\dot{Q}}{2\pi kL} = -r\frac{dT}{dr} = Cons\tan t = C_1 \tag{4.13}$$

which is a first-order ordinary differential equation for T(r) and can be integrated easily:

$$\frac{dT}{dr} = \frac{C_1}{r} \tag{4.14}$$

combined with two boundary conditions of temperature T_1 and T_2, we can easily find the constant C, which is

$$C_1 = \frac{T_1 - T_2}{\ln(r_2/r_1)} \tag{4.15}$$

$$C_2 = T_1 + \frac{T_1 - T_2}{\ln(r_2/r_1)}\ln r_1 \tag{4.16}$$

substituting back in equation (4.14) and rearranging gives the temperature distribution, we finally obtain the heat flow

$$\dot{Q} = \frac{2\pi kL(T_1 - T_2)}{\ln(r_2/r_1)} \tag{4.17}$$

Equation 4.17 is again in the form of Ohm's law, and the thermal resistance of the cylindrical shell is

$$R = \frac{\ln(r_2/r_1)}{2\pi kL} \tag{4.18}$$

when $r_2 = r_1 + \delta$ and $\delta/r_1 << 1$, equation 4.18 reduces to the resistance of a slab, $\delta/2\pi r_1 kL = \delta/kL$.

4.1.2 Contact Resistance

If heat conduction through a composite wall which is perfectly contacted, as shown in Figure 4.4, two mathematical surfaces, the u- and s- surfaces, are located on each side of and infinitely close to the real interface, we know from the law of energy conversation,

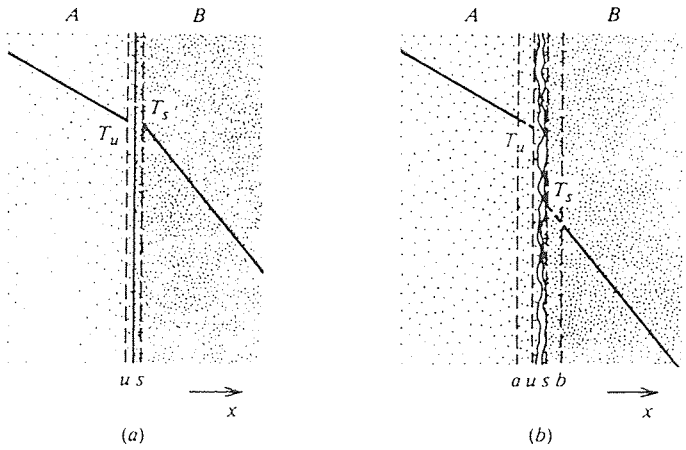

Figure 4.4 Interfaces Between Two Layers of a Composite Wall
(a) Smooth Surfaces (b) Rough Surfaces [43]

$$\dot{Q}|_u = \dot{Q}|_s \qquad \text{or} \qquad -k_A \frac{dT}{dx}|_u = -k_B \frac{dT}{dx}|_s \tag{4.19}$$

Also, since the distance between the u- and s- surface is negligible, we have $T_u = T_s$. However, the two contacted surfaces are not perfectly contacted due to degree of roughness of each surface in realistic situation. The solid materials are in contact at relatively few places, and the gaps may contain a fluid or, in some applications, a vacuum. The heat flow in the interface region is complicated: the condition is three-dimensional as the heat tends to "squeeze" through the contact areas, and there are parallel paths of conduction and radiation through the gaps. The u- and s- surface are located just on either side of a somewhat arbitrarily defined interface location. In addition, a- and b- surfaces are located just far enough from the interfaces for the heat conduction to be one-dimensional. No temperature profile is shown between the a- and b- surfaces since no unique profile T(x) exists there; instead, the temperature profiles are extrapolated from the bulk materials to the interface as shown, thereby defining the temperatures and temperature gradients at the u- and s- surfaces. As was the case for the perfectly smooth surfaces, the first law requires

$$-k_A \frac{dT}{dx}|_u == -k_B \frac{dT}{dx}|_s \tag{4.20}$$

but now there is no continuity of temperature at the interface; that is, $T_u \neq T_s$. The thermal resistance to heat flow at the interface is called the contact resistance and is usually expressed in the term of an interfacial conductance h_i (W/m^2K), defined in an analogous manner to Newton's law of cooling, namely,

$$\dot{Q} = h_i A(T_u - T_s) \tag{4.21}$$

or $$-k_A \frac{dT}{dx}\Big|_u = h_i(T_u - T_s) = -k_B \frac{dT}{dx}\Big|_s \qquad (4.22)$$

4.1.3 Heat Convection

Convection or convective heat transfer is the term used to describe heat transfer from a surface to a moving fluid, as shown in Figure 4.5. The surface may be the inside of a pipe, outside of a pipe, or the skin of a hypersonic aircraft. The flow may be forced, as in the case of liquid pumped through the pipe; or be natural (or free), as in the case of a natural-draft cooling tower. Both forced and natural flows can be either laminar or turbulent. Flow in a pipe becomes turbulent when the dimensionless group called Reynolds Number, $\mathrm{Re}_D = VD/\upsilon$, exceeds about 2300, where υ is he velocity (m/s), D is the pipe diameter (m), and υ is the kinematic viscosity of the fluid (m^2/s). Heat transfer rates tends to be much higher in turbulent flows than in laminar slows, owing to the vigorous mixing of the fluid.

In an internal forced flow, the rate of heat transfer is approximately proportional to the difference between the bulk temperature T_s and averaged fluid temperature called the bulk temperature T_b . The constant of proportionality is called the convective heat transfer coefficient h_c:

$$q_s = h_c \Delta T \qquad (4.23)$$

where $\Delta T = T_s - T_b$, q_s is the heat flux from the surface of pipe into the fluid (W/m^2), and h_c has units ($\mathrm{W}/m^2\mathrm{K}$). Equation 4.23 is called Newton's law of cooling but is a definition of h_c rather than a true physical law.

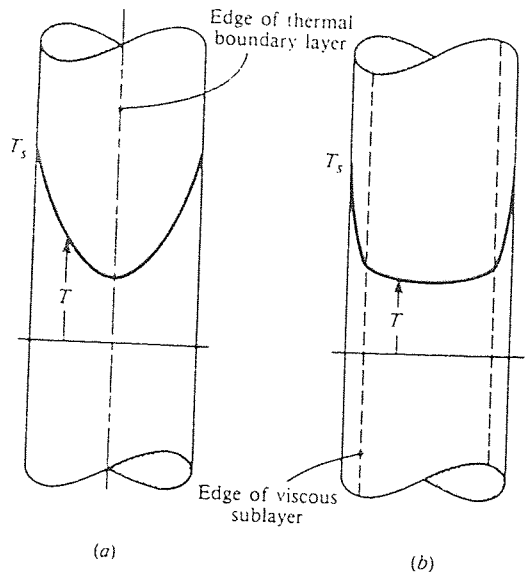

Figure 4.5 Temperature Profiles for Laminar and Turbulent Flow in a Tube
(a) Laminar Flow (b) Turbulent Flow [43]

4.1.4 Dimensional Analysis

Experimental data for convective heat transfer coefficients, as well as the results of analysis, can be conveniently and concisely organized as relationship between dimensionless groups of the pertinent variables. The Reynolds number mentioned above is example of such groups. Momentum transfer to a wall is made dimensionless as the Skin Friction Coefficient C_f :

$$C_f = \frac{\tau_s}{(1/2)\rho V^2} \tag{4.24}$$

where $\tau_s (N/m^2)$ is the wall shear stress. In pipe flows, the pressure gradient is made dimensionless as friction factor, f:

$$f = \frac{\Delta P / L}{(1/2)\rho V^2 / D} \tag{4.25}$$

where $\Delta\rho$ (N/m^2) is the pressure drop over a length L of a pipe with diameter D. This friction is called the Darcy factor. If the flow in the pipe is hydrodynamically fully developed, that is, if the velocity profile is unchanged with axial position, then f and C_f are simply related as

$$f = 4\ C_f \tag{4.26}$$

Nusselt number, Nu, is another dimensionless group of convective heat transfer

$$Nu = \frac{h_c L}{k} \tag{4.27}$$

where the characteristic length L may be the distance along a flat plate, the diameter of a cylinder in cross-flow, or pipe diameter for flow in a pipe, h_c is the convective heat transfer coefficient, k is the thermal conductivity.

Prandtl number, Pr, is the third group that fluid properties affect heat transport in the fluid

$$\Pr = \frac{C_p \mu}{k} = \frac{\nu}{k/lC_p} = \frac{\nu}{\alpha} \tag{4.28}$$

where μ is dynamic viscosity, C_p is the fluid specific heat, ν is the kinematic viscosity, α is the thermal diffusivity. So actually the Prandtl number is the ratio of Momentum diffusivity to thermal diffusivity. It will be seen that the convective heat transfer characteristic of a fluid are very much dependent on its Prandtl number.

Stanton number, $St = \frac{h_c}{\rho C_p V} = \frac{h_c}{C_p G}$, is an alternative dimensional heat transfer coefficient and is related to the Nusselt number as

$$St = NU/Re\ Pr \tag{4.29}$$

mass velocity G = $\dot{m}/A_c$, where $\dot{m}$ is the mass flow rate and A_c is the cross-sectional area for flow.

4.1.5 Forced Flow in Tubes and Ducts

For laminar flow sufficiently far from the entrance of a tube or pipe, where the flow is hydrodynamically fully developed and has the characteristic parabolic velocity profile of Poiseuille flow, some simple analytical results are available. The friction factor has a constant value

$$f = \frac{64}{\mathrm{Re}_D} \qquad (4.30)$$

$$\mathrm{Re}_D = \frac{GD}{\mu} \qquad (4.31)$$

Where D is the tube diameter and G is the mass velocity . Note the use of the subscript D to indicate that the characteristic length in the Reynolds number is the tube diameter. If the wall temperature is uniform, for example, if steam is condensing on the outside of tube wall, then sufficiently far downstream of where heat starts, the flow becomes thermally fully developed, the shape of the temperature profile is unchanging, and the Nusselt number has a constant value

$$\mathrm{Re}_D = 3.66 \qquad (4.32)$$

If, on the other hand, the heat flux through the tube wall is uniform, for example, if the tube is round with an electrical resistance wire at constant pitch, then

$$Nu_D = \frac{48}{11} = 4.364 \qquad (4.33)$$

Transition to turbulent tube place at $\mathrm{Re}_D \approx 2300$, although the turbulent becomes fully established only for $\mathrm{Re}_D > 10{,}000$. For hydrodynamically fully developed flow, the friction factor can be obtained from a Moody chart or, for a smooth wall, from Petukhov's formula [46]:

$$f = (0.790 \ln \mathrm{Re}_d - 1.64)^{-2} \quad ; \quad 10^4 < \mathrm{Re}_D < 5 \times 10^6 \qquad (4.34)$$

In contrast to laminar flow, the effect of wall boundary condition is unimportant for turbulent flow of all fluid except low-Prandtl number liquid metals. For thermally fully developed flow in a smooth tube with Pr > 0.5, a simple power law formula is

$$Nu_D = 0.023 \, \mathrm{Re}_D{}^{0.8} \, \mathrm{Pr}^{0.4} \qquad \mathrm{Re}_D > 10{,}000 \quad ; \quad \mathrm{Pr} > 0.5 \qquad (4.35)$$

If more accurate results are desired, Gnielinski's formula is recommended [47]

$$Nu_D = \frac{(f/8)(\mathrm{Re}_D - 1000)\mathrm{Pr}}{1 + 12.7(f/8)^{1/2}\left(\mathrm{Pr}^{2/3} - 1\right)} \qquad 3000 < \mathrm{Re}_D < 10^6 \; ; \; \mathrm{Pr} > 0 \qquad (4.36)$$

4.1.6 Heat Exchanger

When the temperature of a fluid changes as it flows through a passage, it causes the heat transfer between the passage walls and the fluid. This is the situation which we encounter in our thermal analysis of tool holder. Mills [43] define that a heat exchanger is a device that facilitates transfer of heat from one fluid stream to another. So our device is not an exact heat exchanger according to Mills definition of heat exchanger, because we only use water, one fluid, to remove the heat from tool holder, which is not a fluid. That is why we call it a cooling device. One important classification of heat exchanger is into single-stream exchanger and two-stream exchangers. A single-stream exchanger is one in which the

temperature of only one stream changes in the exchanger; a two-stream exchanger is one in which the temperature of both streams change in the exchanger. A sketch of the expected fluid temperature variations along the exchanger is shown in Figure 4.6.

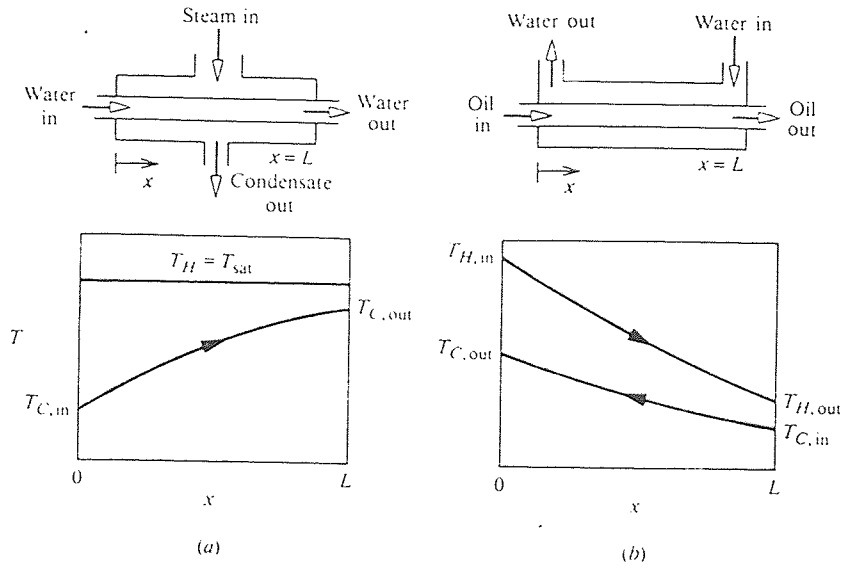

Figure 4.6 Temperature Variations Along Heat Exchanger [43]

4.1.7 Analysis of a Condenser

In a simple single-tube condenser, pure saturated vapor enters the shell at the top and condenses on a horizontal tube. The condensate forms a thin film on the outside of the tube, drops off the bottom, and leaves the shell through a drain. The vapor condenses at the saturation temperature corresponding to the pressure in the shell. Hence, the condensate film surface temperature is constant. The enthalpy of condensation is transferred by conduction across the thin condensate film, by conduction across the tube

wall, and by convection into the coolant. As a result, the coolant temperature rises as it gains energy flowing along the tube.

An energy balance on the exchanger as a whole is formulated by writing down the steady-flow energy equation for a control volume enclosing the exchanger. If the exchanger is well insulated, there is no heat loss to the surroundings, the enthalpy inflow equal the enthalpy outflow:

$$\dot{m}_H\, h_{H,in} + \dot{m}_c\, h_{c,in} = \dot{m}_H\, h_{H,out} + \dot{m}_c\, h_{c,out} \tag{4.37}$$

where h is specific enthalpy (J/kg) and subscripts "in" and "out" denote inlet and outlet values, respectively. Rearranging gives

$$\dot{m}_c\left(h_{c,out} - h_{c,in}\right) = \dot{m}_H\left(h_{H,in} - h_{H,out}\right) = \dot{Q} \tag{4.38}$$

where $\dot{Q}$ is quantity of heat exchanged in the process.

To determine the variation of coolant temperature along the exchanger, we make an energy balance on a differential element of the exchanger Δx as the independent variable and T_c as the dependent variable. When the steady-flow energy equation is applied to the control volume of length Δx, the contribution to $\dot{Q}$ due to x-direction conduction in the coolant is small and can be neglected. Thus, the coolant flow rate times its enthalpy increase must equal the heat transfer across the tube wall:

$$\dot{m}_c\, c_{pC}\left(T_C\big|_{x+\Delta x} - T_C\big|_x\right) = UP\Delta x\left(T_{sat} - T_C\right) \tag{4.39}$$

and letting $\Delta x \rightarrow 0$, gives

$$\dot{m}_C\, c_{pC}\left(\frac{T_C\big|_{x+\Delta x} - T_C|x}{\Delta x}\right) = UP\left(T_{sat} - T_C\right) \tag{4.40}$$

Rearranging,

$$\frac{dT_C}{dx} - \frac{UP}{\dot{m}_C c_{pC}}\left(T_{sat} - T_C\right) = 0 \tag{4.41}$$

this equation is a first-order ordinary differential equation for $T_C(x)$; it requires one boundary condition, which is

$$\text{x} = 0: \; T_C = T_{C,in} \tag{4.42}$$

To integrate equation 4.41, let $\theta = T_{sat} - T_C$; then $dT_c/dx = -d\vartheta/dx$; and the equation becomes

$$\frac{d\theta}{dx} + \frac{UP}{\dot{m}_C c_{pC}}\theta = 0 \tag{4.43}$$

if U is assumed constant along the exchanger, the solution is

$$\theta = Ae^{-\left(UP/\dot{m}_C c_{pC}\right)x} \tag{4.44}$$

where A is the integration constant., Substituting for θ and using the boundary condition

$$T_{sat} - T_C = Ae^0 = A \tag{4.45}$$

Thus the solution of equation 4.41 is

$$T_{sat} - T_C = \left(T_{sat} - T_{C,in}\right)e^{-\left(UP/\dot{m}_C c_{pC}\right)x} \tag{4.46}$$

which is the desired related $T_C(x)$, showing an exponential variation along the exchanger. Of particular interest is the coolant outlet temperature $T_{C,out}$ which is obtained by letting x = L, the length of the exchanger, in equation 4.46 :

$$T_{sat} - T_{C,out} = \left(T_{sat} - T_{C,in}\right)e^{-\left(UPL/\dot{m}_C c_{pC}\right)} \tag{4.47}$$

the product of primeter and length PL is the area of the heat transfer surface. The exponent in equation 4.47 is dimensionless, since a watt is a joule per second. This dimensionless group is called the number of transfer units, with abbreviation NTU of the symbol N_{tu}. The NTU can be viewed as a measure of the heat transfer "size" of the exchanger.

For the forced turbulent flow in a pipe, when the pipe wall temperature is constant, and assumption of the flow is hydrodynamically fully developed at the commencement of cooling, we can use the above formula to obtain the average heat transfer coefficient. The tube is essentially a single-stream heat exchanger with the number of transfer unit N_{tu}. It is good practice to calculate N_{tu} and think in term of its value. If $N_{tu} << 1$, $T_{b,out} \approx T_{b,in}$; if N_{tu} >3 or 4, $T_{b,out} \approx T_s$.

4.2 Finite Element Analysis for the Model of Metal Cutting

The problem considered is the two dimensional steady state calculation of the temperature distribution in the tool and tool holder and chip and work material. Heat is generated by plastic flow in the chip and by friction between the chip and the tool. Heat transfer within the tool and tool holder is by conduction and convection.

4.2.1 The Governing Equation of the Model

Heat generation has been localised, in a common approximation [1,2], to the surfaces S_{q1} and S_{q2} of Figure 4.7. On Sq1, the primary shear plane , the internal specific work rate q_1 is kU_1, where k is the shear flow stress of the chip and U_1 is the velocity change

from the work to the chip. On the S_{q2}, the friction specific work rate q_2 is τU_c, where τ is the friction stress and U_c is the chip sliding speed. To this approximation, in which there is no volume heat generation, the governing equation in each of the three regions I, II and III of Figure 4.7 is, using standard notation.

$$k\left(\frac{\partial^2 T}{\partial x^2}+\frac{\partial^2 T}{\partial y^2}\right) - \rho\, c\left(U_x \frac{\partial T}{\partial x} + U_y \frac{\partial T}{\partial y}\right) = 0 \qquad (4.48)$$

Where: k is the thermal conductivity

T is the temperature

ρ is the mass density

c is the specific heat

and U_x and U_y are the components of the velocity in directions x and y, subject to the boundary conditions

(I) $T = T_s$ on surfaces S_T

(ii) $-k\frac{\partial T}{\partial n} = 0$ on surfaces S_{q_0}

(iii) $-\left(k\frac{\partial T}{\partial n}\right)_I - \left(k\frac{\partial T}{\partial n}\right)_{II} = q_1$ on surface S_{q1}

(iv) $-\left(k\frac{\partial T}{\partial n}\right)_{II} - \left(k\frac{\partial T}{\partial n}\right)_{III} = q_2$ on surface S_{q2}

(v) $-\left(k\frac{\partial T}{\partial n}\right) = h\,(T - To)$ on surface S_h

or $T = T_h$ constant wall temperature of tool holder

where n is the direction normal to S_{q_0}, S_{q1}, or S_{q2} and S_h as appropriate and To is the ambient temperature.

Boundary condition (v) contains the wet cutting conditions which already studied by Childs et al. [40], convective cooling from the tool and tool holder with heat transfer coefficient h. In practice, convective cooling also takes place from the surfaces of the chip and work material. However, this has been ignored (boundary condition (ii)) in the interests of reduced numerical computation. The speeds of the chip and material results in little influence of cooling of the chip and workpiece on the tool temperature, the examination of being the main purpose of the present work. finally, in the present work T_s and T_o have been taken to be equal with an ambient value of 10 °C and K, ρC, and h have been assumed to be independent of temperature.

It has been shown by Hiroaka and Tanaka that solving equation (4.48) subject to the boundary conditions (4.49) is equivalent to minimizing the functional I(T) defined as

$$I(T) = \int_A \frac{K}{2} \left[\left(\frac{\partial T}{\partial x} \right)^2 + \left(\frac{\partial T}{\partial y} \right)^2 \right] dA + \int_A \rho c \left(U_x \frac{\partial \bar{T}}{\partial x} + U_y \frac{\partial \bar{T}}{\partial y} \right) T \, dA$$

$$+ \int_{S_q} q T \, dS + \int_{S_h} h \left(T^2/2 - T T_o \right) dS \qquad (4.50)$$

where A and S indicate area and surface integrals, respectively, and the temperature gradients $\frac{\partial T}{\partial x}$ and $\frac{\partial T}{\partial y}$ are variationally invariant. This is the basis of the finite element formulation already used in Stevenson et al [41]. The development for a mesh of the global thermal stiffness matrix

$$[H]\{T\} + \{F\} = 0 \qquad (4.51)$$

is summarized in the following. Equation (4.51) has been solved by Crout decomposition for fixed values of K and ρC, but for a range of values of h from 0 to 10^5 W $m^{-2}K^{-1}$.

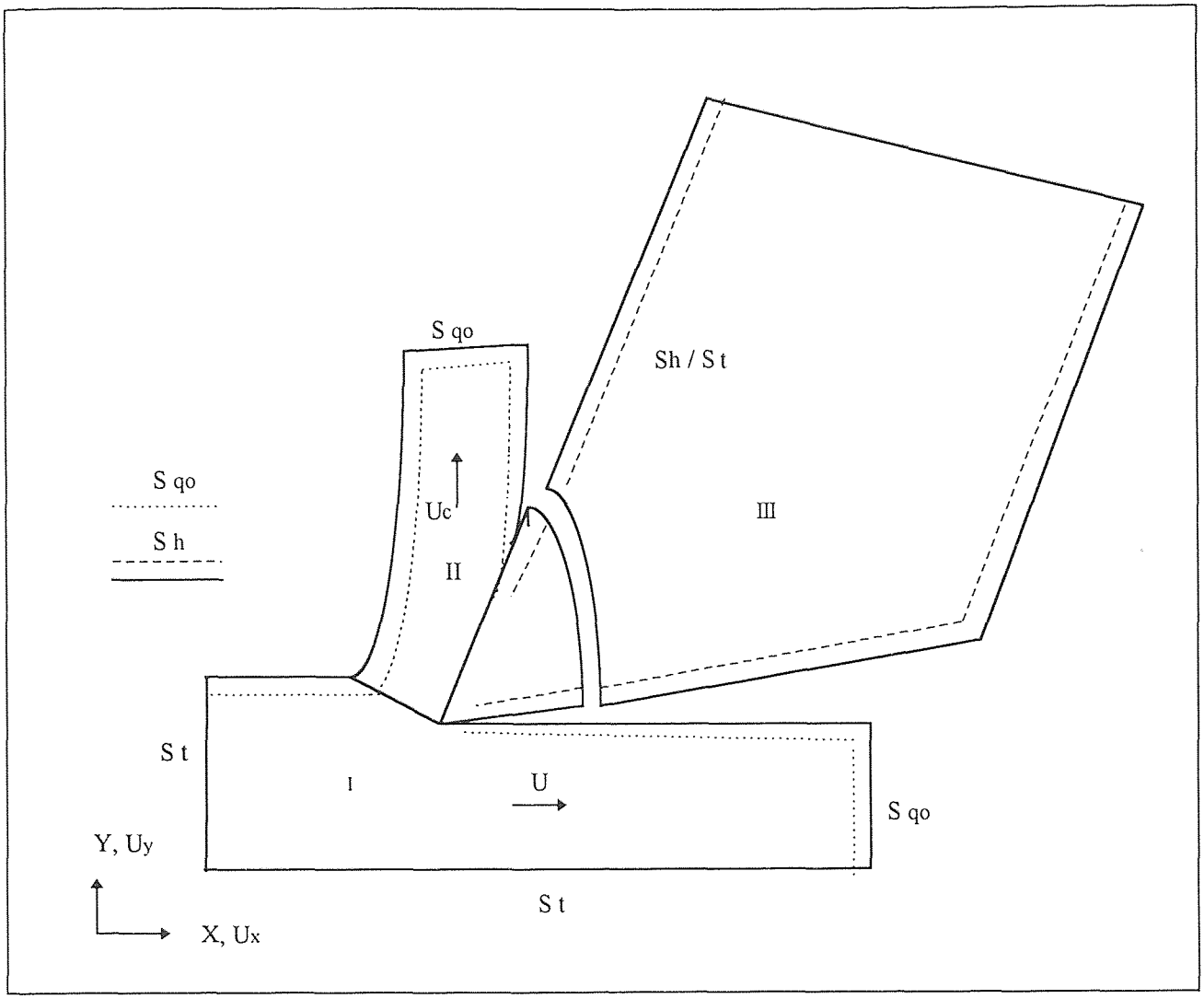

Figure 4.7 Model Structure

4.2.2 Matrix of Finite Element Analysis

The finite element method approximates the temperature distribution and, hence, also the functional I(T) (equation (4.49)) to a function of the temperatures t_i at the nodes of the

mesh. If there are N nodes, the temperatures are found by solving the N equations

$$\frac{\partial I(T)}{\partial T_i} = 0 \tag{4.52}$$

where I = 1 to N. The value of I(T) is evaluated and differentiated, element by element, with respect to nodal temperatures. Inspection of equation (4.50) shows I(T) to be composed of four parts: area integrals relating to conduction and convection and surface integrals related to heat generation and surface heat transfer. For convenience the contribution I^e to I(T) from one element e may be written, in the same order as equation (4.50),

$$I^e = I_k^e + I_u^e + I_q^e + I_h^e \tag{4.53}$$

The differentiation of I^e with respect to its nodal temperatures leads to three equations which in matrix notation may be written

$$\left\{\partial I / \partial T_i\right\}^e = [H]_k^e \{T_i\} + [H]_u^e \{T_i\} + [H]_h^e \{T_i\} + \{F\}_q^e + \{F\}_h^e \tag{4.54}$$

where H and F are coefficients to be determined and the subscripts k, u, q, and h, as in equation 4.53, refer to each of the integrals in equation 4.50 in order. The setting to zero, as dictated by equation 4.52, of the sum over all elements of equation 4.54 gives equation 4.51.

It is noted in passing that expressions for heat generation required, in addition to the temperature, to evaluate I^e have already been given ($q_1 = kU$, $q_2 = \tau U_c$). Values for u_x and u_y are also required: in the present application

$$\left.\begin{aligned} &u_x = U,\ u_y = 0 \quad in\ region\ I \\ &u_x = U_c \sin\alpha,\ u_y = U_c \cos\alpha \quad in\ region\ II \\ &u_x = u_y = 0 \qquad in\ region\ III \end{aligned}\right\} \tag{4.55}$$

where α is rake angle.

1. Conduction Term

From equation 4.50

$$I_k^e = \int_A \frac{K}{2}\left[\left(\frac{\partial T}{\partial x}\right)^2 + \left(\frac{\partial T}{\partial y}\right)^2\right] dA \tag{4.56}$$

If the temperature is interpolated to vary linearly in the element, the gradients $\partial T/\partial x$ *and* $\partial T/\partial y$ are constants over the area of integration and equation 4.56 becomes

$$I_k^e = \frac{KA}{2}\left[\left(\frac{\partial T}{\partial x}\right)^2 + \left(\frac{\partial T}{\partial y}\right)^2\right] \tag{4.57}$$

where A is the area of element e.

Differentiation of equation 4.57 with respect to the nodal temperatures gives

$$\frac{\partial I_k^e}{\partial T_i} = KA\left[\frac{\partial T}{\partial x}\frac{\partial}{\partial T_i}\left(\frac{\partial T}{\partial x}\right) + \frac{\partial T}{\partial y}\frac{\partial}{\partial T_i}\left(\frac{\partial T}{\partial y}\right)\right] \tag{4.58}$$

A mesh element with nodes i,j,k and nodal positions and temperatures (x, y, and T)$_{i,j,k}$ is used. It is a standard result of finite element analysis which may be checked by substitution that a linear interpolation of the temperature T within the element is

$$T = \left[\left(a_i + b_i x + c_i y\right)T_i + \left(a_j + b_j x + c_j y\right)T_j + \left(a_k + b_k x + c_k y\right)T_k\right] / 2A \qquad (4.59)$$

where A is the area of the element and

$$\left.\begin{aligned} a_i &= x_j y_k - x_k y_j \\ b_i &= y_j - y_k \\ c_i &= x_k - x_j \end{aligned}\right\} \qquad (4.60)$$

with similar expressions for a_j, b_j, c_j *and* a_k, b_k, c_k .

Differentiation of equation 5.59 gives

$$\left.\begin{aligned} \partial T/\partial y &= \left(c_i T_i + c_j T_j + c_k T_k\right)/2A \\ \partial T/\partial x &= \left(b_i T_i + b_j T_j + b_k T_k\right)/2A \end{aligned}\right\} \qquad (4.61)$$

the variation of these gradients with respect to nodal temperatures is

$$\left.\begin{aligned} \frac{\partial}{\partial T_i}\left(\frac{\partial T}{\partial x}\right) &= \frac{b_i}{2A} \\ \frac{\partial}{\partial T_i}\left(\frac{\partial T}{\partial y}\right) &= \frac{c_i}{2A} \end{aligned}\right\} \qquad (4.62)$$

substitution of equation 4.61 and 4.62 into equation 4.58 leads to

$$\left\{\frac{\partial I_k}{\partial T_i}\right\}^e = \frac{K}{4A}\begin{bmatrix} b_i b_i + c_i c_i & b_j b_i + c_j c_i & b_k b_i + c_k c_i \\ b_i b_j + c_i c_j & b_j b_j + c_j c_j & b_k b_j + c_k c_j \\ b_i b_k + c_i c_k & b_j b_k + c_j c_k & b_k b_k + c_k c_k \end{bmatrix}\begin{Bmatrix} T_i \\ T_j \\ T_k \end{Bmatrix} \qquad (4.63)$$

which is the term $[H]_k^e \{T_i\}$ of equation 4.54.

2. Convection Term

Similarly, from equation 4.50

$$\frac{\partial I_u^e}{\partial T_i} = \rho C\left(u_x \frac{\partial T}{\partial x} + u_y \frac{\partial T}{\partial y}\right)\int_A \frac{\partial T}{\partial T_i} dA \tag{4.64}$$

$\partial T/\partial T_i$ is obtained from equation 4.59. It may be shown that

$$\int_A \frac{\partial T}{\partial T_i} dA = \frac{(2A)^2}{6} \tag{4.65}$$

Substitution of equation 5.61 and 5.65 into equation 5.64 leads to

$$\left\{\frac{\partial I_u}{\partial T_i}\right\}^e = \frac{\rho C}{6}\begin{bmatrix} u_x b_i + u_y c_i & u_x b_j + u_y c_j & u_x b_k + u_y c_k \\ u_x b_i + u_y c_i & u_x b_j + u_y c_j & u_x b_j + u_y c_k \\ u_x b_i + u_y c_i & u_x b_j + u_y c_j & u_x b_k + u_y c_k \end{bmatrix}\begin{Bmatrix} T_i \\ T_j \\ T_k \end{Bmatrix} \tag{4.66}$$

which is the term $[H]_u^e\{T_i\}$ of equation 4.54.

3. Heat Generation Term

Two elements e_1 and e_2 with a common surface ij of length l and of type S_q are considered. Of the total heat flux q generated on S_q, $-q_{e1}$ flows into e_1 and $-q_{e2}$ flows into e_2. The temperature of S_q at a distance s from node i is

$$T = T_i + \left(T_j - T_i\right)(s/l) \tag{4.67}$$

For element e_1, from equation 4.50

$$\frac{\partial I_q}{\partial T_i} = -q_{e1}\int_S \frac{\partial T}{\partial T_i} dS \tag{4.68}$$

Differentiating equation 4.67 with respect to T_i, substituting in equation 4.68, and integrating leads to

$$\left\{\frac{\partial I_q}{\partial T_i}\right\}^e = -q_{e1}\frac{l}{2}\begin{Bmatrix} l \\ l \\ 0 \end{Bmatrix} \tag{4.69}$$

which is the term $\{F\}_q^e$ of equation 4.54. A similar expression is obtained for element e_2, but with q_{e2} substituted for q_{e1}. Although the division of heat between the two elements is not known, summing the contributions of $\{F\}_q^{e1}$ *and* $\{F\}_q^{e2}$ combines q_{e1} and q_{e2} to give the known flux q in the global matrix equation 4.51.

4. Surface Heat Transfer Term

An element for which the surface between nodes I and j is of type S_h is considered as following. the temperature variation along S_h is again given by equation 4.67. From equation 4.50

$$\frac{\partial I_h^e}{\partial T_i} = h\int_S (T - T_o)\frac{\partial T}{\partial T_i}dS \tag{4.70}$$

Substitution of equation 4.67 and expressions for $\partial T/\partial T_i$ into equation 4.70 and integrating leads to

$$\left\{\frac{\partial I_h}{\partial T_i}\right\}^e = \frac{hl}{6}\begin{bmatrix} 2 & 1 & 0 \\ 1 & 2 & 0 \\ 0 & 0 & 0 \end{bmatrix}\begin{Bmatrix} T_i \\ T_j \\ T_k \end{Bmatrix} - \frac{hlT_o}{2}\begin{Bmatrix} 1 \\ 1 \\ 0 \end{Bmatrix} \tag{4.71}$$

which are the terms $[H]_h^e\{T_i\} + \{F\}_h^e$ of equation 4.71.

CHAPTER 5

CASE STUDIES

5.1 Description of the New Cooling Device

From chapter 3 we learn that heat is generated by converting the mechanical energy consumed in metallic deformation; and how the heat transfers among three parts of metal-cutting: workpiece, chip and tool; the heat flows into the tool from the flow-zone raises its temperature. From chapter 1 we learn that tool temperature lowers not only the tool life but also the machining accuracy. In order to lower the tool temperature, it is introduced the coolant. Though coolant do carry away some heat from tool and improve the finish surface of machined parts in some cases, it causes some severe environmental problems and human healthy problems. So many suggestions for clean and environmental safe cooling systems are proposed. Some of systems discussed in chapter 2 represent part of this practice. However, few of the exist cooling systems can realize the objective of both eliminating the toxic coolant and keeping the cutting area clean in the heavy duty practical use.

Billatos and Hanley [16] proposed "A Novel Cooling System" as shown in figure 5.1, which use cool air from a single phase open air cycle cooling system to cool the tool. The system uses air from surroundings, cools it and then channels the cool air through a heat exchanger around the tool. This thesis research change the cooling agent from air to water for the reason of higher coefficient of heat transfer of water than that of air. the research consider the cooling device in more detail, and also give a thermal analysis for the

device. The new cooling device is illustrated in figure 5.3. A portion of the heat generated is conducted from tool-work interface to the tool tip (inset), the into the tool holder and consequently removed by combined conduction and convection using a coolant (water) flowing in a closed cooling cycle system (see Figure 5.4). The closed system uses water at the room temperature to absorb heat. Water is flowed into a heat exchanger consisted of a coiled copper tube or duct around the tool holder. The outlet water is collected into a small cooling tower and recycled again into the system with high pressure. In the system, the pump is used to maintain the system in a desired high pressure, the filter is used to keep the recycling water from foreign particles. The pumping energy and pressure can be varied by using an adjustable valve to control the amount of heat convective coefficient and heat transferred from the tool.

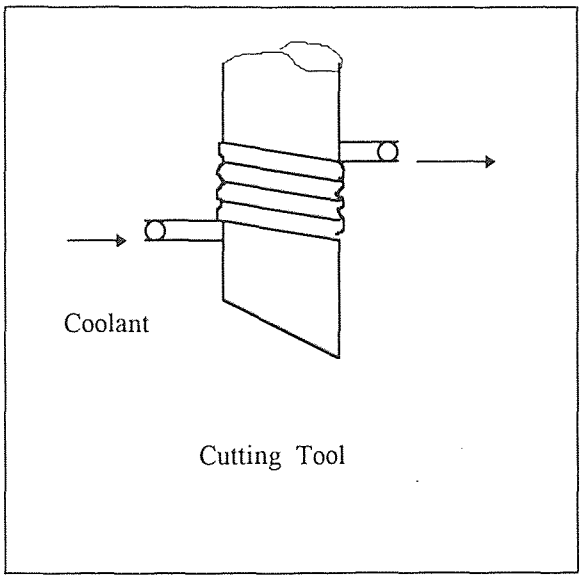

Figure 5.1 Schematic of Cutting Tool

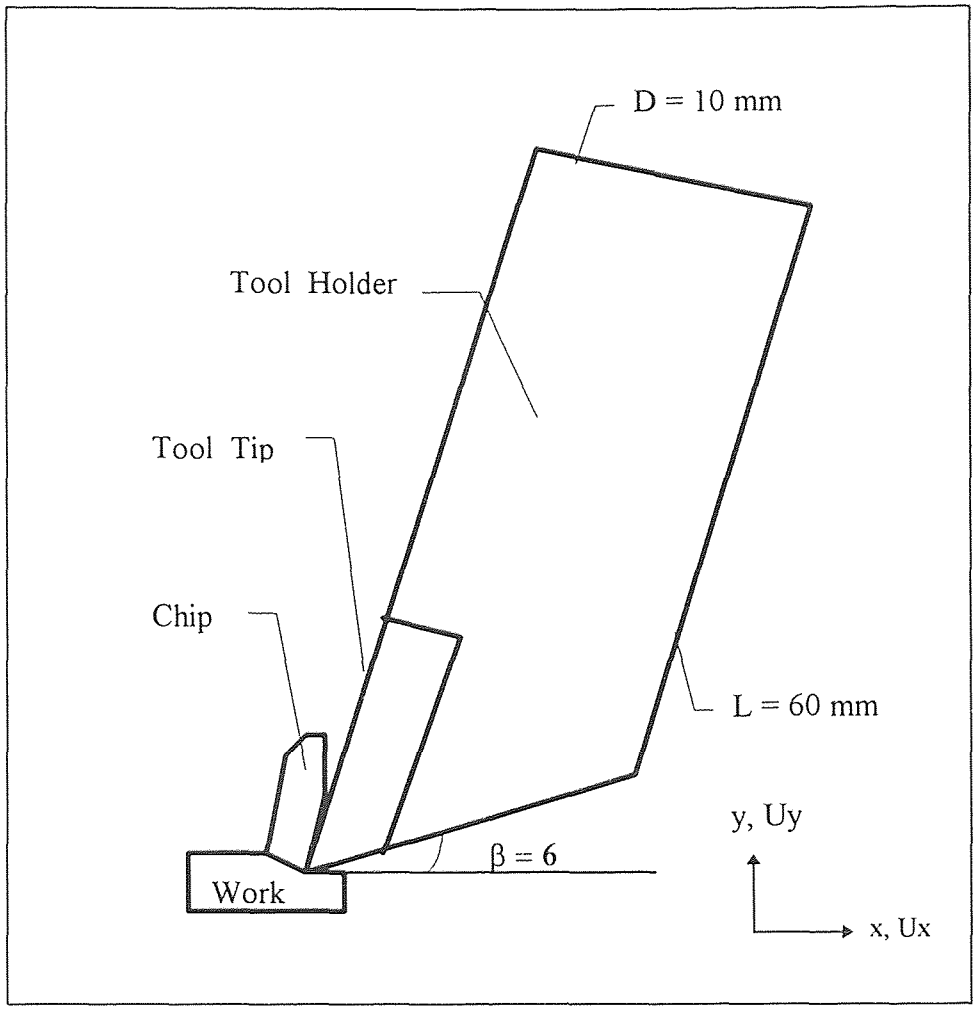

Figure 5.2 Geometry and Dimensions of Cutting Tool

The key component in the system is the cooling device, which must be specially designed to fix the tool holder and obtain the high coefficient of heat transfer. Since most of tool holders using in metal cutting operations have four sharp corners of rectangular shape, the coiled copper tube cannot effectively contact with tool holder, copper is chosen due to its highest heat conduction coefficient.

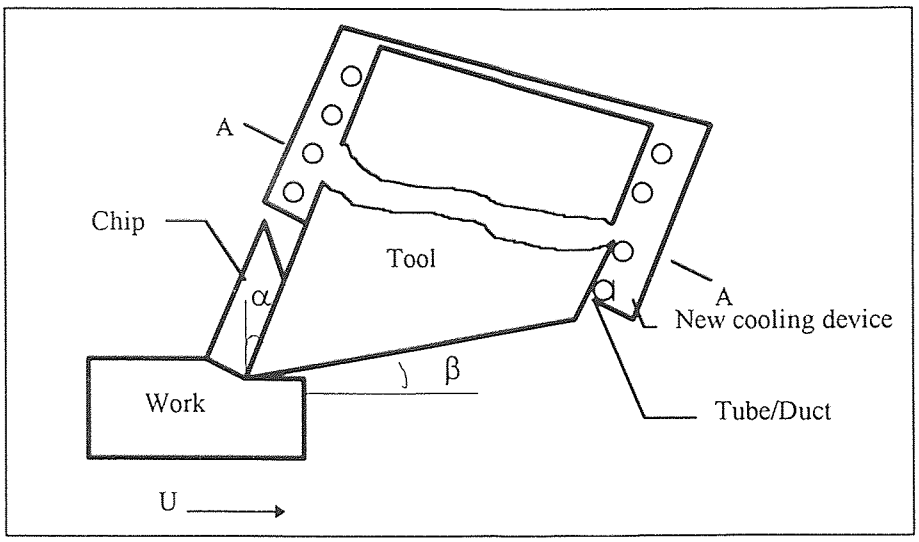

Figure 5.3 New Cooling Device

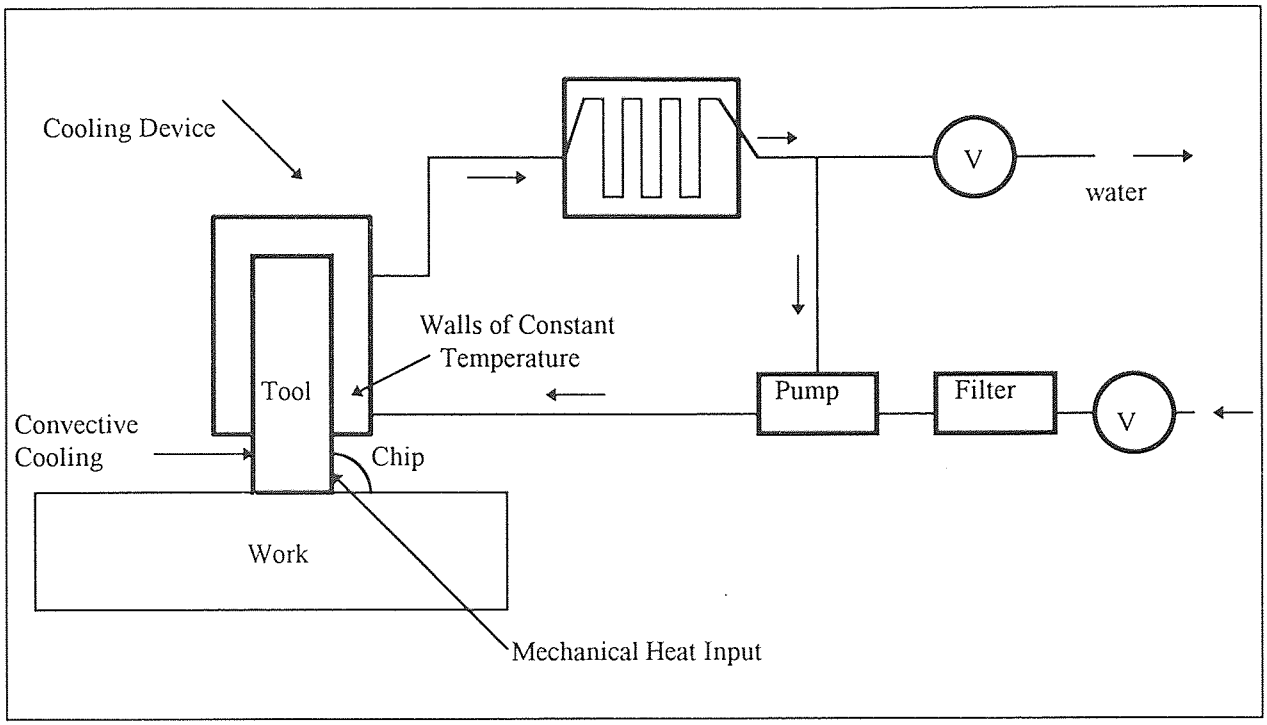

Figure 5.4 System of New Cooling Device

5.2 Calculation of Heat Transfer for the Device

5.2.1 Calculation of Coiled Copper Pipe

Furthermore, we have to consider the possibility and convenience of cooling device installation on the tool holder. In order to achieve these objectives, we can re-design the tool holder as a shape of shank with certain tamper angle, and with a slot along the length of it for guide the direction of cooling device tightly hook up with it and keep excellent contact. Therefore, we let the radius of tool holder be R_1, Let the inner wall of heat-exchanger be ΔL thick, and its outer radius is R_2. The inner and outer diameters of copper tube are D_1 and D_2, respectively. The effective length of heat-exchanger is L.

If the assumption of the quantity of heat exchange from tool holder to cooling device is Q, it is ready to calculate the rate of heat flux through the contact wall of cooling device and further to calculate the temperature difference between two side of the wall by using heat conduction equation A.3 and A.4. Following the same token, it is easy to obtain the temperature of inside surface of cooling device by using the same equation. The heat exchange on the inside surface of the coiling copper pipe, however, is the different from above, now it is the convective heat transfer for cold water to remove the heat from the wall and carry it to the cooling tower. In order to calculate the convective heat transfer coefficient, it must be first to know the rate of fluid flow in the pipe, the inner diameter of the pipe, the velocity of mass flow; then it has to calculate its Reynolds number Re_D , and then to check the material property table to obtain the Prandtl number Pr; after then it is ready to choose a suitable empirical equation to calculate the Nusselt number Nu which matches the range of Re_D and Pr. Once the Nu is obtained, the

convective heat transfer coefficient hc can be obtained by using the Nu definition formula (equation A.27) where L and k are known. At the last step, we can simply use the equation A.23 to calculate the temperature difference between inside surface of pipe and cold water (bulk flow) along the length of pipe. The dimension of new cooling device is given as follows:

L: The effective length of tool holder	L = 60 mm
R_1: The radium of tool holder	R_1= 5 mm
R_2 : The radium of inner wall of cooling device	R_2 = 7 mm
ΔL: the thickness of inner wall of cooling device	ΔL = 2 mm

If Maximum heat-exchange rate is 1.5 kW, we can calculate the temperature difference between two side of inner wall of cooling device by rearranging the equation A.17, where k is heat conduction coefficient of copper and k = 350 W/mK

$$\Delta T = T1 - T2 = \dot{Q} \times \ln(R2/R1)/(2 \times \pi \times k \times L) \qquad (5.1)$$

$$= 3.8\ ^{\circ}C$$

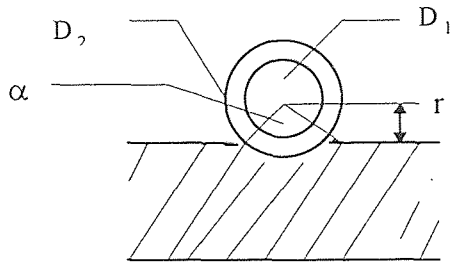

Figure 5.5 Contact Area of Copper Coiled Tube

The size of copper pipe is inside diameter D_1 = 8 mm and outside diameter D_2 = 10 mm, which coil around the inner wall of cooling device. In order to increase the contact area between tube and inner wall. Let copper tube be buried as Figure 5.5 shown

where $$\cos \alpha = \frac{r}{D_2/2} \tag{5.2}$$

$$= 4/5 = 0.8$$

so, $$\alpha = \arccos 0.8$$

$$= 36.86° = 0.643$$

The arc length of AB :

$$R_{ab} = \alpha \times R \tag{5.3}$$

$$= 0.643 \times 5 = 3.21 \text{ mm}$$

The number of cycles around internal wall is:

$$n = L/D_2 \tag{5.4}$$

$$= 60/10 = 6$$

So, the contacted area is

$$A_{out} = n \times (R_{ab} \times \pi \times D_2) \tag{5.5}$$

$$= 8.47 \times 10^{-4} \text{ m}^2$$

$$A_{in} = n \times (\pi \times D_1) \times \pi \times D' \tag{5.6}$$

$$= 6 \times \pi \times 8 \times \pi \times 22$$

$$= 0.01 \text{ m}^2$$

$$A = (A_{out} + A_{in})/2 \tag{5.7}$$

$$= 5.63 \times 10^{-3} \text{ m}^2$$

$$T_2 = \dot{Q} \times \Delta L_3 / (k \times A_{tube}) \qquad (5.8)$$

$$= 1.5\ ^{\circ}C$$

So, the differences of temperature for heat exchanger inner wall and copper coiling pipe are 3.8 °C and 1.5 °C, respectively. The total temperature drop is 5.3 °C.

If water discharge rate: $\dot{m} = 5$ kg/min,

$t_{in} = 20\ ^{\circ}C$

then:

Prandtl number	$P_r = 7.0$
Thermal conductivity	$k = 0.601$ w/m.k
Density	$\rho = 998\ kg/m^3$
Specific heat at constant pressure	$C_p = 4180$ J/kg.k
Kinematic velocity	$\upsilon = 0.98 \times 10^{-6}\ m^2/s$
Diameter	$D_1 = 0.008$ m

For fully developed flow

Discharge rate $\dot{m} = \rho\, v \pi\, d^2 / 4 \qquad (5.9)$

$$V = \dot{m} / (\rho\, \pi\, d^2 / 4)$$

$$= 5/ (998 \times 60 \times \pi \times (0.008/2)^2)$$

$$= 1.66 \text{ m/s}$$

Reynolds number

$$Re_d = d \times V/\upsilon$$

$$= 1356$$

To calculate the flow friction factor (f) for fully developed turbulent flow for a smooth circular tube, it should choose the equation A.34 as follows:

$$f = (0.79 \ln Re_d - 1.64)^{-2} \qquad 10000 < Re_d < 5\times10^6 \qquad (A.34)$$

then we can obtain f = 0.02895

Also, to get Nusselt number by using equation 4.36:

$$\overline{Nu_d} = (f/g) (Re_d - 1000) Pr / (1 + 12.7 \times (f/g)^{1/2} * (Pr^{2/3}-1)) \qquad (A.36)$$

$$3000 < Re_d < 10^6$$

So, $\overline{Nu_d} = 104.95$

and since $Nu = h d / k$ (A.27)

Then: $h = \overline{Nu_d}\ k / d = 7884.7\ w/m^2\ k$

For the heat convection

$$\dot{Q} = h \times A_{tube}\ \Delta T \qquad (A.6)$$

$$A_{tube} = n \times (\pi \times d) \times (\pi \times D')$$

where : D' is the mean diameter of tube coiling , (see Figure 6.6)

D_1 is the inner diameter of tube

so, $A_{tube} = 6 \times \pi^2 \times 0.008 \times 0.022$

$= 0.0104\ m^2$

$\Delta T = \dot{Q} / (h A_{tube})$

$= 18.25\ °C$

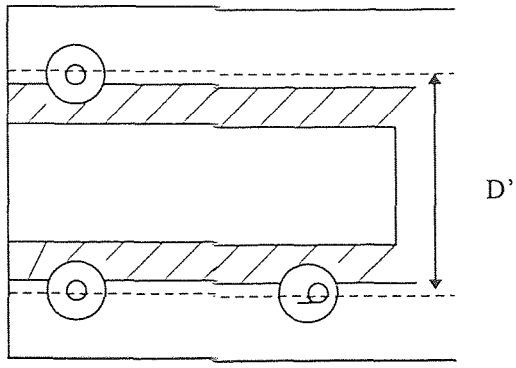

Figure 5.6 Section A-A of New Device:
Copper Tube Partially Burred Within Inner Wall of the Device

To calculate the temperature increase of water, the following equation can be used:

$$\dot{Q} = \dot{m}\, C_p\, \Delta T \qquad (5.10)$$

$$\Delta T_{water} = \dot{Q} / (\dot{m}\, C_p)$$

$$= 1500 \times 60 / (5 \times 4180) = 4.3\ ^\circ C$$

This means that difference of temperature of water from into to out of tube is only 4.3 °C,

Above calculation of heat-exchanger capacity shows that even when the heat flux increase up to 1.5 kW. (In our example conditions, the heat flux is less than 1.2 kW). the heat-exchanger still can remove the heat from tool high efficiently (average difference of temperature is 18.25 °C).

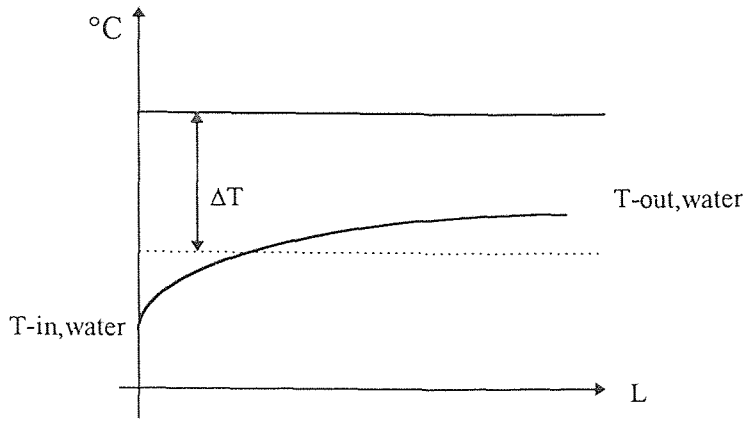

Figure 5.7 Temperature Difference Between Tube and Water Along Running Distance

5.2.2 Calculation of Coiled Copper Duct

The other one design of heat-exchanger use the duct instead of tube for some practical reason, such as use copper cast part in commercial stages. It is shown as Figure 5.8 . The dimension of duct is 2 × 4 mm. There are 10 duct circles around the internal wall of heat exchanger.

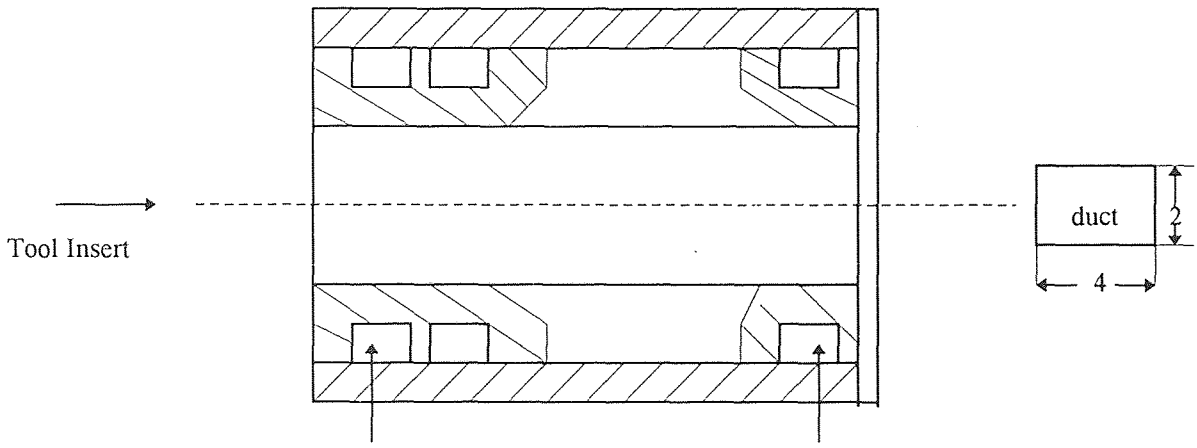

Figure 5.8 Water Running Along Coiled Duct to Remove the Heat from Cutting Tool

The Hydraulic Diameter of the duct is determined by following equation:

$$Dh = 4 * A / P \qquad (5.11)$$

where :

A = cross area

P = wetted perimeter

Dh = 16/6 = 2.67 mm

Fellow the same procedures as calculation of copper tube, we can obtain:

V = 10.44 m/s

$\overline{Re_{Dh}} = 284.44$

f = 0.02394

$\overline{N_{uDh}} = 36.287$

$\overline{h'} = 8168$ w/m^2 k

$A_{duct} = 0.004523$ m^2 (contacted Area)

$\Delta T_{duct} = 1500 / (8168 * 0.004523) = 40.6$ °C

(average difference of temperature between wall and water)

$\Delta T_{d,water} = 1500 * 60/ (5 * 4180) = 4.3$ °C

Comparison results of copper tube and duct, we find that coiling copper tube gives higher capacity because it need lower temperature difference (18.25 °C) to remove the same heat flux (1.5 kW), however, the duct needs much higher temperature difference (40.6 °C).

5.3 Cutting Conditions

It is observed by Childs et al experiment at three different cutting speeds (33, 46 and 61 m/min) turning a 0.43% carbon steel workpiece with BT42 grade high speed steel (HSS). In our finite element analysis model, It is assumed that cutting edge is sharp and there is no build-up edges attached cutting edge. The experimental evidence for the values of work rates q_1 and q_2 required in the calculations are recorded. The thermal constants used in the calculations are given in Table 5.1. The thermal conductivity data for BT42 HSS of 22 W $m^{-1}K^{-1}$ is an estimate from the values of other tungsten HSS with or without cobalt [42].

Table 5.1 Thermal properties used in present calculations

Material	Work & Chip (0.43%C Steel)	Tool Tip or Insert (HSS)	Tool Holder (low carbon steel)
Specific heat ρC MJm^{-3}	4.3	4.3	4.3
Thermal conductivity (at T=400(c))	43.6 w/m.k	22.0 w/m.k	45.0 w/m.k

The full extents of the chip models, but, for reasons of size, only a small part of the work and tool models are shown in Figure 5.1. The geometry and dimensions of the cutting tool

of our model is showed in Figure 5.2. The effective length of tool holder L is about 60 mm and its diameter is about 10 mm. The rectangular outline in the tool, surrounding the cutting edge, defines the boundary of the HSS tip; the remainder is the low carbon steel tool holder. In the calculations, the interface between tool and tool holder has been assumed to have zero thermal resistance.

The experiment of cutting conditions are given as follows: Turning process on a lathe using a water based coolant subject to the tool side rake angle and clearance angle were 14° and 6° , respectively. The feed rate was 0.254 mm rev^{-1} and depth of cut was 2.54 mm. The cutting speeds of 33, 46, and 61 m min^{-1} covered the range from the onset of cratering almost to thermal collapse of these tools [40]. The chip geometry and cutting force related data required for the temperature calculations obtained from quick stop and force measurement tests subsidiary to the main wear tests and the microstructural and microhardness changes observed in both the quick stop and main wear test tools which enable estimates to be made of tool temperature distributions.

The general friction stress distributions are shown in Figure 5.9. Experiment results of quick stop sections of the chips formed at cutting speeds of 33, 46, and 61 m min^{-1}, after 57 m cut distance are shown in Figure 6.10 . Added to each section to the same scale is a scanning electron micrograph of the tool face that formed the chip. It has been possible to match the estimated and measured friction forces by assigning a friction stress near the cutting edge of 410, 440, and 420 MN m^{-2} to the cutting tests at 33, 46, and 61 m min^{-1}, respectively. The cutting and thrust forces measured and friction forces from stress distributions on Figure 5.10 are given in Table 5.2. The Table 5.2 also gives

the values of shear angles ϕ and shear stress k on the primary shear plane, obtained from the measured forces and ϕ. Finally, in the Table 5.2 are also given the values of U_1 and U_c obtained from the tests and used with τ and k in the temperature calculations.

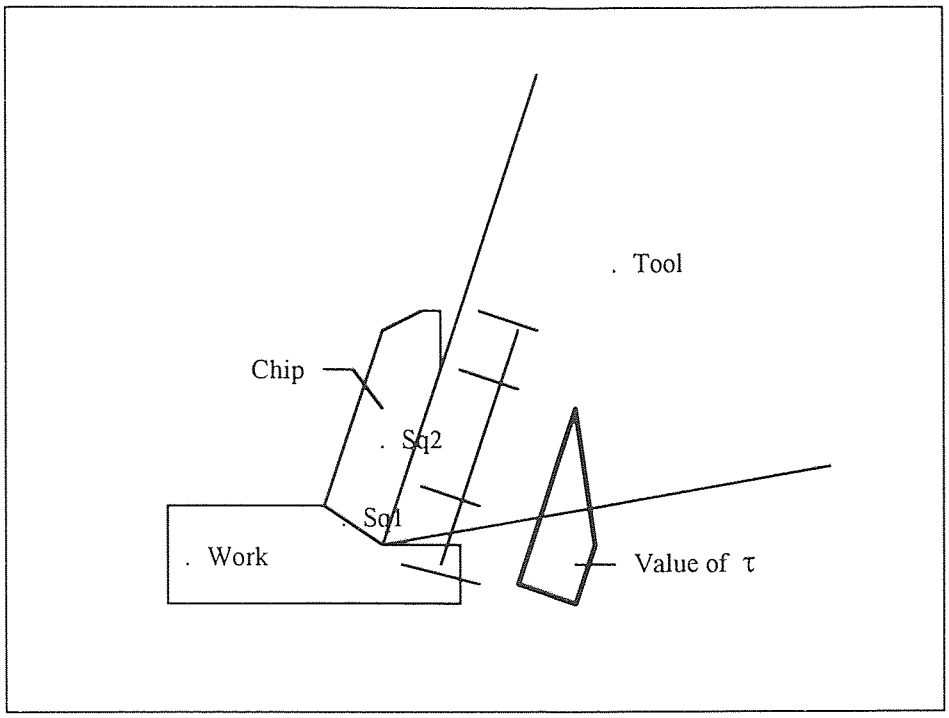

Figure 5.9 Friction Stress Distribution

5.3 Determination of Heat Transfer Coefficient

There is no direct experimental information in the metal machining literature on heat transfer coefficients from the cutting tool and holder to the coolant. Two geometric conditions present themselves:

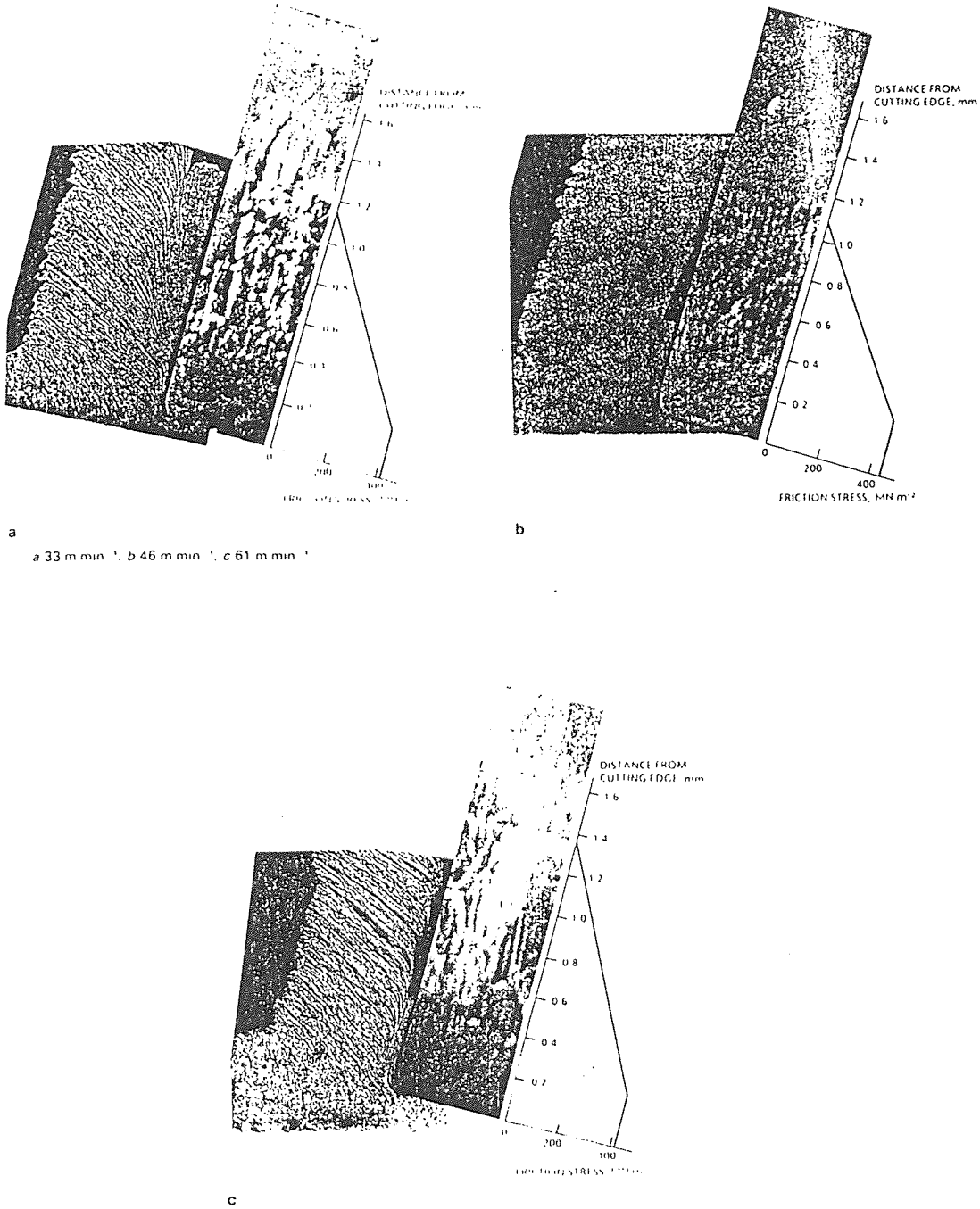

a 33 m min $^{-1}$, *b* 46 m min $^{-1}$, *c* 61 m min $^{-1}$

Figure 5.10 Data of Friction Stress Obtained by Experiment [40]

(I) cooling from the tool holder sufficiently remote from the cutting edge that coolant has unimpeded access to the surface to be cooled.

(II) cooling from the flank surfaces of the tool so close to the cutting edge that access of coolant may be severely restricted by the proximity of the work material.

The finite element calculations presented by Childs et al [40] demonstrate that, in the absence of cooling in the conditions considered , temperatures above 200 °C are generated in large regions of the tool remote from the cutting edge; close to the cutting edge, free surface temperature up to 900°C are estimated. Therefore, film boiling conditions must be considered. [43]

A recent review of water cooling for continuous casting is relevant to cooling of the tool holder remote from cutting edge. The immersion of steels in water has been found to give a reduction in heat transfer coefficients from $2\times10^{4}\,Wm^{-2}K^{-1}$ at 300°C to $2\times10^{3}\,Wm^{-2}\,K^{-1}$ at 700°C. In spray cooling conditions, the water spray intensity is important. At spray intensities of $\geq$ 1500 l $m^{-2}\,\min^{-1}$, the heat transfer coefficient is reduced from 2×10^{4} to $8\times10^{3}\,Wm^{-2}K^{-1}$ as surface temperature increases from 300 to 700°C. A reduction of the spray intensity to 70 l $m^{-2}\,\min^{-1}$ reduces the heat transfer coefficient over the same temperature range to 5×10^{3} to $10^{3}\,Wm^{-2}K^{-1}$.

Thus, the best estimates in the absence of direct experimental measurements of heat transfer coefficients from a cooled cutting tool are in the range $10^{3}-10^{4}\,Wm^{-2}K^{-1}$ (this levels of transfer greatly exceed effects resulting from radiation, estimated at up to 100 W $m^{-2}K^{-1}$).

Although, it is believed, measurements of heat transfer in metal cutting have not been made previously, heat transfer coefficient values could have been found if previous measurements of temperature gradients in cutting tips [4] had been combined with temperature analysis. This is the approach taken in the present work.

5.5 Case Studies

Table 5.2 Data of Three Cutting Conditions

Cutting Speed m/min	Cutting Force Fc, N	Thrust Force Ft, N	Friction From Fc, From Ft	Force, N From Measuring	Shear plane Angle ϕ,deg	Shear stress k, MN/m2	Chip speed U1	m/min Uc
33	1100+/-100	600+/-100	650+/-50	640	27+/-1	58-+/-90	36	16
46	1100+/-100	500+/-100	750+/-100	760	29+/-1	540+/-90	45	23
61	1200+/-100	550+/-50	870+/-100	875	27+/-2	500+/-90	59	28

We also have three different cooling cases (methods):

5.5.1 Case 1: Dry Cutting

The boundary surface S_h is the surface of the natural convective heat transfer for both of the tool and the tool holder. Since air is a bad heat conductor and the temperatures on S_h are not

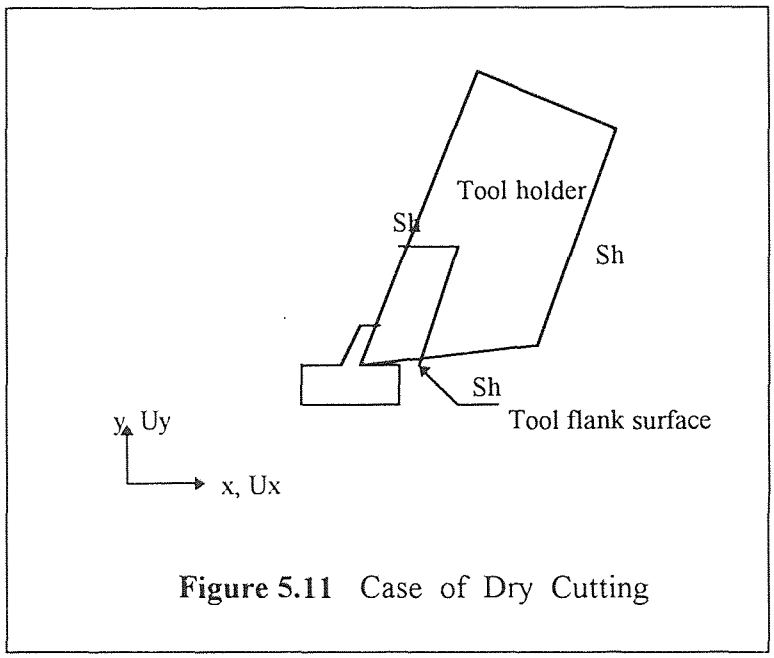

Figure 5.11 Case of Dry Cutting

extremely high, heat losses to the air by conduction, convection and radiation are negligibly small [45]. Childs et al [40] showed that within about 1 mm of the cutting edge on the tool flank surface the closeness of this surface can result in conductive heat losses in dry air with mean heat transfer coefficient, h, of about $10^3\ W m^{-2} K^{-1}$. Therefore, a small value of h ($10\ W m^{-2} K^{-1}$) is used on all the external surface S_h except at this small surface, mentioned above on the tool flank . The ambient temperature $T_o = 10\ ^o C$ is applied on all external surfaces.

5.5.2 Case 2: New Cooling Device

The copper tube is used to coil the tool holder to remove heat by cold water flows in the tube, and there is no heat convection along the tool holder surfaces. The nearest point of effective heat exchange is 3 mm from tool tip, and effectively up to top of tool holder. The effective length of tool holder is L = 60 mm long.

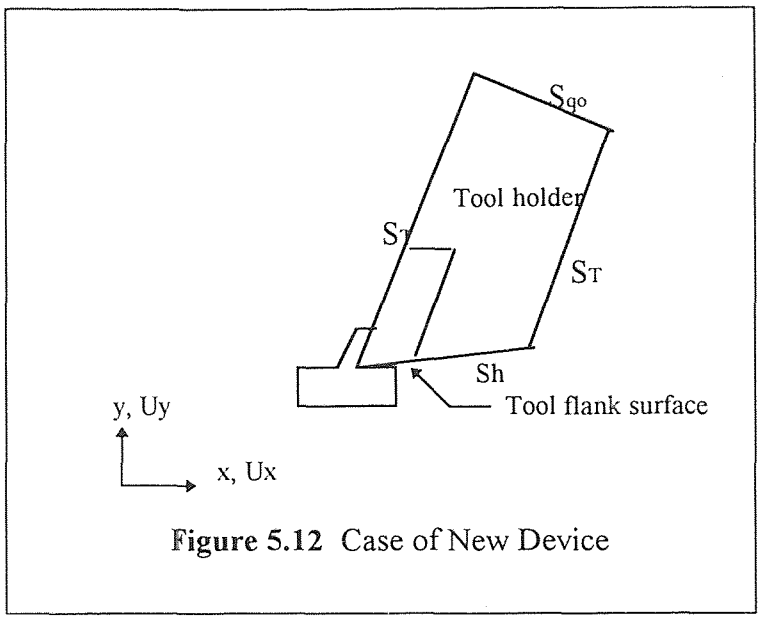

Figure 5.12 Case of New Device

5.5.3 Case 3: Wet Cutting

The value of convective heat transfer coefficient, h, from the tool to the coolant, isdetermined from previous published work [44] in the range of 10^3 *to* 10^4 $Wm^{-2}K^{-1}$. Therefore, the value of h is averaged at

$$h = 5 \times 10^3 \ Wm^{-2}K^{-1}$$

to give the most reasonable results for the effect of coolant in this case. Also, the ambient temperature $T_o = 10\,^{\circ}C$.

In our model, all these conditions with constant surface temperature of workpiece far from shear zone and surface of chip is thermal insulation as showed in Figure 6.5. The temperature field of tool and tool holder with combinations of different cutting speeds and cooling methods is calculated by using the commercial finite element analysis package ANSYS. Some results from ANSYS calculations for these combinations of cutting speeds and cooling conditions are showed in from Figure 5.13.

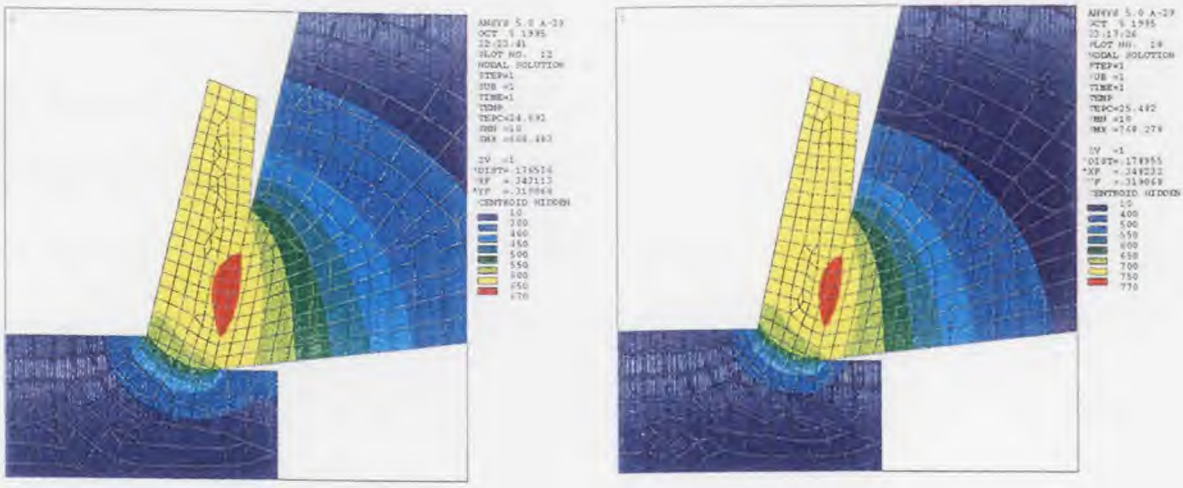

(a) U = 33 m/min

(b) U = 46 m/min

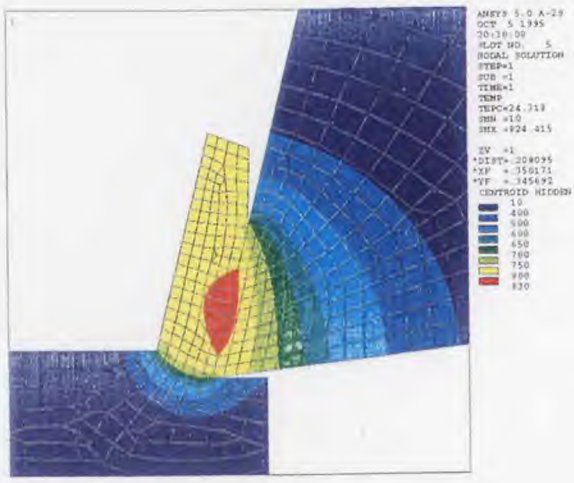

(c) U = 61 m/min

Figure 5.13 Results of Temperature Distributions for Three Cutting Conditions by Using Proposed Cooling Device

CHAPTER 6

ANALYSIS OF RESULTS

6.1 Maximum Temperature on Rake Face

The maximum temperature on rake face of cutting tool are shown in Figure 6.1. We find that wet cutting has the lowest maximum temperature, new cooling device has middle one and, dry cutting has highest temperature on rake face of tool. Comparison of three cutting speed U, we also find that highest cutting speed (U1 = 61 m/min) results in the highest maximum temperature on the rake face of tool; middle cutting speed (U2 = 46 m/min) gets the middle one; and also the lowest cutting speed (U3 = 33 m/min) obtains the lowest maximum temperature on rake face of tool. With almost same difference of cutting

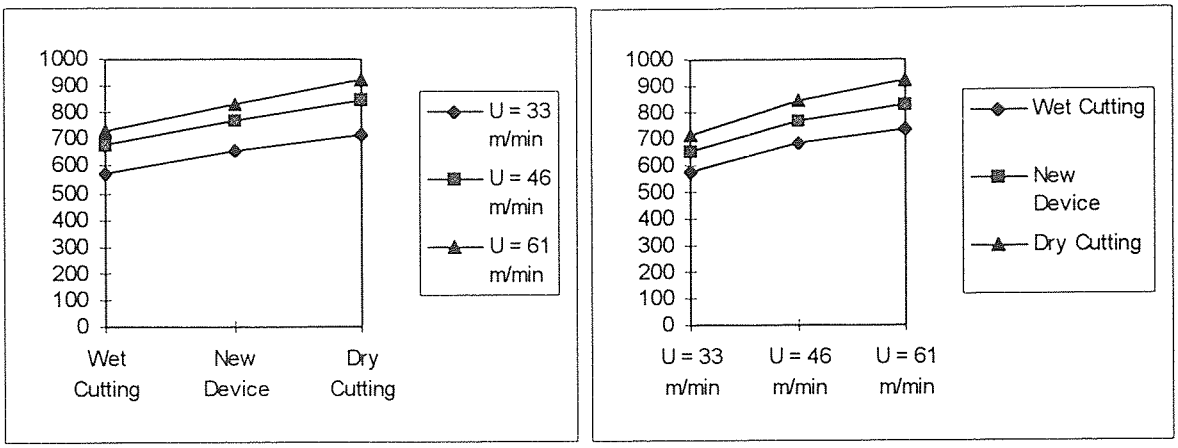

(a) (b)

Figure 6.1 Maximum Temperature on Rake Face of Tool

speeds, $\Delta U1 = U1 - U2 = 15$ m/min and $\Delta U2 = U2 - U3 = 13$ m/min, the maximum temperature increase much more from lowest to middle cutting speed (from U3 to U2)

than that of from middle to highest (from U2 to U1). Study of the increase rate of maximum temperature, we can say that they are almost the same among three cooling methods. The reason of this kind of temperature distribution is based on quantity of heat generated from different cutting speeds, how and where the heat is removed from its source. The wet cutting let coolant remove heat directly from its source, rake face and flank face which we will discuss later. The new device, however, remove the heat a certain distance from its source due to its constructure, so it results in the maximum temperature of tool rake face relatively higher than wet cutting. The dry cutting only let tool cool by natural convection through surrounding air, of course, it raise the highest maximum temperature of tool.

6.2 Maximum Temperature on Flank Face

Figure 6.2 shows that the maximum temperature of flank face of tool for the dry cutting and new device are very close, which means that new device has few effect on maximum temperature of flank face of tool, it is because that effective area of heat exchange new device is far from flank face. We also find that new device has better effect for higher cutting speed than lower speed because the temperature increase rate is reduced when cutting speed increasing. However, the temperature increase rate of dry cutting and wet cutting are almost the same when cutting speed increasing.

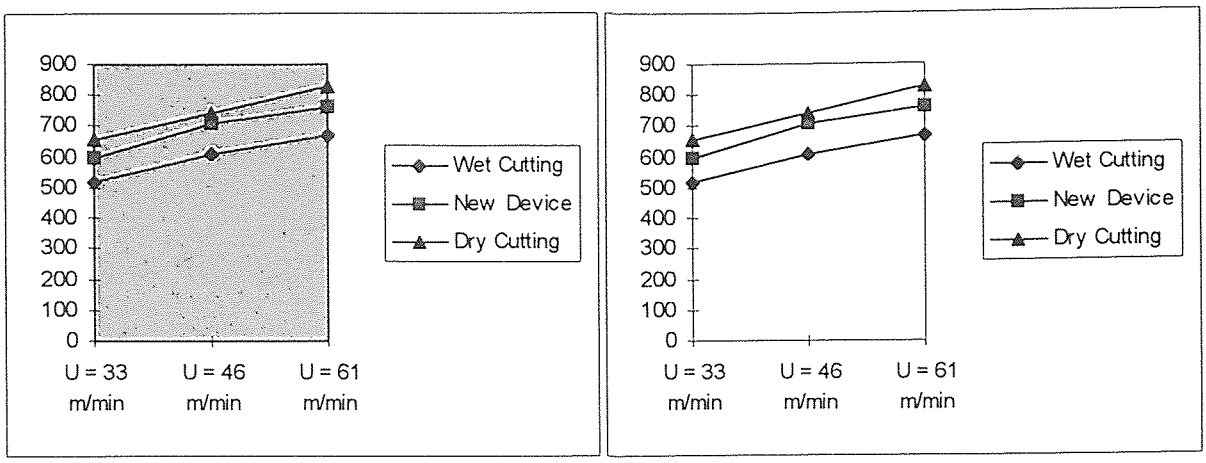

(a) (b)

Figure 6.2 Maximum Temperature on Flank Face of Tool

6.3 Distance of Temperature Bounday Beneath Rake Face

Figure 6.3 shows that if we set an absolute value of temperature (here is 600° C) the temperature diffusive length is the way in Figure 6.3. New device has a much close to wet

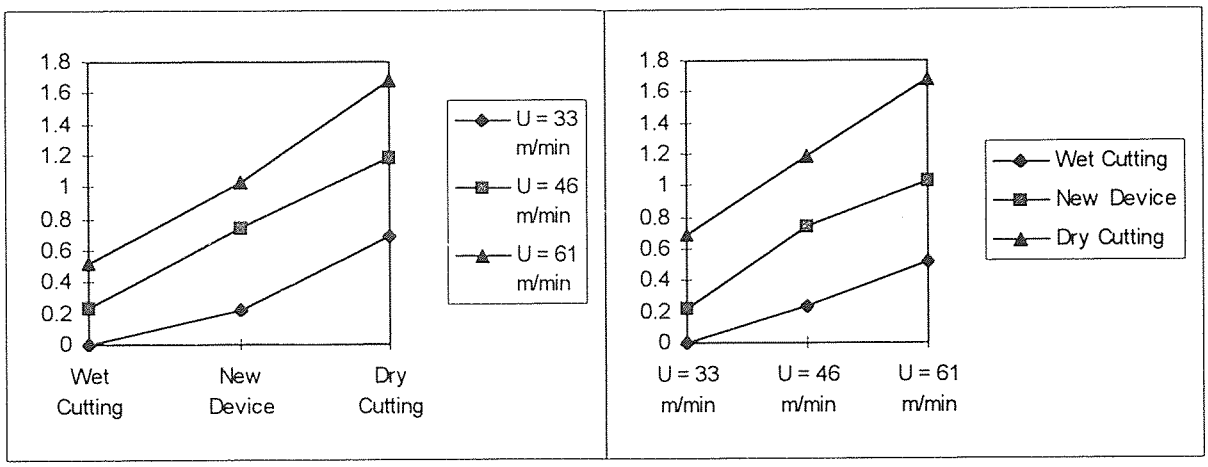

(a) (b)

Figure 6.3 The Distance of Temperature (T = 600° C) Boundary Beneath of Rake Face

cutting in three different cutting speed. Though the rate increases with the cutting speed increases, new device insure the rate increase much lower in higher cutting speed comparing with both dry cutting and wet cutting. The tendency means new device will has great temperature gradient in higher cutting speed.

6.4 Temperature Around BUE Area

If we take a fix length L = 0.25 mm from the tool tip up to rake face of the tool, the temperature range in this area which covers the normal build-up-edge (BUE) area is showed in the Figure 6.4. We can find that both low and high temperature boundary of proposed device is lied in between the Wet Cutting and Dry Cutting. The low temperature boundary of the proposed device, for different cutting conditions, is showed in (a) and (b) of Figure 6.4. The high temperature boundary is showed in (c) and (d) of Figure 6.4. When U = 33 m/min, they are close to Wet Cutting; when the cutting speed increases such

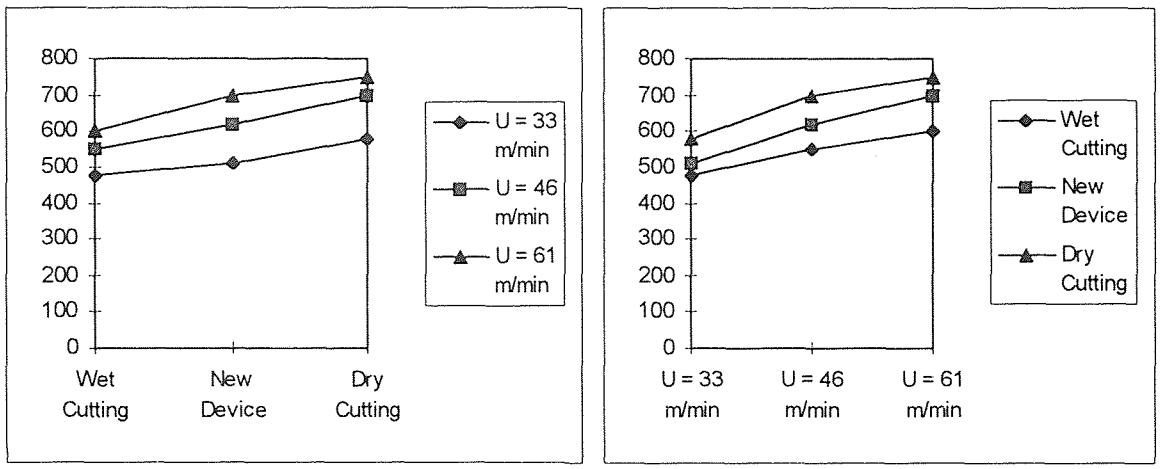

(a) (b)

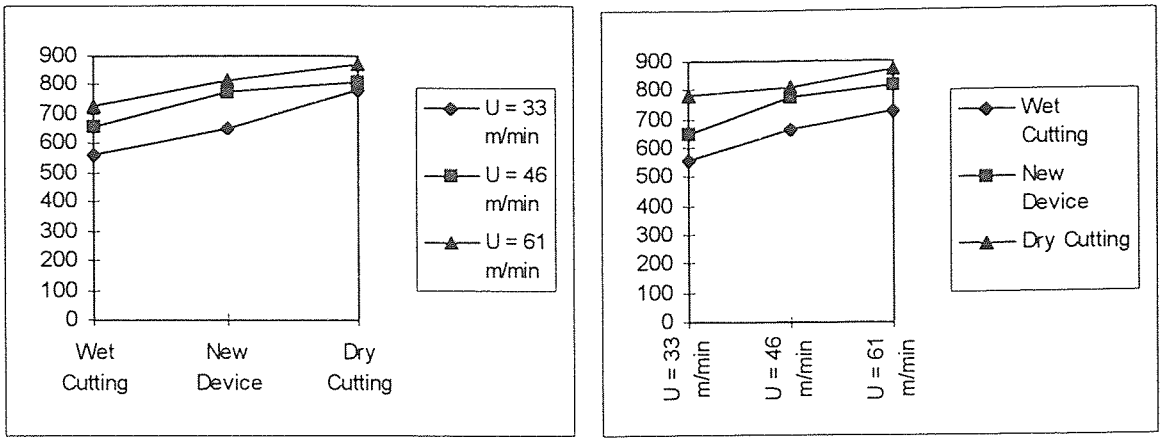

(c) (d)

Figure 6.4 Temperature Range in Build-Up-Edge
When Take Length L = 0.25 mm From Tool Tip
(a) & (b) are Lower Temperature Boundary ; (c) & (d) are High Temperature Boundary

as U = 61 m/min, they are close to Dry Cutting. That means the heat exchange of device can not effectively reach the BUE area due to its structure.

6.5 Thermal Stress of Cutting Tool

We have learned that temperature of tool ant tool holder is proportional to the thermal force of them, which is $T \propto F$. In our two-dimensional model, the length L represents the area A, that is $L \propto A$. However, we also know that stress of tool and tool holder i determined by it definition formula:

$$s = \frac{F}{A} \propto \frac{T}{L} \tag{6.1}$$

So there are three different combinations of changes with T and L which will affect the tool and tool holder stress (s):

(i) If temperature T decreases while Length L decreases too, then the change of stress (s) whether increase or decrease will be determined by the ratio of both changes of T and L. This is the good case because the change of tool stress may decrease even if it increases but only with small rate.

(ii) If temperature T decreases while length L increases, then we can simply determine that stress will decreases by its definition formula. This is the optimal choice when consider the changes of temperature field of tool during different cutting conditions. It will insure that we can have a longer tool life.

(iii) If temperature increases while length L decreases, then we also can say that the change of tool stress (s) will increase. This is the worst case because it will reduce the tool life of machining.

Table 6.1 Temperature and Its Length and Width of Boundary Near Cutting Edge

		Dry	*Cutting*		*New*	*Device*		*Wet*	*Cutting*		
		A	B	C	A	B	C	A	B	C	D
	T (C)	900	850	800	800	750	700	720	700	650	600
U = 61	L (mm)	.79	1.266	1.39	.82	1.226	1.39	.69	.98	1.28	1.405
m/min	W (mm)	.078	.30	.62	.082	.328	.58	.051	.10	.28	.485
	T (C)	830	800	750	750	700	650	660	620	550	
U = 46	L (mm)	.545	.858	1.05	.54	.87	.985	.616	.938	1.14	
m/min	W (mm)	.049	.14	.402	.049	.203	.443	.049	.165	.428	
	T (C)	720	700	650	650	600	550	570	550	500	450
U = 33	L (mm)	.63	.91	1.158	.77	1.109	1.23	.72	.93	1.17	1.26
m/min	W (mm)	.0526	.14	.479	.088	.37	.64	.0675	.15	.36	.585

If we take a look at the temperatures of areas A, B and C which are maximum temperature zones that along the contact area between chip and tool, where area A is the highest temperature zone, area B is the area close to area A and has a higher temperature

too and, the area C is next to area B and its temperature boundary very close to contact area. The temperatures, their length and width among these areas are shown as follows based on the data in Table 6.1 obtained from calculations:

Now we take a look at the results of temperature field obtained by calculations of ANSYS, we find that, in the same cutting speed such as at U = 61 m/min, the length of temperature boundary decreases with the temperature increases in different cooling

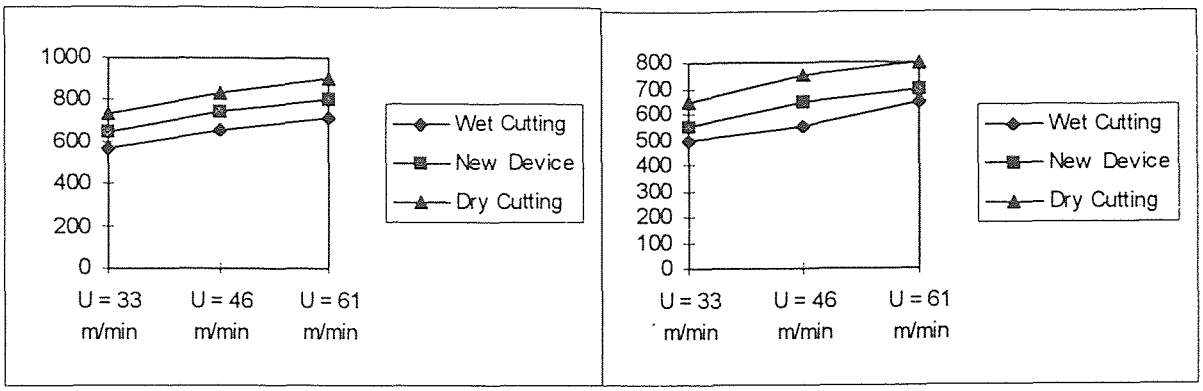

(a) Zone A (b) Zone B

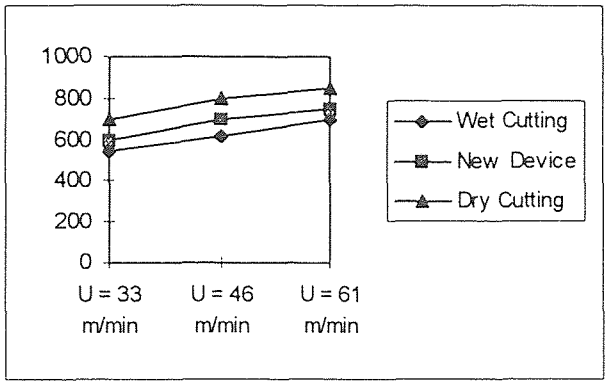

(c) Zone C

Figure 6.5 Temperature of Three Zones A, B and C

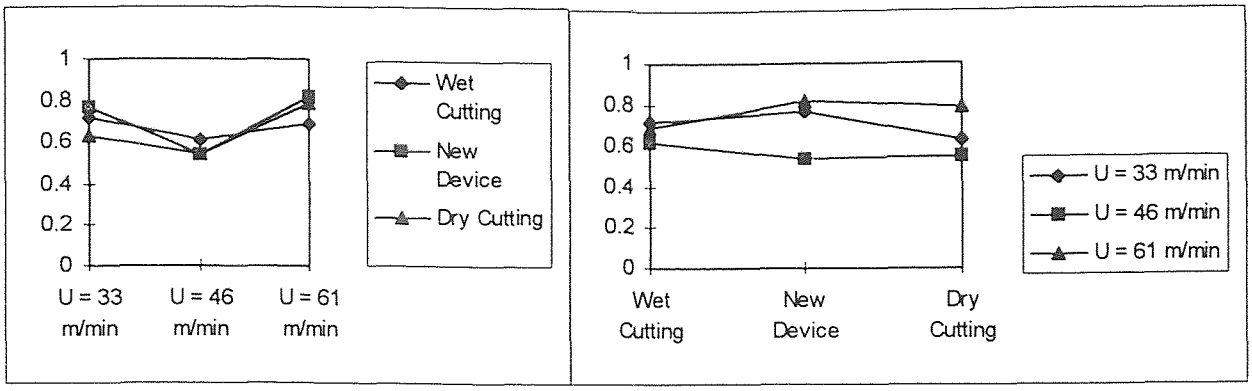

(a) Zone A

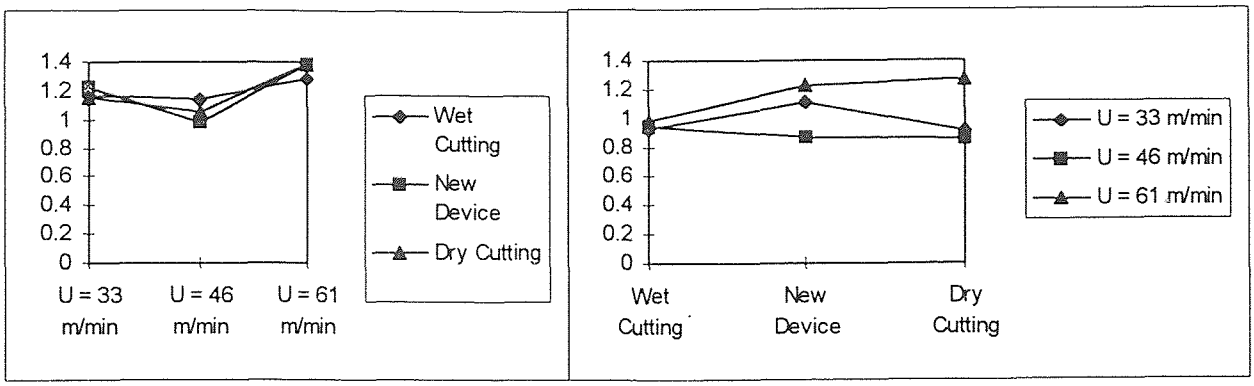

(b) Zone B

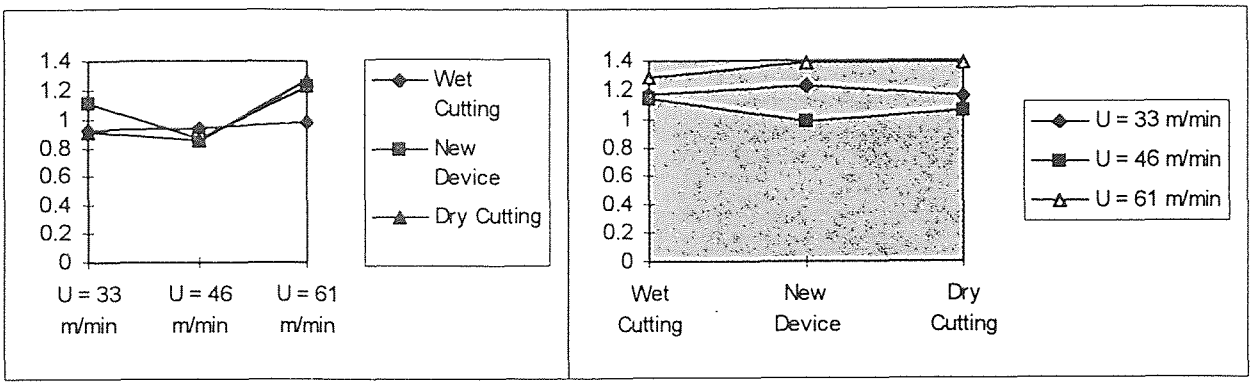

(c) Zone C

Figure 6.6 Length of Temperature Boundary for Three Zones A, B and C

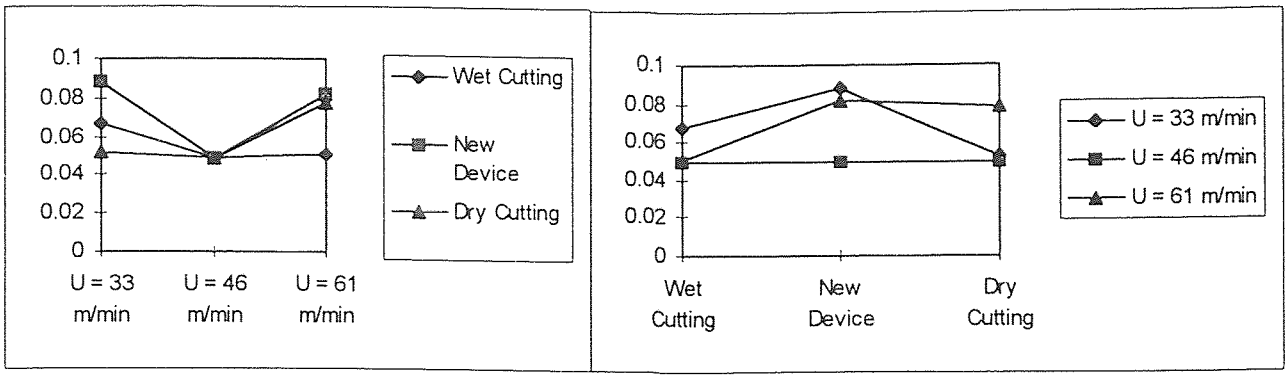

(a) Zone A

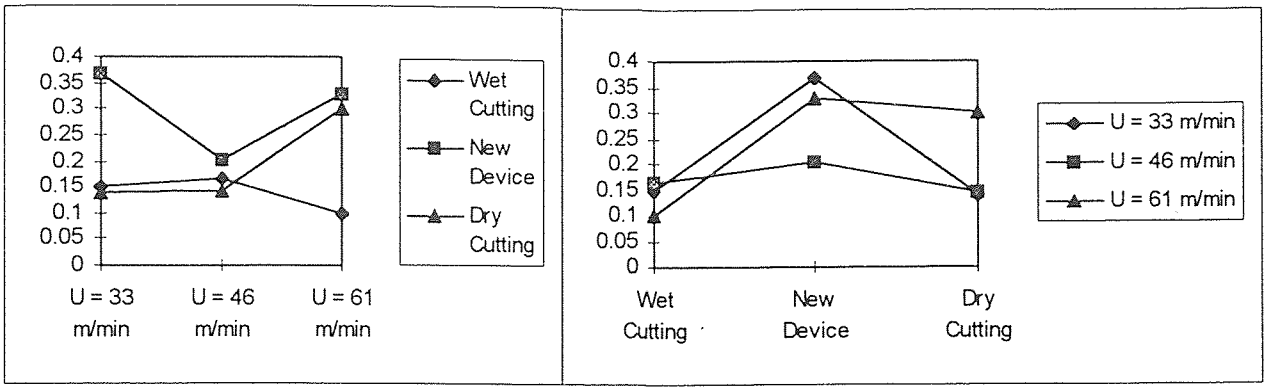

(b) Zone B

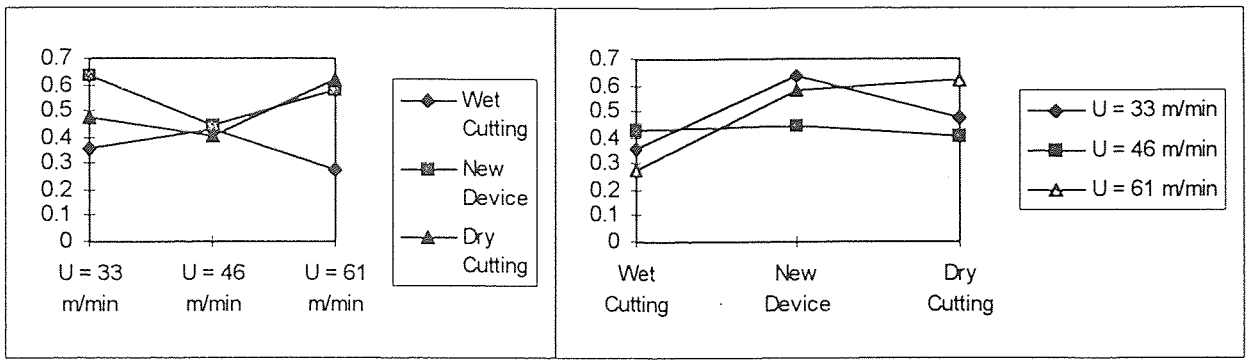

(c) Zone C

Figure 6.7 Width of Temperature Boundary for Three Zones A, B and C

methods. For example, when temperature T is 850 °C the length of temperature boundary L is 1.266 mm in Dry Cutting situation; when temperature T is 750 °C the temperature boundary L is 1.226 mm in New Device cooling situation; and when temperature T is 700 °C the temperature boundary L is only 0.98 mm in Wet Cutting. These results match the situation (i) we have discussed above. From these data we can say that thermal stress of tool and tool holder may be highest in the Dry cutting, middle level in the New Device cooling, and lowest in the Wet Cutting. The rate of change for different cooling conditions is much higher from Dry Cutting to New Device cooling condition and relatively lower from New Device to Wet Cutting.

If we take a look at the results further, we can find that there is the situation as temperature decrease the length of temperature boundary increase in different cooling conditions. For example, when we take the temperature T at 850 °C, the length of temperature boundary L become 1.266 mm long in the Dry Cutting; similarly if we take the temperature T at 700 °C the length L is 1.39 mm long for the New Device cooling; and when temperature T is 600 °C the length L is 1.405 mm long for Wet Cutting. This matches the situation (ii) we have discussed above which also is the optimal situation for the cutting tool thermal design because it will ensure the low thermal stress of the tool. In our three different cases, the thermal stress of tool is highest to lowest as the order of Dry Cutting, New Device and Wet Cutting, respectively. Though Wet Cutting make the thermal stress of tool lowest, the New Device make its thermal stress much close to Wet Cutting from the data of our results.

CHAPTER 7

CONCLUSION AND RECOMMENDATIONS

The proposed cooling device does reduce the maximum temperature of cutting tool comparing with the Dry Cutting, but it also increases the maximum temperature and temperature boundary of cutting tool comparing with Wet Cutting. The results of Table 6.1 shows that proposed cooling device has much lower thermal stress (very close to lowest one - Wet Cutting) among three cooling environments for some cutting condition. Under the consideration of these situations, we can say that it is a good choice to use the proposed cooling device, when it is mandatory to eliminate the biological and environmental effects of the cutting fluids and the maximum temperature of tool by using the device is below its thermal failure temperature.

From the results and plots, it can be concluded that a significant amount of the cooling effect of the cutting fluid can be compensated by the use of the new device. Overheated area at the tip is reduced compared to the case of dry cutting, and consequently, less wear and longer tool life can be achieved. This also minimize the tooling and production costs. Benefits realized from this new device are enormous, precision engineering of components used in aircraft, space shuttles, automobiles, etc.

However, there are some limitations of the proposed cooling device. One is that the device itself cannot substitute the lubrication function of cutting fluids. It will be good in use for the self lubrication materials. The other is that it still cause higher maximum

temperature than that of Wet Cutting, so this restrict its applications only in certain cutting conditions that do not cause tool thermal failure.

Some recommendations have been given to improve the proposed device in the following. The most important one is that a under cooling method proposed by Dr. Billatos can be introduced into this device. The modified device will further reduce the maximum temperature of tool due to adding a heat transfer area which is much closer to tool tip.

One more aspect of the work which requires further study is the suggestion that the main friction heat source because of sliding between the chip and the tool remained in the plane of the original rake face, even when the tool became deeply cratered.

The other aspect of the work needed further study is to change the boundary conditions of main friction heat source between tool tip and chip as there is not prefect contact considered. So it should be introduced heat resistance into the model.

Furthermore, if it is necessary to obtain the more accuracy model compared with the actual situation, a three-dimensional model has to be established instead of present two-dimensional model. However, it is expected that much more experimental and analytical work should be carried out for such change.

APPENDIX A

RESULTS OF TEMPERATURE DISTRIBUTIONS FOR WET CUTTING

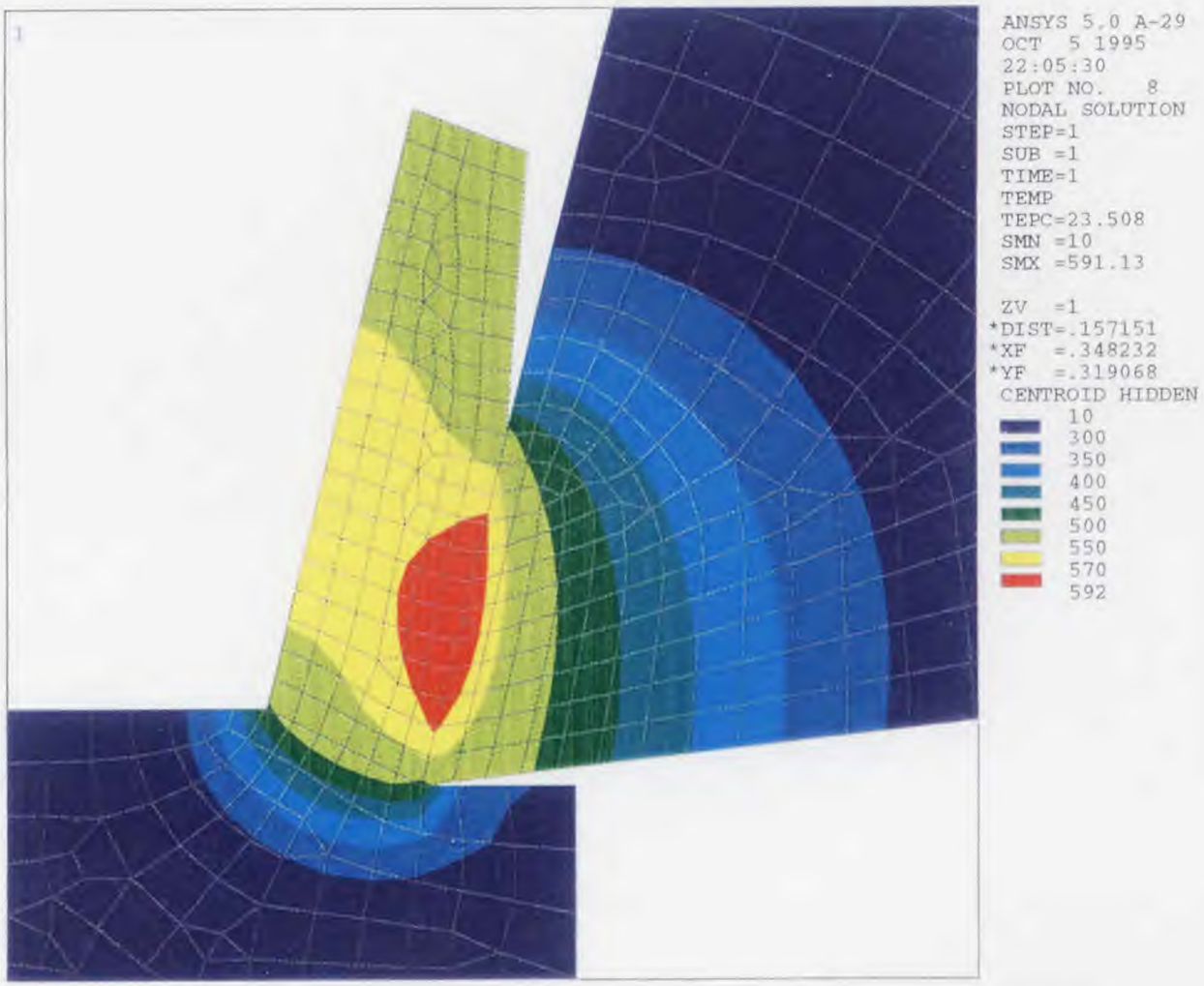

Figure A.1 Temperature Distributions Around Cutting Edge For Speed U = 33 m/min

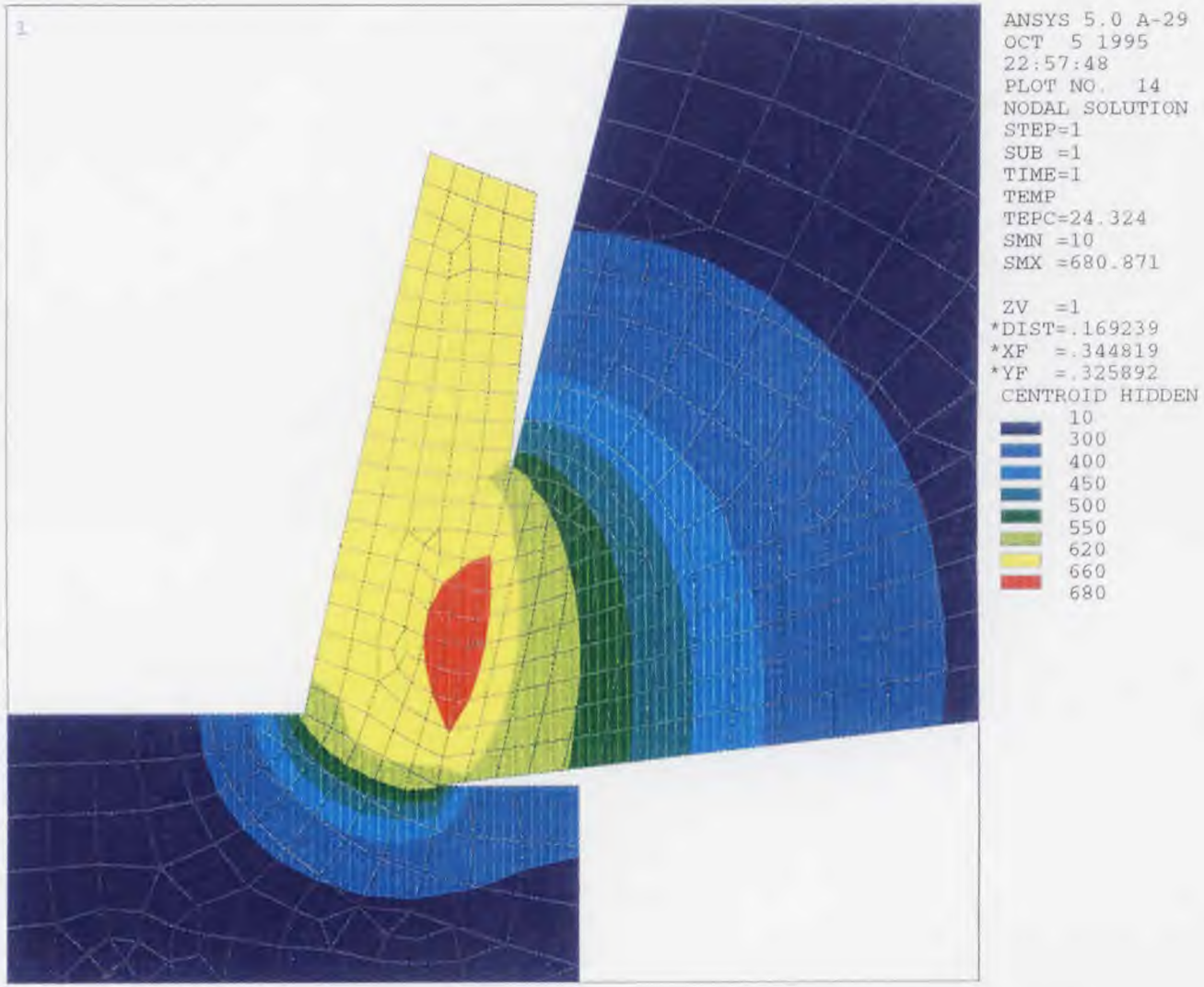

Figure A.2 Temperature Distributions Around Cutting Edge for Speed U = 46 m/min

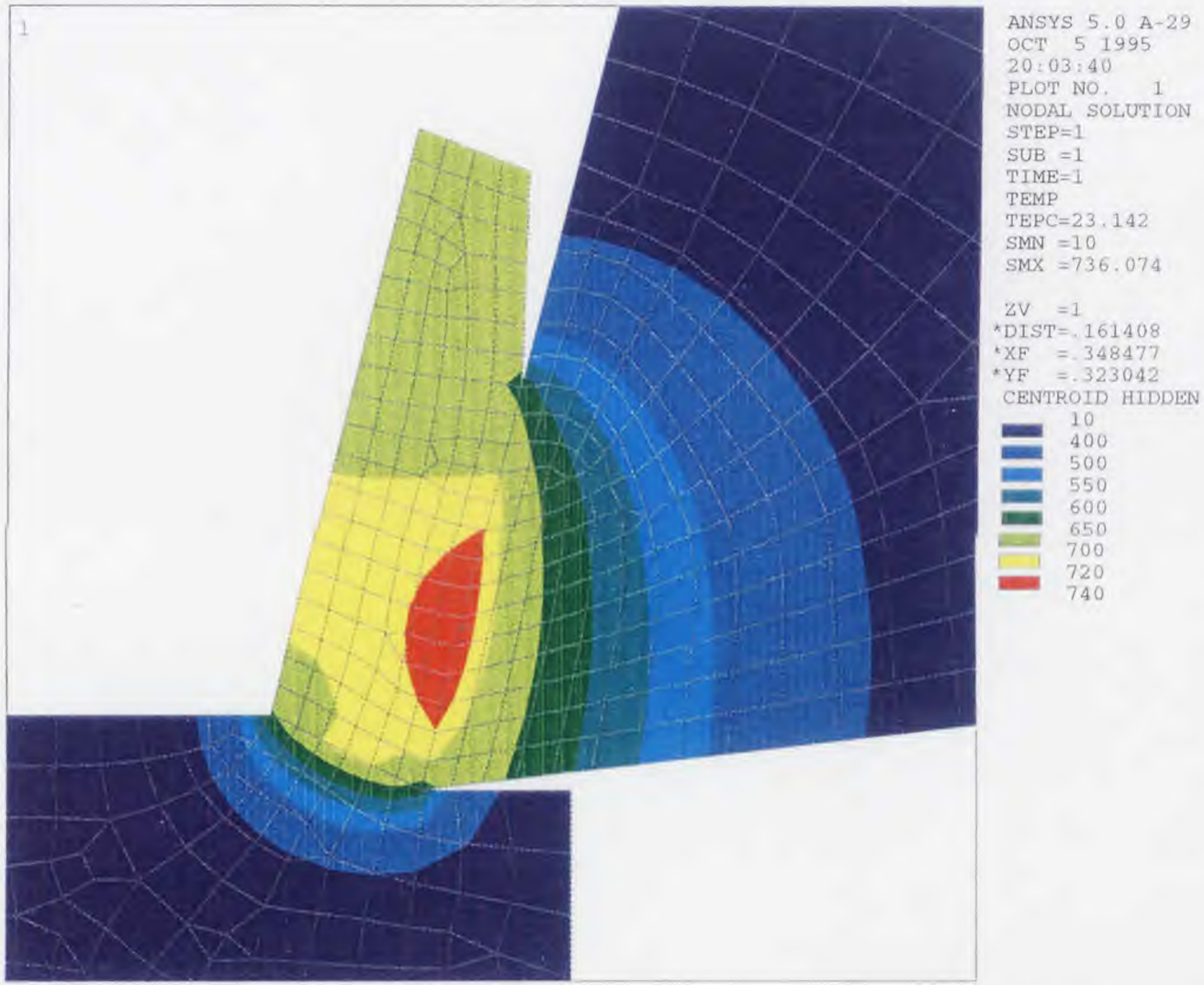

Figure A.3 Temperature Distributions Around Cutting Edge for Speed U = 61 m/min

APPENDIX B

RESULTS OF TEMPERATURE DISTRIBUTIONS FOR NEW DEVICE

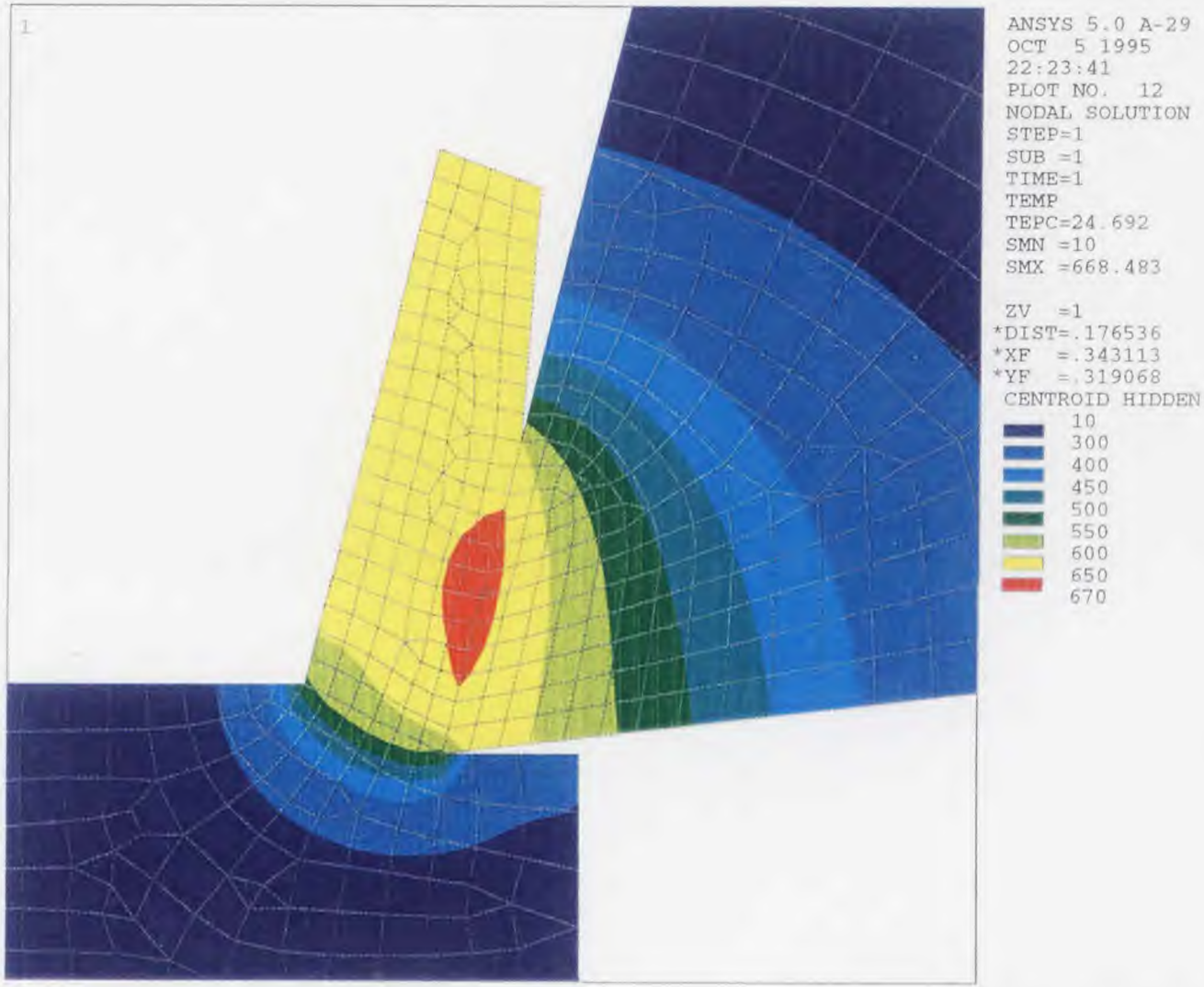

Figure B.1 Temperature Distributions Around Cutting Edge for Speed U = 33 m/min

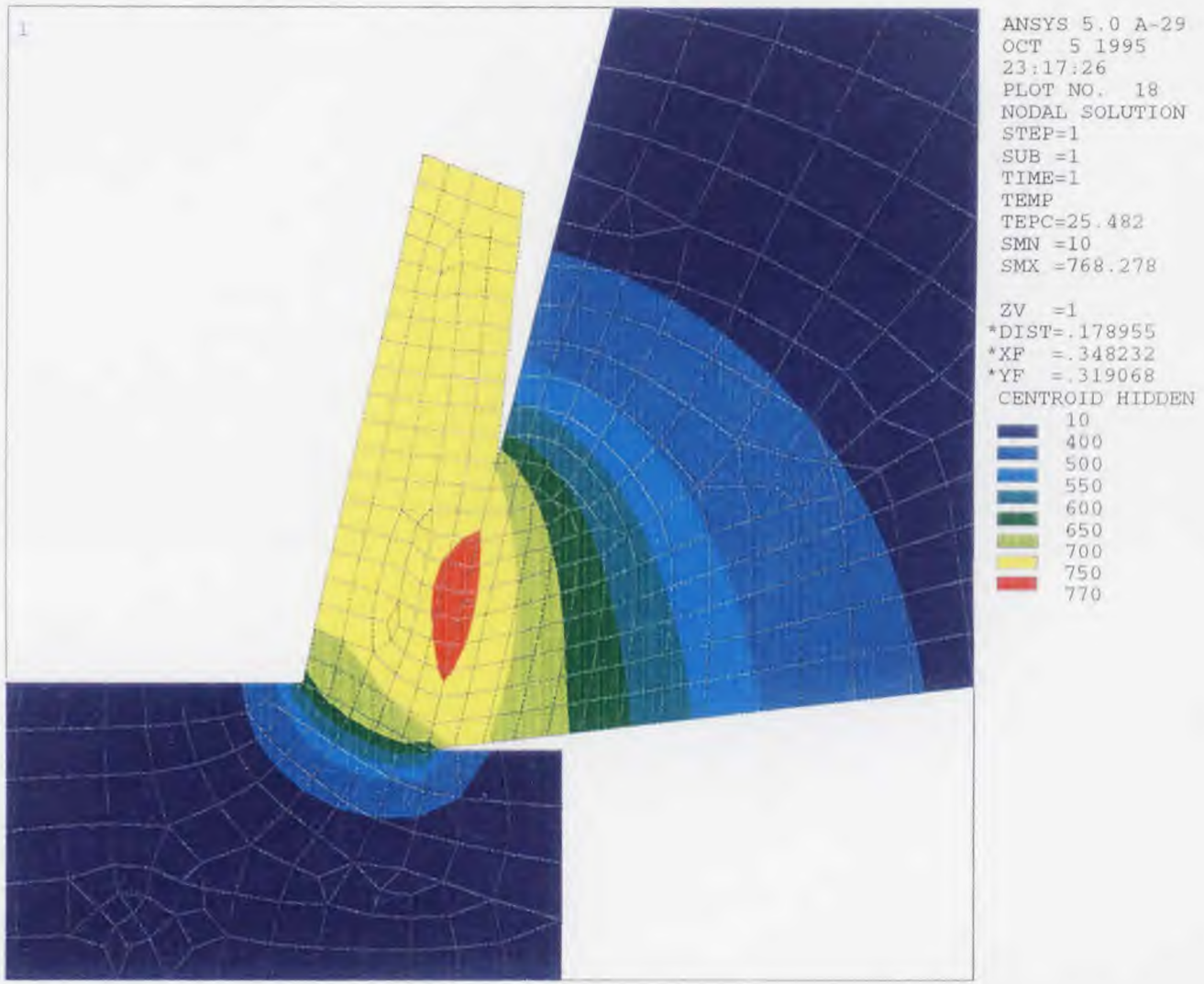

Figure B.2 Temperature Distributions Around Cutting Edge for Speed U = 46 m/min

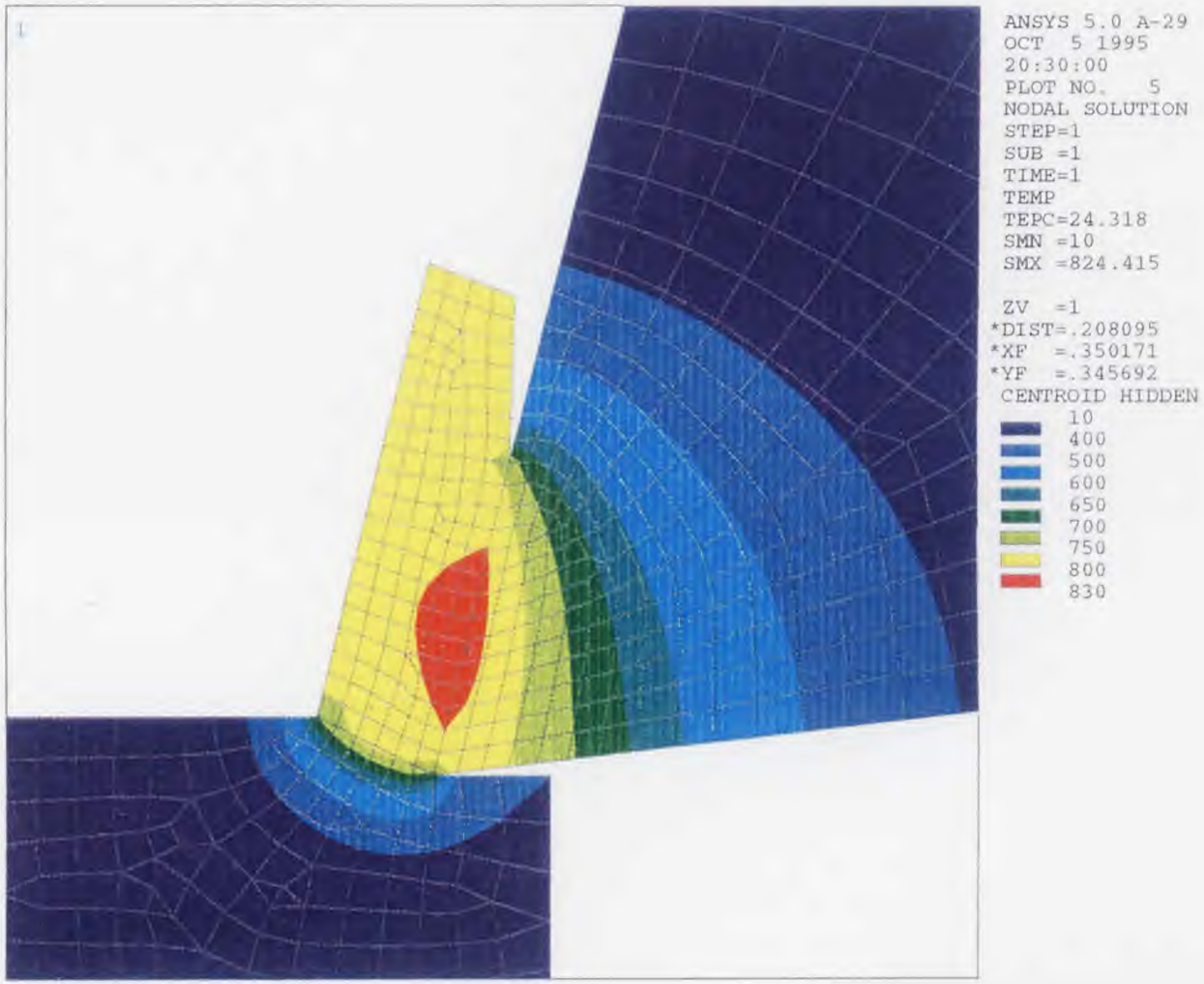

Figure B.3 Temperature Distributions Around Cutting Edge for Speed U = 61 m/min

APPENDIX C

RESULTS OF TEMPERATURE DISTRIBUTIONS FOR DRY CUTTING

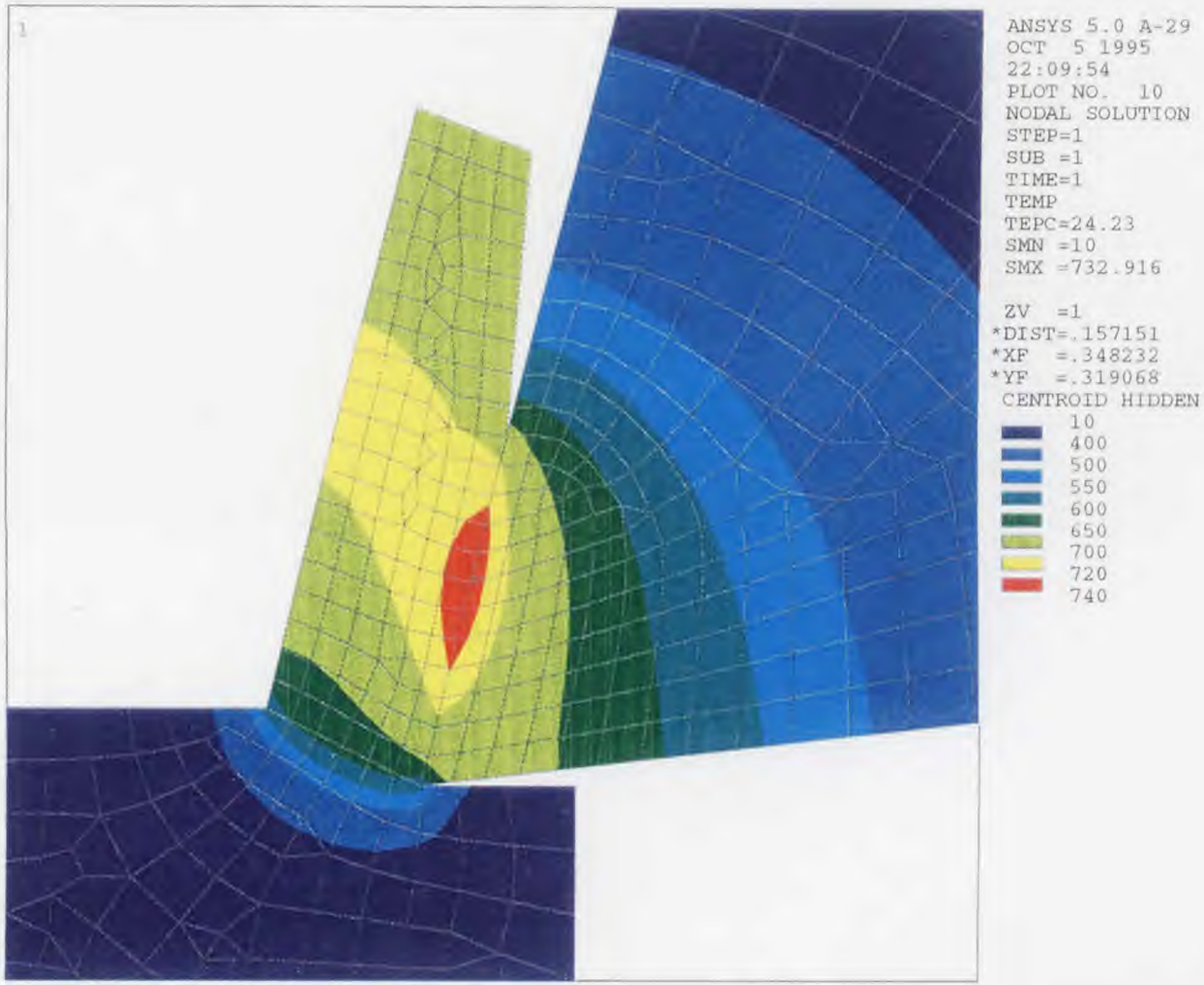

Figure C.1 Temperature Distributions Around Cutting Edge for Speed U = 33 m/min

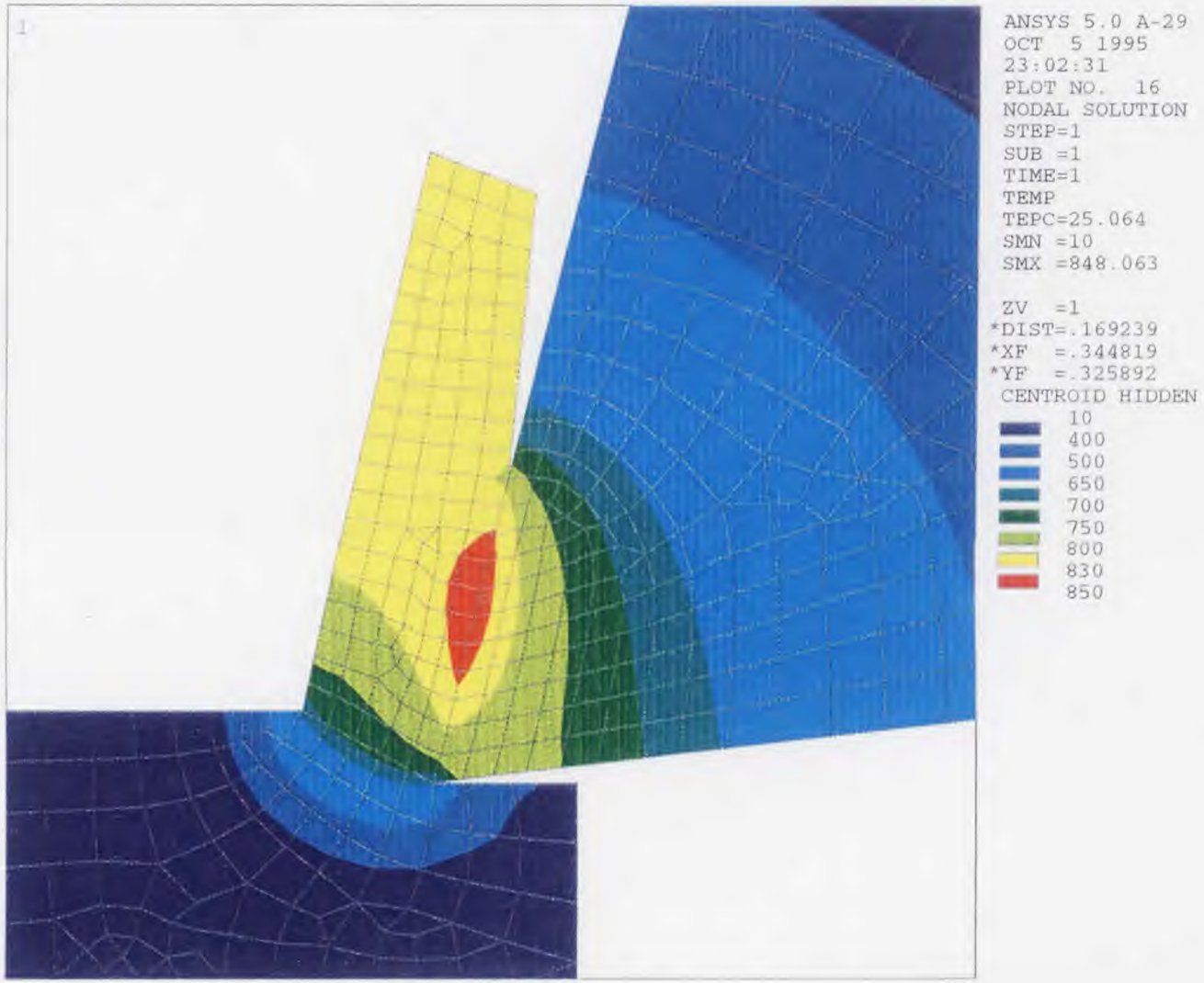

Figure C.2 Temperature Distributions Around Cutting Edge for Speed U = 46 m/min

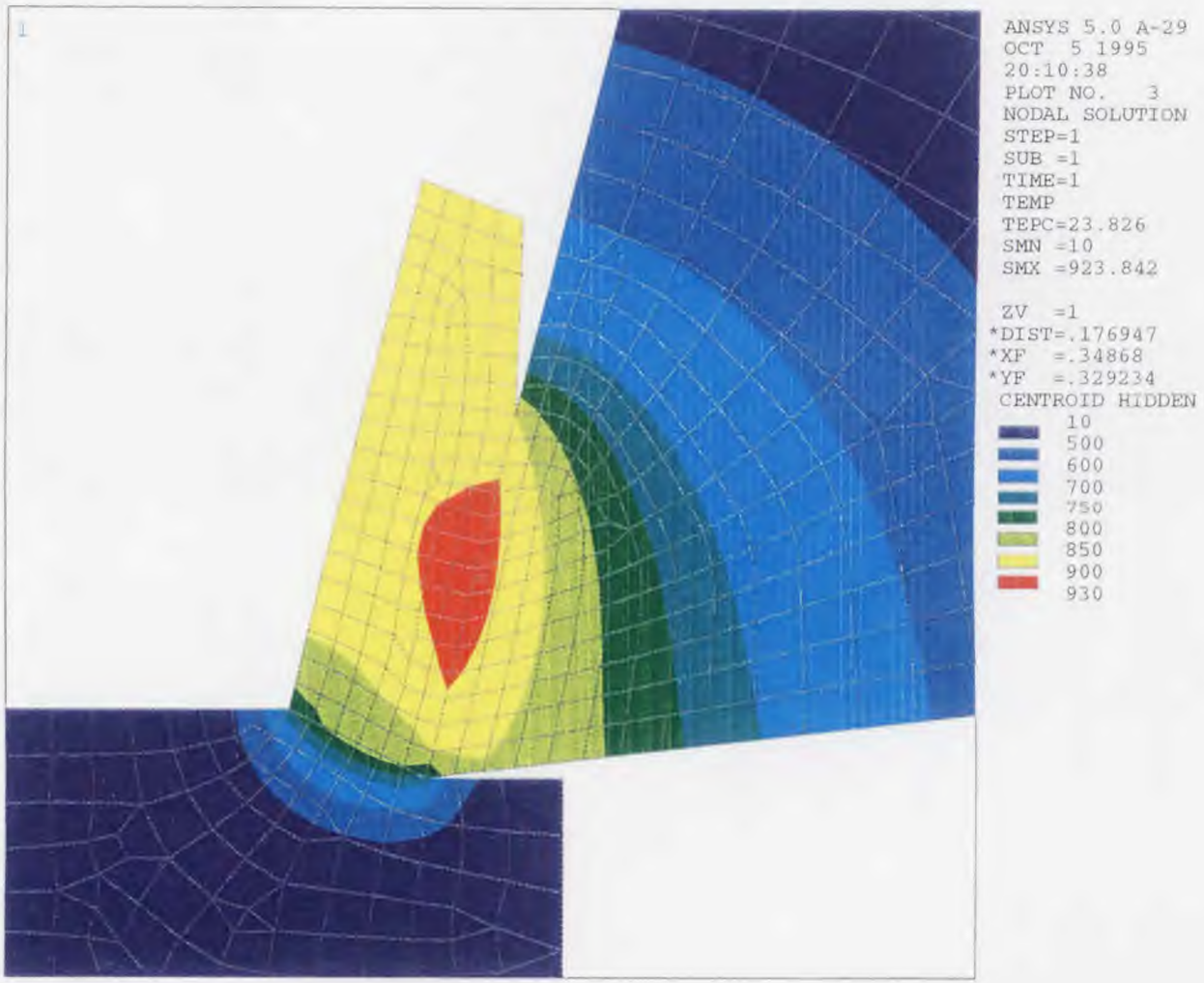

Figure C.3 Temperature Distributions Around Cutting Edge for Speed U = 61 m/min

REFERENCES

1. B. I. Juneja, G.S. Sekhor, Fundamentals of Metal Cutting and Machine Tools , Wiley Eastern Ltd., New Delhi, India 1987.

2. M. C. Shaw, Metal Cutting Principles, Oxford University Press, New York, 1984.

3. M. C. Shaw, "In Metal Transformation", Gordon and Breach, New York, 1968.

4. E. M. Trent, Metal Cutting, Butterworths, Boston, Massachusetts, 1977.

5. G. Boothroyd, Fundamentals of Metal Machining and Machine Tools, McGraw - Hill Book Company, New York, 1975.

6. P. L. B. Oxley, Mechanics of Machining, Ellis Horward Ltd., England, 1989.

7. A. P. Gwiazdonwski, Tool Engineering, McGraw - Hill Book Co., New York, 1951.

8. J.A. McGeough, Advanced Methods of Machining, Chapman and Hall Ltd., New York, 1988.

9. P.H. Black, Theory of Metal Cutting, McGraw-Hill Book Co., New York, 1961.

10. F. W. Wilson, R.W. Cox, Machining the Space- Age Metals, ASTME, Dearborn, Michigan, 1965.

11. E. Dow Whitney, Ceramic Cutting Tools, Noyes Publications, Park Ridge, New Jersey, 1994.

12. M. Jouaneh, S. S. Rangwala, "Precision Machining: Technology and Machanic Development and Improvement", The Winter Annual Meeting of ASME, Anaheim, California, 1992.

13. S. B. Billatos, N.A. Malak, "A Design for the Environment Application in Machining", Fifth World Conference on Robotics Research, September 1994.

14. L. Rozeanu, D. Pnueli, "Two Temperature Gradients Model for Friction Failure", Journal of Lubrication Technology, October 1987, Vol. 100 , pp. 479-485.

15. S. A. Tobias, F. Koenigsberger, "Coolants and Cutting Tool Temperatures", Fifteenth International Machine Tool Design and Research Conference, Birmingham, United Kingdom, September 1974.

16. S. Billatos, P. Hanley, "Analysis of Machining Systems", To be Published.

17. R. Radulescu, S. G. Kapoor, "An Analytical Model for Prediction of Tool Temperature Fields During Continuous and Interrupted Cutting", Journal of Engineering for Industry, May 1994, pp. 135-143.

18. B. R. Kim and et al, "Biological Removal of Organic Nitrogen and Fatly Acids From Metal-Cutting-Fluid Wastewater", Water research, Vol. 28, No.6, pp. 1453-1461.

19. L.Montgomery, "Mist Cooling for High-Speed Machining", American Machinist, October 1962, pp. 86

20. H.R. Leep, M.A. Deak, "Drilling Models for a Synthetic Cutting Fluid", Lubrication Science 6-2, Jan. 1994, pp. 133-147.

21. E. Lenz, Z. Katz, A. Ber, "Investigation of the Flank Wear of Cemented Carbide Tools", J. of Engineering for Industry, Feb. 1976, pp. 246-257.

22. A.Ber, M. Goldblatt, "The Influence of Temperature Grqdient on Cutting Tool's Life", Annals of the CIRP, Vol. 38, Jan.1989, pp.69-73.

23. F.W. Taylor, "On the Art of Cutting Metals", Transactions of the ASME, Vol. 28, No. 1119, pp. 31-350, 1907.

24. Rowe, G.W. and Spick, P.T., Transactions of the ASME 89B, 530 (1976).

25. Childs, T.H.C. and Rowe, G.W., Reports on Progress in Physics, 36,3,225 (1973).

26. Kalpakjian, S., Manufacturing Engineering and Technology, Addison Wesley, 1992.

27. Kurimoto, T. and Barrow, G., "The Influence of Aqueous Fluids on the Wear Characteristics and Life of Carbide Cutting Tools", Annals of the CIRP, Vol. 31/1/1982.

28. George M. Duelley, "Machine Tool having Internally Touted Cryogenic Fluid for Cooling Interface Between Cutting Edge of Tool and Workpiece", US Patent No. 3,971,114, July 27,1976.

29. R.S. Figlioka, and D. E. Beasley, Theory and Design for Mechanical Measurements, Wiley Eastern Ltd., New Delhi, India, 1991.

30. G. L. Davis, Thermo-Eletric Cooler Technology, Mullard Mitchham, C.M.L. United Kingdom.

31. H.J. Goldsnid, Applications of Thermoelectricity, Methuen, London, 1960.

32. EXAIR Corporation, Cold Gun Air Coolant System, EXAIR Catalog.

33. Marian Mazurkiewics, "High Pressure Lubricooling Machining of Metals", US Patent No. 5,148,728, September 22,1992.

34. Rozeanu, L., Dnueli, D., " Two Temperature Gradients Model for Friction Failure", ASME Transaction Paper No. - Lab.-28, 1977.

35. Rozeanu, L., " Trobology", a Publicaion of the Technion, Israel (in Hebrew), pp. 138-152 and pp. 352-378, 1978.

36. K. Maekawa, I. Ohshima, R. Murata, "Finite Element Analysis of Temperature and Stress within an Internally Cooled Cutting Tool", Bull., Japan Society of Process engineering, Vol. 23, No. 3, September 1989.

37. H. Ernst, "Physics of Metal Cutting, Machining of Metals", America Society for Metal, 1938.

38. P. L. B. Oxley, "Note: Allowing for Friction in Estimating Upper Bound Loads". Int. J. Mech. Sci. 5, pp. 183-184, 1963.

39. J. T. Nicolson, The Engineer, England, 99, 1905, pp. 385.

40. T. H. C. Childs, K. Maekawa, P. Malllik, " Effects of Coolant on temperature Distribution in metal machining", Materials Science and Technology, Nov. 1988, Vol. 4, pp. 1006-1019.

41. M.G. Steveson, P. K. Wright, and J. G. Chow: Journal of Engineering for Industry (Trans. ASME),1983, 105, pp. 149-154.

42. Y. S. Touloukian, R. W. Powell, C. Y. Ho, and P. G. Klemens: Thermophysical Properties of Matter, Vol. 1, 1970, Plenum Press, New York.

43. Anthony F. Mills, Heat Transfer, Richard D. Irwin, Inc., 1992.

44. M. Bamberger and B. Prinz, Material Science Technology, 1986, 2, (4), pp. 410-415.

45. A. O. Tay, M. G. Stevenson, and G. de Vahl Davis, " Using The Finite Element Method to Determined Temperature Distributions in Orthogonal Machining", Proc. Mech. Engrs. Vol. 188, pp. 627-638, 1974.

46. Petukhov, B. S., " Heat Transfer and Friction in Turbulent Pipe Flow With Variable

Physical Properties", in Advances in Heat Transfer, Vol. 6, eds. J. P. Hartnett and Irvine, Academic Press, New York, (1970).

47. Gnielinski, V., "New Equations for Heat and Mass Transfer in Turbulent pipe and Channel Flow", Int. Chemical Engineering, 16, pp. 359-368. (1976).